Molecular Bonding in an Alternative Approach to Orbital-Free Density Functional Theory

by

Spencer Sillaste

A thesis
presented to the University of Waterloo
in fulfillment of the
thesis requirement for the degree of
Master of Science
in
Physics

Waterloo, Ontario, Canada, 2021

Author's Declaration

I hereby declare that I am the sole author of this thesis. This is a true copy of the thesis, including any required final revisions, as accepted by my examiners.

I understand that my thesis may be made electronically available to the public.

Abstract

An alternative approach to orbital-free density functional theory based on polymer self-consistent field theory for modelling diatomic molecules is proposed. The ability of the theory to accurately model the bonding characteristics of diatomic molecules will elevate the theory beyond simple atomic system calculations. Homonuclear diatomic molecules H_2, N_2, O_2 and F_2 modelled using this theory exhibit molecular bonding in agreement with known results. Heteronuclear diatomic molecules CO and HF also exhibit molecular bonding. The calculated electron density contours are found to be in agreement with known density functional theory results. Bond lengths for the majority of diatomic molecules studied are found to deviate less than 8% when compared to accepted experimental results and less than 9% when compared to Kohn-Sham density functional theory results, with the exception of O_2 and F_2, which deviated significantly from both results. The bond dissociation energy for H_2 is found to be within 16% of the accepted experimental value, but the fundamental vibrational frequency does not agree well with experimental results. The main approximations in the theory are a Fermi-Amaldi factor in the electron-electron interaction that corrects for electron self-interactions and Pauli potential based on excluded volume arguments to account for the Pauli exclusion principle. The governing modified diffusion equation is solved in terms of a basis set that encodes the cylindrical symmetry of diatomic molecules.

Acknowledgements

I would like to thank my research supervisor, Professor Russell Thompson, for his complete support and skillful guidance throughout the project.

I would also like to thank my committee members, Professor Nasser Abukhdeir, Professor Jeff Chen and Professor Qing-Bin Lu, for critically examining my research performance and providing insightful feedback.

Thank you, as well, to my family, friends and Suzy Lim for their constant love and support.

Table of Contents

List of Figures vii

List of Tables viii

1 Introduction 1
- 1.1 Motivation . . . 1
- 1.2 Objectives . . . 3
- 1.3 Overview . . . 3

2 Background 5
- 2.1 Introduction . . . 5
- 2.2 Density Functional Theory . . . 6
  - 2.2.1 Hohenberg-Kohn Theorems . . . 6
  - 2.2.2 Kohn-Sham Density Functional Theory . . . 10
  - 2.2.3 Orbital-Free Density Functional Theory . . . 13
- 2.3 Self-Consistent Field Theory for a Gaussian Polymer in an External Field . 18

3 Theory 25
- 3.1 Introduction . . . 25
- 3.2 Self-Consistent Field Theory Equations . . . 26
  - 3.2.1 Mean Field Quantities . . . 27
  - 3.2.2 Modified Diffusion Equation . . . 32
  - 3.2.3 Spectral Solution to the Modified Diffusion Equation . . . 34
- 3.3 Cylindrically Symmetric Basis Set . . . 38
- 3.4 Potentials and Fields . . . 39
  - 3.4.1 External Potential . . . 39
  - 3.4.2 Electron-Electron Potential . . . 43
  - 3.4.3 Pauli Potential . . . 45

3.4.4 Nuclei Potential 50
3.5 Helmholtz Free Energy 51

4 Diatomic Molecules **53**
4.1 Introduction 53
4.2 Computational Methods 54
4.3 Electron Density 55
4.4 Bond Lengths 59
4.5 Bond Dissociation Energy and Fundamental Vibrational Frequency for Hydrogen 62
4.6 Limitations 63

5 Conclusions **65**

References **67**

APPENDICES **71**

A Derivation of Cylindrically Symmetric Basis Set **72**

B Gamma Tensor **78**

C Quantum and Classical Partition Function **81**

D Kac-Feynman Differential Equation Solution **86**

List of Figures

4.1 Flowchart of the computational algorithm used to determine the electron density of diatomic molecules. 54
4.2 Total electron density contour plot of homonuclear diatomic molecules, (a) H_2, (b) N_2, (c) O_2, (d) F_2. For (a), both axes are identically spaced from -4 to 4 Bohr radii, a_0. The outermost contour is 0.001 e/a_0^3 and the innermost contour is 0.2 e/a_0^3. For the remaining contour plots (b), (c), and (d) both axes are identically spaced from -3 to 3 a_0. The outermost contour is 0.04 e/a_0^3 and the innermost contour is 8 e/a_0^3. 56
4.3 Total electron density contour plot of heteronuclear diatomic molecules, (a) CO, (b) HF. For (a) and (b), both axes are identically spaced from -3 to 3 a_0. The outermost contour is 0.04 e/a_0^3 and the innermost contour is 8 e/a_0^3. In (a), the carbon nucleus is on the bottom and the oxygen nucleus is on the top. In (b), the hydrogen nucleus is on the bottom and the fluorine nucleus is on the top. 58
4.4 Free energy for two hydrogen atoms at different atomic separations. The position coordinate is in reference to the origin, the actual distance between the two atoms will be twice the position value. The dot marks the free energy minimum. 62

List of Tables

4.1 Differences in OF-DFT based on SCFT, KS-DFT and experimental bond lengths for diatomic molecules. [a]Using B3LYP exchange-correlation functional and the 6-31G(d,p) basis set. [b]Using B3LYP exchange-correlation functional and the aug-CC-PVDZ basis set. 60

Chapter 1

Introduction

1.1 Motivation

Predicting the properties of quantum systems of electrons is fundamental to understanding how the universe behaves at small length scales. Specifically, understanding the characteristics of molecular bonding in diatomic molecules provides insight into the foundation of how all molecules behave. The study of diatomic molecules is essential to a variety of applications, such as understanding oxidation in materials [1], or the role of nitrogen in greenhouse-gas balance in the atmosphere [2].

The Thomas-Fermi model was one of the first well-known attempts at a comprehensive theoretical model to describe quantum systems of electrons [3]. This model assumed that the system's kinetic energy term in the Hamiltonian was the same as that of a uniform electron gas. As might be expected, the model performed poorly when describing most quantum systems, including atoms and molecules, since the distribution of their electrons is far from uniform. The successor to the Thomas-Fermi model is density functional theory (DFT) which is regarded by many as the most well-known and accurate theoretical model that can predict the behaviour of quantum systems of electrons. DFT was originally formulated by Kohn and Sham in 1965 [4, 5]. Through the Hohenberg-Kohn theorems [6] and the theorems of DFT, it is proven that DFT is an exact theory; however, finding the exact form is difficult. Instead, approximations are made, and finding more accurate approximations of the theory is the central motivation for continued studies of DFT. The theme of DFT is that instead of using the many-body quantum wave function to describe the system and then solving the Schrödinger equation, a single-body electron density is used to describe the system, and then an eigenvalue equation or equivalent is solved. The advantage of this

method is that the single-body electron density is much easier to construct compared to the many-body wave function. As well, it provides an easy-to-implement approximation scheme that has been utilized since DFT's inception. In the Hamiltonian, for the multi-particle system, the kinetic energy term and potential energy term are approximated as their non-interacting counterparts, and all these ignored interactions are grouped into a third term called the exchange-correlation energy. The exchange-correlation energy only contributes a small fraction of the total energy of the system, and so will not significantly affect the accuracy of the calculations. If the exact exchange-correlation energy were to be found, it would make all DFT calculations exact. There is extensive research on determining its exact form, but it is yet to be found [3, 4]. The useful approximation method and the fact that DFT is exact in principle is what has given DFT its popularity as the most powerful computational tool for describing quantum systems of electrons.

There are two general approaches to DFT that take on different advantages and disadvantages. The first is Kohn-Sham density functional theory (KS-DFT), which sacrifices computational efficiency for improved accuracy [7]. This manifests in the use of artificial orbitals to describe the electron density instead of working with the electron density itself. The orbitals allow the non-interacting kinetic energy to be written exactly; however, the governing equation is an eigenvalue equation that needs to be solved for each electron in the system. The second is orbital-free density functional theory (OF-DFT), which takes the opposite approach and sacrifices accuracy for improved computational efficiency [8]. OF-DFT works with the electron density directly, and so the non-interacting kinetic energy must be approximated; however, only a single eigenvalue equation or equivalent must be solved for the entire system. So, in addition to searching for the exact exchange-correlation energy, OF-DFT also concerns itself with finding the exact non-interacting kinetic energy expressed with respect to the electron density directly.

Currently, KS-DFT has gained greater widespread use over OF-DFT due to its improved accuracy. However, if the exact non-interacting kinetic energy were to be found for OF-DFT, it would become the leading DFT theory overnight as it would be equally accurate but far more computationally efficient. For that reason, it is worth investigating and formulating different approaches to OF-DFT that might be able to solve the non-interacting kinetic energy problem, increase the accuracy of the approximations or provide an alternative perspective on the problem that could potentially lead to advancements in the future. One such proposal is the present theory, which uses an alternative approach to OF-DFT based on ideas from self-consistent field theory (SCFT). Proving that this theory can accurately model diatomic molecules is a great first step in validating its ability to predict molecular bonding and how the theory compares to other OF-DFT methods. Additionally, the theory offers an alternative ensemble perspective into constructing OF-DFT and offers

a comparison between classical and quantum mechanics.

1.2 Objectives

The OF-DFT theory presented here offers an alternative viewpoint, with the potential to provide more accurate results compared to other OF-DFT methods if a rigorous exchange-correlation energy is implemented, as the inexactness of the non-interacting kinetic energy has been pushed to the exchange-correlation energy. The alternative approach to OF-DFT is based on a statistical mechanics ensemble interpretation of DFT, compared to the usual formulation based on ideas from quantum mechanics. Additionally, the theorems of DFT are not used to construct the theory, but instead, ideas from polymer SCFT are used.

The advantage of polymer SCFT as the basis of this OF-DFT approach is that it provides readers who are familiar with SCFT the opportunity to understand the theory without previous knowledge of DFT. It also provides a comparison of the similarity between Gaussian distributed ring polymers in SCFT and quantum particles in DFT.

The primary objective of this research is to construct a representation of the current OF-DFT theory that can model a variety of quantum systems. Specifically, provide accurate quantitative results for the physical properties of homonuclear and heteronuclear diatomic molecules.

The secondary objective is to demonstrate that the current theory provides a more accurate model of diatomic molecules compared to other OF-DFT formulations that rely on basic approximations for the non-interacting kinetic energy. Specifically, demonstrating that the theory can model the correct electron density structure and predict molecular bonding.

To achieve these objectives, the alternative approach to OF-DFT is derived in its entirety, starting from basic concepts in quantum mechanics and statistical mechanics. This allows for all the differences from traditional DFT approaches to be examined, as well as identify the approximations made to construct the theory. How these differences and approximations affect the results when modelling diatomic molecules is also investigated.

1.3 Overview

The thesis consists of five chapters. Chapter 2 describes the foundational concepts that motivate this research. An overview of DFT is provided in section 2.2, where the Hohenberg-Kohn theorems are proven in subsection 2.2.1, the Kohn-Sham formulation of DFT is

constructed in subsection 2.2.2 and OF-DFT is constructed along with different approximations for the non-interacting kinetic energy term in subsection 2.2.3. A description of SCFT for Gaussian distributed polymers in an external field is given in section 2.3.

In chapter 3 the present theory on the alternative approach to OF-DFT is derived. Section 3.2, constructs the majority of the necessary equations needed to describe the theory, including the solution to the modified diffusion equation that governs the theory. Section 3.3 provides a description of the basis set necessary to model diatomic molecules. Section 3.4, investigates the spectral forms of the potentials and fields that are present in systems of diatomic molecules. Section 3.5 brings together all components of the theory to construct the Helmholtz free energy.

Chapter 4 investigates the results when modelling diatomic molecules using the present theory. Section 4.2 discusses the computational methods used to generate the physical properties of diatomic molecules. Section 4.3 examines the qualitative aspects of the calculated electron density contours for the diatomic molecules. Section 4.4 provides a summary of the bond lengths for the various diatomic molecules and quantitatively compares the results to known values. Section 4.5 briefly describes the calculation process for determining the bond dissociation energy and fundamental vibrational frequency of diatomic molecules using the current theory. Section 4.6 discusses the limitations of the theory and necessary steps to improve the results.

Chapter 5 gives concluding remarks on the modelling of diatomic molecules using the current implementation of the alternative approach to OF-DFT.

Chapter 2

Background

2.1 Introduction

Shortly after the discovery of quantum mechanics, in the early 20^{th} century, physicists were using it to theoretically study the characteristics of a variety of microscopic systems. This process was improved further, when Schrödinger published his eponymous equation in 1926 [9]. The Schrödinger equation gained widespread use in the physics community for its ability to describe the dynamics of any quantum system exactly. Although it is an extremely useful tool, for complex systems, solving the Schrödinger equation in a closed-form is typically not possible and even finding the solution can be difficult. Such as in the case of quantum systems of atoms or molecules, where the analytical Schrödinger equation solution exists only for the hydrogen atom. Directly finding the solution to the Schrödinger equation for atoms or molecules with more particles can be tedious, if not unsolvable. To avoid this complication, approximations are made to the Schrödinger equation or an approximate equivalent governing equation is used. One of the most primitive models for determining the properties of atoms and molecules that did not explicitly solve the Schrödinger equation, is the Thomas-Fermi model [3].

The Thomas-Fermi model allows the complicated electron wave function from the Schrödinger equation to be replaced with a much simpler electron density. It assumes that the electrons are uniformly distributed throughout phase space and so, as one would expect, does not give accurate results for atoms and molecules, as these systems are highly non-uniform. Regardless of the quantitative accuracy of the Thomas-Fermi model, it represents one of the earliest methods for replacing the wave function with the electron density and is often considered as the forerunner to the much more accurate, density functional

theory [3].

In 1964 and 1965, Hohenberg, Kohn and Sham [6, 5] greatly improved upon the Thomas-Fermi model and the idea that the many-body wave function can be replaced with a single-body electron density. They formulated an exact complete theory, density functional theory, that is equivalent to solving the Schrödinger equation. This allows for the study of complex quantum systems where solving the Schrödinger equation would be intractable. They showed that there exists an exact functional of the electron density that completely characterizes the quantum system, specifically the ground-state energy, and outlined a process for determining this density. Although they were unable to find the exact ground-state electron density, an approximation scheme and calculation process was demonstrated. The proof that there is an exact ground-state energy functional has been the driving force behind the advancement of DFT since its inception.

Improving upon the different approximations present when calculating the ground-state electron density in DFT has become a massive area of research and discussion in the physics community [4]. There is a wide array of different approaches and approximation methods for improving the accuracy, computational efficiency or providing a more in-depth understanding of the various functionals present in the theory. Each category of these improvements marches DFT forward, expanding its applicability in modelling and understanding a wider variety of quantum systems.

The chapter begins with an introduction to DFT, discussing the Hohenberg-Kohn theorems that form the foundation of DFT. The two popular approaches to DFT, Kohn-Sham and orbital-free, are then discussed. Following is an introduction to SCFT, specifically the theory of a Gaussian distributed polymer in an external field, which is relevant to the discussion on the alternative approach to OF-DFT presented in the theory chapter.

2.2 Density Functional Theory

2.2.1 Hohenberg-Kohn Theorems

The origins of DFT start with the seminal paper by Hohenberg and Kohn from 1964 [6], where the two fundamental theorems that form the basis of the theory are discussed. The overall theme of the theorems is that the total ground-state energy of a quantum system of electrons is uniquely determined by the electron density.

Consider the total energy of a quantum system of electrons that is a functional of the electron density, $E[n]$. The system is under the influence of an external potential and all the inter-electron interactions are still present. The total energy can be written as [3, 10]

$$E[n] = \int d\mathbf{r} n(\mathbf{r}) V_{ext}(\mathbf{r}) + G[n], \tag{2.1}$$

where $G[n]$ is the contribution of all the inter-electron interactions to the total energy and is also a functional of the electron density. $G[n]$ can be written as,

$$G[n] = K[n] + V_{ee}[n] \tag{2.2}$$

where $K[n]$ is the total kinetic energy and $V_{ee}[n]$ is the total Coulombic electron-electron interaction energy. It should be noted that the Hohenberg-Kohn theorems give no recipe for finding the functional forms of $K[n]$ and $V_{ee}[n]$ [3, 6].

In terms of operator notation, the total energy of the system can be rewritten as the expectation value of the Hamiltonian,

$$E = \langle \psi | \hat{H} | \psi \rangle = \langle \psi | \hat{V}_{ext} | \psi \rangle + \langle \psi | \hat{G} | \psi \rangle \,, \tag{2.3}$$

where $\hat{V}_{ext}$ and $\hat{G}$ are the operator forms of $V_{ext}(\mathbf{r})$ and, $G[n]$ respectively, before the expectation value has been taken and a basis chosen. To avoid obscuring the results when proving the theorems, the most basic case will be assumed, the ground-state energy of the system is non-degenerate.

Theorem 1: For a quantum system of electrons in an external potential, $V_{ext}(\mathbf{r})$, the ground-state electron density, $n_{GS}(\mathbf{r})$, uniquely determines $V_{ext}(\mathbf{r})$ to within a trivial additive constant [3, 6, 10].

Assume there is a ground-state electron density of the system, $n_{GS}(\mathbf{r})$, with an external potential, $\hat{V}_{ext,1}$, and a total ground-state energy, $E_1 = \langle \psi_1 | \hat{H}_1 | \psi_1 \rangle$, where ψ_1 is the wave function that is a ground-state energy eigenstate of the Hamiltonian, H_1. Now, assume there is another external potential, $\hat{V}_{ext,2}$, and another total ground-state energy, $E_2 = \langle \psi_2 | \hat{H}_2 | \psi_2 \rangle$, where ψ_2 is the wave function that is a ground-state energy eigenstate of the Hamiltonian, H_2, that leads to the same ground-state electron density, $n_{GS}(\mathbf{r})$. The total energy of these two states are,

$$E_1 = \langle \psi_1 | \hat{H}_1 | \psi_1 \rangle = \hat{V}_{ext,1} + \hat{G} \tag{2.4}$$

$$E_2 = \langle \psi_2 | \hat{H}_2 | \psi_2 \rangle = \hat{V}_{ext,2} + \hat{G}. \tag{2.5}$$

First, it needs to be proven that the two different external potentials that differ by more than a constant, lead to two different ground-state wave functions [3, 10]. Taking the difference of equations 2.4 and 2.5,

$$E_1 - E_2 = \langle\psi_1|\hat{H}_1|\psi_1\rangle - \langle\psi_2|\hat{H}_2|\psi_2\rangle = \langle\psi_1|\hat{V}_{ext,1}|\psi_1\rangle - \langle\psi_2|\hat{V}_{ext,2}|\psi_2\rangle\,. \tag{2.6}$$

Assume that the systems have the same ground-state wave function, $\psi_1 = \psi_2$, and since the operators are local, the wave functions can be dropped. So, equation 2.6 becomes,

$$E_1 - E_2 = \hat{V}_{ext,1} - \hat{V}_{ext,2}. \tag{2.7}$$

The difference in energies is a constant, so if these two external potentials are to have the same ground-state wave function they must differ only by a constant, proving the first part of the theorem. Thus, for every external potential, $\hat{V}_{ext}$, there is a corresponding unique wave function ψ.

The second part in proving the theorem relies on proof by contradiction and the variational principle that is given by,

$$E \leq \langle\psi|\hat{H}|\psi\rangle\,, \tag{2.8}$$

where E is the ground-state energy, H is the Hamiltonian and ψ is an arbitrary eigenstate of the Hamiltonian. It needs to be proven that if there are two different wave functions, they cannot lead to the same ground-state electron density [3, 10]. Start with the system of two different external potentials and different ground-state energies from before. Assume that, $\psi_1 \neq \psi_2$ but both wave functions have the same ground-state density $n_{GS}(\mathbf{r})$. Applying the variational principle,

$$\begin{aligned} E_1 < \langle\psi_2|\hat{H}_1|\psi_2\rangle &= \langle\psi_2|\hat{H}_2|\psi_2\rangle + \langle\psi_2|\hat{H}_1 - \hat{H}_2|\psi_2\rangle \\ E_1 &< E_2 + \int d\mathbf{r} n_{GS}(\mathbf{r})\left(V_{ext,1}(\mathbf{r}) - V_{ext,2}(\mathbf{r})\right), \end{aligned} \tag{2.9}$$

where the external potential has been written in the position basis with respect to ψ_2. Similarly,

$$E_2 < \langle \psi_1 | \hat{H}_2 | \psi_1 \rangle = \langle \psi_1 | \hat{H}_1 | \psi_1 \rangle + \langle \psi_1 | \hat{H}_2 - \hat{H}_1 | \psi_1 \rangle$$

$$E_2 < E_1 + \int d\mathbf{r} n_{GS}(\mathbf{r}) \left(V_{ext,2}(\mathbf{r}) - V_{ext,1}(\mathbf{r}) \right), \tag{2.10}$$

where the external potential has been written in the position basis with respect to ψ_1. In both sets of equations that use the variational principle, the external potential can be written in the same form, as both systems yield the same ground-state electron density. Now, summing equations 2.9 and 2.10,

$$E_1 + E_2 < E_1 + E_2. \tag{2.11}$$

Giving the desired contradiction, both systems with a different wave function cannot lead to the same ground-state electron density. Combining the results of both proofs, the theorem is proven, the electron density uniquely determines the external potential.

Theorem 2: The ground-state electron density can be determined from the ground-state total energy functional through the variation principle by varying only the electron density [3, 6, 10].

From the first Hohenberg-Kohn theorem, the total energy of a quantum system of electrons is a functional of the electron density, and therefore the eigenstate wave functions of the Hamiltonian are also a functional of the electron density. Using the variational principle, the total energy for an arbitrary eigenstate of the Hamiltonian obeys the relation,

$$E[n] = \langle\ \psi[n]\ |H|\ \psi[n]\ \rangle \geq E_{GS}[n_{GS}], \tag{2.12}$$

where the equality holds when $n(\mathbf{r}) = n_{GS}(\mathbf{r})$. The ground-state electron density can then be found by minimizing the total energy functional through variations of the electron density. The electron density that minimizes the total energy will be the ground-state electron density. A Lagrange multiplier is included in the total energy equation to enforce conservation of particle number. The variation of the total energy with respect to the electron density is,

$$\frac{\delta}{\delta n(\mathbf{r})} \left(E[n] - \mu \left(\int d\mathbf{r}' n(\mathbf{r}') - N \right) \right) = 0, \tag{2.13}$$

where μ is the Lagrange multiplier and N is the total number of electrons. Bringing through the functional derivative, equation 2.13 becomes,

$$\frac{\delta E[n]}{\delta n(\mathbf{r})} = \mu, \tag{2.14}$$

where the functional derivative, $\delta n(\mathbf{r}')/\delta n(\mathbf{r}) = \delta(\mathbf{r}' - \mathbf{r})$, has been used and the Lagrange multiplier, μ, corresponds to the chemical potential. The value that minimizes the variation of the total energy with respect to the electron density is the chemical potential, and from that condition the ground-state total energy can be determined.

The second Hohenberg-Kohn theorem has now been proven, and the path towards formulating a complete theory based on these theorems lies ahead.

2.2.2 Kohn-Sham Density Functional Theory

Following in the footsteps of Hohenberg and Kohn, in 1965 Kohn and Sham fully developed DFT [5, 6]. DFT is often regarded as the most accurate computational method for calculating the properties of complex quantum systems such as atoms, molecules, and periodic systems/solid-state lattices [3, 4]. This "original" approach to DFT is commonly known as Kohn-Sham DFT after the creators of the theory and is discussed in this section. Natural units are used throughout the section, $m_e = \hbar = e = \frac{1}{4\pi\epsilon_0} = 1$.

As mentioned above, the Hohenberg-Kohn theorems do not specify the functional forms of $K[n]$ and $V_{ee}[n]$, so the first step of the KS-DFT approach is determining these forms. Specifically, instead of directly finding the functional forms with respect to the electron density, a set of Slater determinant orthonormal orbitals Ψ_i are chosen, that are typically expressed in the position basis [7, 11]. The orbitals are related to the electron density by,

$$n(\mathbf{r}) = 2\sum_{i=1}^{N} |\Psi_i(\mathbf{r})|^2, \tag{2.15}$$

where the factor of 2 is included to account for the two electrons populating each orbital due to spin. Allowing only two electrons per orbital provides partial enforcement of the Pauli exclusion principle. To describe $K[n]$ and $V_{ee}[n]$ using orbitals, the kinetic energy is approximated as a kinetic energy for non-interacting electrons, and the electron-electron potential energy is approximated as a classical Coulomb potential energy. The non-interacting kinetic energy is,

$$K_0[n] = -\frac{1}{2}\sum_{i=1}^{N} 2\int d\mathbf{r}\Psi_i^*(\mathbf{r})\nabla^2\Psi_i(\mathbf{r}). \tag{2.16}$$

The Coulomb or Hartree potential energy is,

$$J[n] = \frac{1}{2}\int\int d\mathbf{r}d\mathbf{r}'\frac{n(\mathbf{r})n(\mathbf{r}')}{|\mathbf{r}-\mathbf{r}'|}, \tag{2.17}$$

where the factor $\frac{1}{2}$ is to correct for electron self-interactions. The errors made in approximating the kinetic energy and electron-electron potential energy are grouped into the exchange-correlation energy, $E_{XC}[n]$. The energy attributed to the Pauli exclusion principle is also grouped into $E_{XC}[n]$. The total energy of the system is,

$$E[n] = K_0[n] + J[n] + \int d\mathbf{r}n(\mathbf{r})V_{ext}(\mathbf{r}) + E_{XC}[n]. \tag{2.18}$$

The benefit of using the approximations $K_0[n]$ and $J[n]$ is that they are easily calculated, closed-form expressions and that $E_{XC}[n]$ only contributes a small part to the total energy [4].

Using the second Hohenberg-Kohn theorem, the ground-state energy of the system is determined through variational minimization of the total energy with respect to the electron density. Since the electron density is expressed in terms of orbitals, the ground-state can be equivalently determined through variation of the orbitals, specifically, Ψ_i^* [3]. In terms of Kohn-Sham functionals, the ground-state energy obeys the condition,

$$\begin{aligned}&\frac{\delta K_0[n]}{\delta\Psi_i^*(\mathbf{r})} + \frac{\delta J[n]}{\delta\Psi_i^*(\mathbf{r})} + \frac{\delta}{\delta\Psi_i^*(\mathbf{r})}\int d\mathbf{r}'n(\mathbf{r}')V_{ext}(\mathbf{r}') + \frac{\delta E_{XC}[n]}{\delta\Psi_i^*(\mathbf{r})}\\ &-\frac{\delta}{\delta\Psi_i^*(\mathbf{r})}2\sum_{j=1}^{N}\sum_{k=1}^{N}\epsilon_{jk}\left(\int d\mathbf{r}'\Psi_j^*(\mathbf{r}')\Psi_k(\mathbf{r}') - \delta_{jk}\right) = 0,\end{aligned} \tag{2.19}$$

where ϵ_{ij} is the Lagrange multiplier that enforces the orthonormality condition of the orbitals,

$$\int d\mathbf{r}\Psi_i^*(\mathbf{r})\Psi_j(\mathbf{r}) = \delta_{ij}. \tag{2.20}$$

The conservation of the number of particles is automatically enforced if the orbitals are orthonormal.

For functionals of the electron density directly, the chain rule is used when functionally differentiating,

$$\frac{\delta X[n]}{\delta \Psi_i^*(\mathbf{r})} = \sum_{j=1}^{N} \frac{\delta n(\mathbf{r})}{\delta \Psi_j^*} \cdot \frac{\delta \Psi_j^*}{\delta \Psi_i^*} \cdot \frac{\delta X[n]}{\delta n(\mathbf{r})} = 2\Psi_i(\mathbf{r}) \frac{\delta X[n]}{\delta n(\mathbf{r})}, \tag{2.21}$$

where $X[n]$ is an arbitrary functional of the electron density directly. The definition of the electron density in terms of orbitals, from equation 2.15, has been used to complete the chain rule identity. Expanding the functionals and taking the functional derivatives, equation 2.19 becomes,

$$-\frac{1}{2}\nabla^2\Psi_i(\mathbf{r}) + \left(\int d\mathbf{r} \frac{n(\mathbf{r})}{|\mathbf{r} - \mathbf{r}'|} \right) \Psi_i(\mathbf{r}) + V_{ext}(\mathbf{r})\Psi_i(\mathbf{r}) + \frac{\delta E_{XC}[n]}{\delta n(\mathbf{r})}\Psi_i(\mathbf{r}) - \sum_{j=1}^{N} \epsilon_{ij}\Psi_j(\mathbf{r}) = 0. \tag{2.22}$$

All the operators are Hermitian, and so the orbitals can be unitarily transformed into a basis diagonal in ϵ_{ij} [3]. The result is called the Kohn-Sham equation,

$$-\frac{1}{2}\nabla^2\Psi_i(\mathbf{r}) + V_{KS}(\mathbf{r})\Psi_i(\mathbf{r}) = \epsilon_{ij}\Psi_i(\mathbf{r}), \tag{2.23}$$

where $V_{KS}(\mathbf{r}) = \int d\mathbf{r} \frac{n(\mathbf{r})}{|\mathbf{r}-\mathbf{r}'|} + V_{ext}(\mathbf{r}) + \frac{\delta E_{XC}[n]}{\delta n(\mathbf{r})}$ and ϵ_{ij} are the Kohn-Sham orbital eigenvalues. Comparing 2.14 with 2.23, the maximum eigenvalue, ϵ_{max}, corresponds to the chemical potential, μ [3]. Other eigenvalues do not have a well-defined physical interpretation. The Kohn-Sham equation is the governing equation in KS-DFT, and the solution to the equation is the ground-state energy of the system.

The only contribution to the total energy that is yet to be determined is the exchanged correlation functional, $E_{XC}[n]$. In all approaches to DFT, the exchange-correlation functional must be approximated. There is extensive literature in finding the most accurate exchange-correlation functional [12]. A common yet simple approach for approximating $E_{XC}[n]$ is the local density approximation that assumes the exchange-correlation density effects are the same as a local uniform electron gas [5, 13]. The local-density approximation is,

$$E_{XC}^{LDA}[n] = -\frac{3}{4}\left(\frac{3}{\pi}\right)^{1/3}\int d\mathbf{r} n(\mathbf{r})^{4/3}. \tag{2.24}$$

There are more complicated approaches to determining the exchange-correlation functional, but they will not be discussed [12]. All components of Kohn-Sham DFT have been fully specified, and the ground-state total energy and electron density can be determined by self-consistently solving the Kohn-Sham equation.

2.2.3 Orbital-Free Density Functional Theory

Orbital-free DFT follows more closely the original spirit of the Hohenberg-Kohn theorems, as the total energy of the system is determined directly from the electron density. Since the electron density is the fundamental function of the theory, compared to the mathematically constructed orbitals in KS-DFT, there is no ambiguity in the physical meaning of any of the constants, variables, functions or functionals in the system [8, 14]. Specifically, the Kohn-Sham orbitals and their corresponding eigenvalues do not have a physical meaning in the quantum system they describe.

To determine the ground-state energy of the system in OF-DFT, a very similar procedure from KS-DFT is followed. However, since there are no orbitals, the non-interacting kinetic energy functional from KS-DFT cannot be used. Instead, the non-interacting kinetic energy must be approximated and be a functional of the electron density directly [15]. Additionally, since the Kohn-Sham orbitals partially enforce the Pauli exclusion principle, without them the full Pauli exclusion principle must be approximated and included in the non-interacting kinetic energy functional, exchange-correlation functional or as an additional term in the total energy functional [16].

There is extensive literature attempting to find the exact or most accurate non-interacting kinetic energy functional in OF-DFT [14]. It is important to note that the non-interacting kinetic energy is of the same magnitude as the total energy, as demonstrated through the virial theorem, and so the approximation scheme for the non-interacting kinetic energy has a significant effect on the accuracy of the theory [14].

The first attempt at approximating the kinetic energy was borrowed from the Thomas-Fermi model and assumes the kinetic energy of the system is the same as a uniform electron gas [8]. The Thomas-Fermi kinetic energy will be determined using the Sommerfeld model of electrons [17].

The derivation of the Thomas-Fermi kinetic energy is written independently; however, it should be noted that the derivation borrows on ideas from Ashcroft and Mermin [17].

Starting from the time-independent Schrödinger equation for a free particle with periodic boundary conditions, the Schrödinger equation is,

$$H\psi(\mathbf{r}) = -\frac{\hbar^2}{2m}\nabla^2\psi(\mathbf{r}) = E\psi(\mathbf{r}). \tag{2.25}$$

With solution,

$$\psi_{\mathbf{k}}(\mathbf{r}) = \frac{1}{\sqrt{V}}e^{i\mathbf{k}\cdot\mathbf{r}}. \tag{2.26}$$

where V is the volume of the box that the periodic boundary conditions need to satisfy, and

$$\mathbf{k} = \frac{2mE}{\hbar^2} \tag{2.27}$$

is a position-independent vector. The $1/\sqrt{V}$ factor is the normalization condition of the wave function. For a box of length L, the boundary conditions for the wave function is given by

$$\begin{aligned}\psi(x,y,z) &= \psi(x+L,y,z)\\ \psi(x,y,z) &= \psi(x,y+L,z)\\ \psi(x,y,z) &= \psi(x,y,z+L).\end{aligned} \tag{2.28}$$

For the boundary conditions to be satisfied, the wave function at the boundary must be

$$e^{ik_xL} = e^{ik_yL} = e^{ik_zL} = 1. \tag{2.29}$$

This only occurs if,

$$k_x = \frac{2\pi n_x}{L}, \quad k_y = \frac{2\pi n_y}{L}, \quad k_z = \frac{2\pi n_z}{L}, \tag{2.30}$$

where n_x, n_y, n_z are integers. Each k value must reside in a volume $\left(\frac{2\pi}{L}\right)^3$ and the number of k points in a volume Ω of k-space is

$$\frac{\Omega}{(2\pi/L)^3} = \frac{\Omega L^3}{8\pi^3}. \tag{2.31}$$

For a system of free electrons obeying the Pauli exclusion principle, two electrons will populate each k point in a structure that minimizes the energy of the system. The resulting configuration is a Fermi sphere with volume

$$\frac{4\pi k_F^3}{3}, \tag{2.32}$$

where k_F is the radius of the Fermi sphere and is the highest populated k point. The number of electrons in the Fermi sphere is

$$N = 2 \cdot \left(\frac{4\pi k_F^3}{3}\right)\left(\frac{L^3}{8\pi^3}\right) = \frac{k_F^3}{3\pi^2}V, \tag{2.33}$$

where $V = L^3$ and N is the number of electrons. The electron density of this configuration is

$$n = \frac{k_F^3}{3\pi^2}, \tag{2.34}$$

where n is the electron density. The energy of this system is the sum of all the electrons in the Fermi sphere. To determine the explicit form of the energy, the definition of $\mathbf{k}$ from equation 2.27 is used. The energy is,

$$E = 2 \cdot \frac{\hbar^2}{2m} \sum_{k \leq k_F} k^2. \tag{2.35}$$

Assuming the size of the system is macroscopic and so the spacing between k points is continuous, the sum can be approximated as an integral. The energy density is,

$$\frac{E}{V} = 2 \cdot \frac{\hbar^2}{2m} \int_{k<k_F} \frac{d\mathbf{k}}{8\pi^3} k^2 = \frac{\hbar^2 k_F^5}{10\pi^2 m}. \tag{2.36}$$

Substituting in the value of the electron density from equation 2.34 and setting $\hbar = m = 1$, the energy density takes the form of the Thomas-Fermi energy density,

$$\frac{E}{V} = \left(\frac{3}{10}\right)\left(3\pi^2\right)^{2/3} n^{5/3} = c_0 n^{5/3}. \tag{2.37}$$

where $c_0 = (3/10)\left(3\pi^2\right)^{2/3}$. The Thomas-Fermi kinetic energy is,

$$K_{TF} = \frac{3}{10}\left(3\pi^2\right)^{2/3} \int d\mathbf{r} n(\mathbf{r})^{5/3}. \tag{2.38}$$

Although the Thomas-Fermi kinetic energy takes a simple and easy to compute form, it is crude and does not accurately represent the physical characteristics of most quantum systems. Atoms and molecules have highly non-uniform electron densities and the Thomas-Fermi kinetic energy performs poorly in these cases, failing to predict atomic shell structure and molecular bonding [8, 14]. The use of the Thomas-Fermi kinetic energy is very limited in scope, and a more accurate non-interacting kinetic energy approximation would greatly improve the applicability of OF-DFT.

A well-known improvement to the Thomas-Fermi kinetic energy is the von Weizsäcker non-interacting kinetic energy functional, which includes gradients of the density and does not assume the kinetic energy of the system is the same as a uniform electron gas. To construct the von Weizsäcker functional, the orbitals from KS-DFT in equation 2.15 are used. The electron density for the individual orbitals will also be used,

$$n(\mathbf{r}) = 2\sum_{i=1}^{N} n_i(\mathbf{r}), \tag{2.39}$$

where $n_i(\mathbf{r})$ is the electron density of the individual orbitals. Applying the Laplacian operator to equation 2.15 and using the Hermitian property of the gradient operator,

$$\nabla^2 n(\mathbf{r}) = 2\sum_{i=1}^{N}\left(\Psi_i^*(\mathbf{r})\nabla^2\Psi_i(\mathbf{r}) + \nabla\Psi_i(\mathbf{r})\nabla\Psi_i^*(\mathbf{r})\right). \tag{2.40}$$

Integrating both sides of the equation with respect to, $\mathbf{r}$ it can be seen that the first term on the right-hand side is just the Kohn-Sham kinetic energy $K_0[n]$ from equation 2.16. Rearranging equation 2.40,

$$K_0[n] = -\frac{1}{4}\int d\mathbf{r}\nabla^2 n(\mathbf{r}) + \frac{1}{2}\int d\mathbf{r}\sum_{i=1}^{N}\nabla\Psi_i(\mathbf{r})\nabla\Psi_i^*(\mathbf{r}). \tag{2.41}$$

Multiplying each term in the sum by $n_i(\mathbf{r})$ in the numerator and denominator,

$$K_0[n] = -\frac{1}{4}\int d\mathbf{r}\nabla^2 n(\mathbf{r}) + \frac{1}{8}\int d\mathbf{r}\sum_{i=1}^{N}\frac{|\nabla n_i(\mathbf{r})|^2}{n_i(\mathbf{r})}. \tag{2.42}$$

The divergence theorem can be applied to the first term, that is, the integral over the Laplacian of the electron density,

$$K_0[n] = -\frac{1}{4}\oint d\mathbf{r}\nabla n(\mathbf{r}) + \frac{1}{8}\int d\mathbf{r}\sum_{i=1}^{N}\frac{|\nabla n_i(\mathbf{r})|^2}{n_i(\mathbf{r})}. \tag{2.43}$$

For quantum systems with finite extent, such as atoms and molecules, the gradient of the electron density approaches zero at large distances and so the surface integral is zero [8]. If the system under consideration only has one orbital or in the case of OF-DFT, all systems are considered to have only one "orbital", then the non-interacting kinetic energy functional is the von Weizsäcker functional and is given by,

$$K_{vW} = \frac{1}{8}\int d\mathbf{r}\frac{|\nabla n(\mathbf{r})|^2}{n(\mathbf{r})}. \tag{2.44}$$

The gradient-dependent electron density greatly improves the accuracy of the non-interacting kinetic energy in modelling quantum systems. Specifically, the von Weizsäcker functional is exact for two-electron systems and provides a better approximation for systems with quickly varying electron densities than the Thomas-Fermi functional. However, the von Weizsäcker functional does not provide accurate results for multi-orbital systems, such as most diatomic molecules [8]. In some cases, the sum of both the Thomas-Fermi and von Weizsäcker functionals are used as the non-interacting kinetic energy functional, and this combination does slightly improve the accuracy compared to the use of the individual functionals. However, this combination still does not address many of the fundamental issues present in these approximations.

There are many far more advanced and complicated approximations to the non-interacting kinetic energy that improve upon the von Weizsäcker functional that will not be discussed [8, 14, 15]. However, the Thomas-Fermi functional and von Weizsäcker functional are some of the most well-known non-interacting kinetic energy functionals and many of the more advanced methods contain or limit to these more basic functionals. It should be noted that the exact form of the non-interacting kinetic energy is yet to be discovered [15].

The ground-state energy and electron density in OF-DFT is determined in a similar process as KS-DFT, except the total energy is varied with respect to the electron density instead of the complex conjugate of the orbitals. The resulting equation is,

$$\frac{\delta K_{OF}[n]}{\delta n(\mathbf{r})} + \frac{1}{2}\int d\mathbf{r}\frac{n(\mathbf{r})}{|\mathbf{r}-\mathbf{r}'|} + V_{ext}(\mathbf{r}) + \frac{\delta E_{XC}[n]}{\delta n(\mathbf{r})} = \mu \tag{2.45}$$

where $K_{OF}[n]$ is the non-interacting kinetic energy functional of choice that is directly dependent on the electron density. Without the exact form of the non-interacting kinetic energy, OF-DFT is generally less accurate than KS-DFT, since, in addition to the exchange-correlation functional being approximated, the full Pauli potential and non-interacting kinetic energy must be approximated. The advantage to OF-DFT is that only a single governing equation (2.45) must be solved for the entire system, compared to KS-DFT where an eigenvalue equation (2.23) must be solved for each electron in the system [8, 14]. This represents an enormous computational advantage over KS-DFT, especially for systems with a large number of electrons.

The final frontier of DFT is finding the exact form of the exchange-correlation functional and, in the case of OF-DFT, finding the exact form of the non-interacting kinetic energy functional in terms of the electron density as well. If both functionals are found, DFT would be an exact theory, which would represent a significant leap forward in the computational modelling of quantum systems. If only the exact form of the non-interacting kinetic energy functional were to be found, OF-DFT would be the leading choice for DFT calculations as it would offer the same accuracy as KS-DFT but with a significant increase in computational efficiency.

2.3 Self-Consistent Field Theory for a Gaussian Polymer in an External Field

This section is written independently; however, it should be noted that this section borrows on ideas from Matsen [18].

The behaviour of a Gaussian distributed polymer chain melt in an external field is described by self-consistent field theory [18, 19]. For large molecular polymer chains, the microscopic behaviour of all the individual small molecule monomers is extremely difficult to characterize due to the sheer number of particles. However, if the macroscopic properties of the entire polymer are the only characteristics of interest, then many of the individual monomers segments can be grouped and averaged to form a larger segment, these segments are referred

to as coarse-grained segments. The advantage of coarse-graining polymers is that the complex position probability distributions of the individual monomers are grouped together and due to the central limit theorem these coarse-grained segments position probability distributions become Gaussian distributions [18]. This allows the macroscopic characteristics of the polymer to be calculated much more easily while still maintaining accuracy. The disadvantage of the coarse-graining process is that the individual microscopic characteristics of the polymer are lost. The Gaussian distributed coarse-grained segment position probability distribution is

$$\lim_{m\to\infty} p_m(\mathbf{r}) = \left(\frac{3}{2\pi a^2}\right)^{3/2} \exp\left(-\frac{3r^2}{2a^2}\right), \tag{2.46}$$

where a is the statistical length of the segment and m is the number of monomers constituting each coarse-grained segment. The statistical segment length is defined as $a = R_0 N^{-1/2} = bm^{1/2}$, where $R_0 = aN^{1/2}$ and b is a proportionality constant. $N = M/m$, where M is the total number of monomers constituting the polymer. Although the position probability distribution of the coarse-grained segment is only a Gaussian distribution at asymptotically large m, the approximation gives reasonable accuracy at finite m [18].

Consider a polymer chain in the presence of an external static field $w(\mathbf{r})$, assume the field varies slowly enough such that the chain can be divided into N Gaussian distributed coarse-grained segments of volume, ρ_0^{-1}, with the field being constant in the neighbourhood of each segment. The positional configuration of the coarse-grained segments are described by the function, $\mathbf{r}_c(s)$, where $0 \leq s \leq 1$ is the parameterization of the polymer backbone, such that equal intervals of s have the same molecular weight. The subscript c indicates that the position vector is referring to the polymer configuration. The energy of the coarse-grained polymer configuration in an interval, $s_1 \leq s \leq s_2$, is

$$\frac{E[\mathbf{r}_c; s_1, s_2]}{k_B T} = \int_{s_1}^{s_2} ds \left(\frac{3}{2a^2 N}|\mathbf{r}_c'(s)|^2 + w(\mathbf{r}_c(s))\right), \tag{2.47}$$

where $\mathbf{r}_c'(s)$ is the time derivative of the coarse-grained polymer configuration. The first term in the energy resembles a kinetic energy and comes from the Gaussian position probability distribution. The second term resembles a potential energy term and is the energy from the external field.

The partition function of the full polymer is important for characterizing the polymer's behaviour, as the partition function can be used to calculate macroscopic quantities of the system, such as average segment distribution and entropy. The full partition function will

now be constructed. Starting with the first sN segments of the coarse-grained polymer, this will be known as a polymer fragment, with $0 \leq s \leq 1$. The beginning of the fragment obeys, $\mathbf{r}_c(0) = \mathbf{r}_0$, and the end of the fragment obeys, $\mathbf{r}_c(s) = \mathbf{r}$. The energy of the fragment is $E[\mathbf{r}_c; 0, s]$, and its partition function with one of the fragment's ends fixed at $s = 0$ is

$$z(\mathbf{r}, \mathbf{r}_0, s) \propto \int \mathcal{D}\mathbf{r}_c \exp\left(-\frac{E[\mathbf{r}_c; 0, s]}{k_B T}\right) \delta(\mathbf{r}_c(0) - \mathbf{r}_0)\delta(\mathbf{r}_c(s) - \mathbf{r}). \tag{2.48}$$

The delta functions are included in the partition function to ensure the boundary conditions for the fragment ends are obeyed. The functional integral is over all fragment configurations, $\mathbf{r}_c(t)$, where $0 \leq t \leq s$. To transform the proportionality relation in equation 2.48 to an equality, a factor containing the kinetic energy and a functional integral over all the momenta of the monomers should be included. However, the form of the kinetic energy for the fragment allows the momenta to be integrated out and included as a proportionality factor in the partition function. To calculate the exact form of the proportionality factor, the exact degrees of freedom of all monomers in the fragment would be required, but during the coarse-graining process, this information is lost. Overall, the proportionality factor is not necessary to the form of the full partition function being constructed. So, equation 2.48 will be kept as a proportionality relation [18].

Due to the locality of the polymer fragment energy, the energy can be equivalently written as a superposition,

$$E[\mathbf{r}_c; 0, s] = E[\mathbf{r}_c; 0, t] + E[\mathbf{r}_c; t, s]. \tag{2.49}$$

This allows the partition function of the fragment to be written as a recursion relation, this is performed by using the superposition of energies along with inclusion of a delta function for the new coordinate $\mathbf{r}_1$ and then integrating over this new coordinate. The recursion relation is,

$$z(\mathbf{r}, \mathbf{r}_0, s) = \frac{1}{a^3 N^{3/2}} \int d\mathbf{r}_1 z(\mathbf{r}, \mathbf{r}_1, t) z(\mathbf{r}_1, \mathbf{r}_0, s - t) \tag{2.50}$$

where the constant factor $1/a^3 N^{3/2}$, is chosen to ensure the partition function is dimensionless and to assign a value to the proportionality factor. The value of the constant was chosen for convenience and does not have any physical meaning. The recursion relation describes the partition function for the polymer fragment of sN segments in terms of the partition function of two smaller fragments. For a fragment composed of zero segments, the recursion relation implies,

$$z(\mathbf{r}, \mathbf{r}_0, 0) = a^3 N^{3/2} \delta(\mathbf{r} - \mathbf{r}_0), \tag{2.51}$$

since the beginning and end of the chain should be at the same position for a fragment of zero length.

The task of finding the partition function for long fragments can be accomplished by solving the partition function for very short fragments and using the recursion relation to build up progressively longer fragments until the desired fragment length partition function is found. These very short fragments must have a partition function such that the field does not change over the length of the fragment, and so can be regarded as a constant. This partition function is $z(\mathbf{r}, \mathbf{r}_0, \epsilon)$ where ϵ is small and satisfies the constant field condition for the fragment length,

$$|\mathbf{r} - \mathbf{r}_0| \lesssim a(\epsilon N)^{1/2}. \tag{2.52}$$

For this small fragment partition function, the field adds a constant energy of $\epsilon w(\mathbf{r}) k_B T$ for each fragment configuration and so will not affect the position probability distribution of the fragment. Assuming that the position probability distribution obeys a Gaussian distribution as in equation 2.46, using the form of the partition function from equation 2.48, expanding the energy using equation 2.47 and discretizing the integrand, the small fragment partition function is,

$$z(\mathbf{r}, \mathbf{r}_0, \epsilon) \approx \left(\frac{3}{2\pi\epsilon}\right)^{3/2} \exp\left(-\frac{3\left|\mathbf{r} - \mathbf{r}_0\right|^2}{2a^2 N\epsilon} - \epsilon w(\mathbf{r})\right). \tag{2.53}$$

The small fragment partition function for ϵN segments is normalized such that in the limit $\epsilon \to 0$ it reduces to equation 2.51. The large fragment partition function can now be iteratively built up from the small partition function. Using equation 2.50, this relation is given by,

$$z(\mathbf{r}, \mathbf{r}_0, s + \epsilon) = \frac{1}{(a^2 N)^{3/2}} \int d\mathbf{r}_\epsilon z(\mathbf{r}, \mathbf{r} + \mathbf{r}_\epsilon, \epsilon) z(\mathbf{r} + \mathbf{r}_\epsilon, \mathbf{r}_0, s). \tag{2.54}$$

The condition in equation 2.52 indicates that $z(\mathbf{r} + \mathbf{r}_\epsilon, \mathbf{r}_0, s)$ needs to only be accurate for $|\mathbf{r}_\epsilon| \lesssim a(\epsilon N)^{1/2}$ and so, this partition function can be expanded in a Taylor series of $\mathbf{r}_\epsilon$ to second order,

$$z(\mathbf{r}, \mathbf{r}_0, s+\epsilon) = \frac{1}{(a^2N)^{3/2}} \int d\mathbf{r}_\epsilon z(\mathbf{r}, \mathbf{r}+\mathbf{r}_\epsilon, \epsilon) \left[1 + \mathbf{r}_\epsilon \cdot \nabla + \frac{1}{2}(\mathbf{r}_\epsilon \cdot \nabla)^2\right] z(\mathbf{r}, \mathbf{r}_0, s). \quad (2.55)$$

In this form and using equation 2.53, the integration over $\mathbf{r}_\epsilon$ can now be performed. Recognizing that the field term in the exponent can be factored out of the integral and that the integrand is simply a Gaussian over all space, the partition function is,

$$z(\mathbf{r}, \mathbf{r}_0, s+\epsilon) \approx \exp\left(\epsilon w(\mathbf{r})\right) \left(1 + \frac{a^2 N \epsilon}{6} \nabla^2\right) z(\mathbf{r}, \mathbf{r}_0, s). \quad (2.56)$$

Expanding $\exp\left(\epsilon w(\mathbf{r})\right)$ in a Taylor series and truncating the partition function expansion to first order in ϵ, the partition function is,

$$z(\mathbf{r}, \mathbf{r}_0, s+\epsilon) \approx \left[1 + \left(\frac{a^2 N}{6} \nabla^2 - w(\mathbf{r})\right) \epsilon\right] z(\mathbf{r}, \mathbf{r}_0, s). \quad (2.57)$$

Similarly, $z(\mathbf{r}, \mathbf{r}_0, s+\epsilon)$ can be directly expanded in a Taylor series of $s+\epsilon$ centered at s and truncated at first order in ϵ. The partition function for this expansion is,

$$z(\mathbf{r}, \mathbf{r}_0, s+\epsilon) = \left(1 + \epsilon \frac{\partial}{\partial s}\right) z(\mathbf{r}, \mathbf{r}_0, s). \quad (2.58)$$

Equating the Taylor series expanded partition functions from equations 2.57 and 2.58,

$$\frac{\partial}{\partial s} z(\mathbf{r}, \mathbf{r}_0, s) = \left(\frac{a^2 N}{6} \nabla^2 - w(\mathbf{r})\right) z(\mathbf{r}, \mathbf{r}_0, s). \quad (2.59)$$

The resulting modified diffusion equation is used to solve for $z(\mathbf{r}, \mathbf{r}_0, s)$.

Another important quantity of the coarse-grained segment polymer is the local or partial partition function for the polymer fragments with a free end at $s = 0$, this is given by,

$$z(\mathbf{r}, s) \propto \int \mathcal{D}\mathbf{r}_c \exp\left(-\frac{E[\mathbf{r}_c; 0, s]}{k_B T}\right) \delta\left(\mathbf{r}_c(s) - \mathbf{r}\right). \quad (2.60)$$

Equivalently, the partition function in equation 2.60, can be constructed from the partition function with both ends fixed, $z(\mathbf{r}, \mathbf{r}_0, s)$,

$$z(\mathbf{r}, s) = \frac{1}{(a^2 N)^{3/2}} \int d\mathbf{r}_0 z(\mathbf{r}, \mathbf{r}_0, s). \tag{2.61}$$

So, $z(\mathbf{r}, s)$ also satisfies the modified diffusion equation 2.59 as the differential operators are linear and can be moved inside or outside the integral. As well, equation 2.51 can be used to determine the $s = 0$ condition for equation 2.61,

$$z(\mathbf{r}, 0) = 1. \tag{2.62}$$

The partial partition function for a polymer fragment of $(1 - s)N$ segments with the end at $s = 1$ fixed, can be constructed in a similar way as $z(\mathbf{r}, \mathbf{r}_0, s)$. The complementary partition function is,

$$z^\dagger(\mathbf{r}, \mathbf{r}_0, s) \propto \int \mathcal{D}\mathbf{r}_c \exp\left(-\frac{E[\mathbf{r}_c; s, 1]}{k_B T}\right) \delta(\mathbf{r}_c(1) - \mathbf{r}_0)\delta(\mathbf{r}_c(s) - \mathbf{r}). \tag{2.63}$$

The condition when $s = 1$ can also be specified using a recursion relation for the complementary partition function,

$$z^\dagger(\mathbf{r}, \mathbf{r}_0, 1) = (a^2 N)^{3/2} \delta(\mathbf{r} - \mathbf{r}_0). \tag{2.64}$$

The modified diffusion equation for the complementary partition function can be constructed in an equivalent way as was done for the partition function,

$$\frac{\partial}{\partial s} z^\dagger(\mathbf{r}, \mathbf{r}_0, s) = -\left(\frac{a^2 N}{6}\nabla^2 - w(\mathbf{r})\right) z^\dagger(\mathbf{r}, \mathbf{r}_0, s). \tag{2.65}$$

As well, the local or partial complementary partition function for the polymer fragment with a free end at $s = 1$, can be constructed from the complementary partition function,

$$z^\dagger(\mathbf{r}, s) = \frac{1}{(a^2 N)^{3/2}} \int d\mathbf{r}_0 z^\dagger(\mathbf{r}, \mathbf{r}_0, s). \tag{2.66}$$

From equation 2.64, the partial complimentary partition function satisfies the following $s = 1$ condition,

$$z^\dagger(\mathbf{r}, 1) = 1. \tag{2.67}$$

The partition function for the complete coarse grained Gaussian distributed polymer in an external field can be constructed from the integral of the partial partition function and complementary partial partition function, where both ends of the polymer are free. The full partition function is,

$$Z[w] = \int d\mathbf{r} z(\mathbf{r}, s) z^{\dagger}(\mathbf{r}, s) \propto \int \mathcal{D}\mathbf{r}_c \exp\left(-\frac{E[\mathbf{r}_c; 0, 1]}{k_B T}\right) \tag{2.68}$$

The full partition function of a Gaussian distributed coarse-grained polymer in an external field has been determined. The procedure for determining the characteristics of the Gaussian distributed coarse-grained polymer in an external field and the resulting equations follow many of the same steps when deriving the alternative approach to OF-DFT in the theory chapter.

Chapter 3

Theory

3.1 Introduction

In quantum mechanics, determining the ground-state behaviour of stationary many-body systems is often approached using density functional theory [7]. The basis of the theory relies on the Hohenberg-Kohn theorems that prove the ground-state energy of a quantum system is a unique functional of the electron density [6]. The main objective of DFT then is to determine the ground-state electron density of the system. In DFT, the Hamiltonian is approximated as consisting of a non-interacting kinetic energy functional term, a non-interacting potential energy functional term and an exchange-correlation functional term that approximates the correlation characteristics of electrons and the exchange-statistics arising from the fermionic nature of electrons. Within the field, there are two well-established categories that the various approaches to DFT fall under, Kohn-Sham density functional theory and orbital-free density functional theory. The KS-DFT method uses a basis set of functions that are eigenfunctions of the Hamiltonian to solve an eigenvalue equation. The solution to the eigenvalue equation is used to calculate the ground-state electron density. This method generally provides very accurate results but suffers in computational efficiency as an eigenvalue equation must be solved for each electron [3]. In OF-DFT, the non-interacting kinetic energy functional must be approximated and from there the electron density is solved for directly [8]. The advantage, in comparison to KS-DFT, is only one eigenvalue equation or an equivalent governing equation needs to be solved for the entire system, providing computational efficiency. The disadvantage is the non-interacting kinetic energy functional in addition to the exchange-correlation functional must be approximated [20].

There has been extensive research in formulating various approaches to DFT in order to improve its accuracy, increase computational efficiency or provide a more profound insight into the theory [4]. Focusing on the OF-DFT approach and borrowing from the ideas of Feynman and Hibbs [21] on the mapping of classical mechanics to quantum mechanics, it can be shown that an isomorphism exists between SCFT and DFT. Furthermore, it can be shown that an isomorphism exists between 4-D Gaussian distributed ring polymers in thermal space and 3-D quantum particles. SCFT is used extensively in the study of polymers, with the governing equation being a modified diffusion equation that determines the characteristics of the polymer [18, 19]. The focus of this chapter is deriving an alternative approach to OF-DFT using concepts from SCFT and investigating the relationship between quantum particles and polymers. Specifically, using this SCFT based OF-DFT approach to determine the electron density and ground-state energy of a diatomic molecule.

The chapter begins with a derivation of the overall framework of theory, discussing the governing modified diffusion equation and other important equations and their similarities to the ideas of SCFT. The modified diffusion equation is then solved self-consistently using techniques from polymer SCFT. Lastly, the basis set dependent potentials and fields are calculated for diatomic molecules, allowing the electron density and free energy to be determined.

The overall derivation and self-consistent calculation process in the present theory was originally developed by Thompson [20, 22]. However, the theory was only implemented in atomic systems with a spherically symmetric basis set. The goal of the current approach is to improve the results of the initial implementation of the theory by modelling a more complex system, diatomic molecules, using a more advanced cylindrically symmetric basis set while still retaining the original self-consistent calculation process.

3.2 Self-Consistent Field Theory Equations

The overall goal is to construct an alternative approach to OF-DFT theory without the theorems of DFT, based on ideas from quantum mechanics, statistical mechanics and SCFT. This approach starts from "first principles" and is done in the canonical ensemble, contrary to the typically DFT approach where the grand canonical ensemble is used [23, 24]. The canonical ensemble allows for a more convenient derivation as in most cases the number of particles is known and so fixing the number of particles makes calculations easier. The derivation closely follows the work of Thompson [20, 22].

3.2.1 Mean Field Quantities

Consider a quantum system in the canonical ensemble with N identical indistinguishable particles, specifically electrons, of mass m, in a volume V and at temperature T. The quantum Hamiltonian in terms of the kinetic energy $\mathcal{K}$ and the potential energy $\mathcal{U}$ in position representation is,

$$\begin{aligned}\mathcal{H} &= \mathcal{K} + \mathcal{U} \\ &= -\frac{\hbar}{2m}\sum_{i=1}^{N}\nabla_i^2 + U(\{\mathbf{r}\}),\end{aligned} \tag{3.1}$$

where ∇_i^2 is acting on particle i at position $\mathbf{r}_i$ and the potential energy $U(\{\mathbf{r}\})$ acts on the set of all N particle positions $\{\mathbf{r}\} = \{\mathbf{r}_1, \mathbf{r}_2, ..., \mathbf{r}_N\}$. The quantum partition function in the canonical ensemble is given by,

$$Q_N(\beta) = \sum_i e^{-\beta E_i}, \tag{3.2}$$

where E_i are the energy states of the system and $\beta = 1/k_B T$ with k_B as the Boltzmann constant. As will be shown in appendix C, the quantum partition function can be written equivalently in classical form as,

$$Q_N(\beta) = \frac{1}{h^{3N}}\int\cdots\int d\{\mathbf{r}\}d\{\mathbf{p}\}e^{-\beta H}w(\{\mathbf{r}\},\{\mathbf{p}\},\beta), \tag{3.3}$$

where $\{\mathbf{p}\} = \{\mathbf{p}_1, \mathbf{p}_2, ..., \mathbf{p}_N\}$ is the set of all N particle momenta, $d\{\mathbf{r}\}$, $d\{\mathbf{p}\}$ is the integration over all positions and momenta respectively and H is the classical Hamiltonian that takes the usual form,

$$H = \sum_{i=1}^{N}\frac{\mathbf{p}_i}{2m} + U(\{\mathbf{r}\}). \tag{3.4}$$

A factor of $\frac{1}{N!}$ is missing in equation 3.3 as permutation arguments are ignored, this will be justified shortly. For a purely classical system $w(\{\mathbf{r}\},\{\mathbf{p}\},\beta) = 1$. From appendix C, it is shown that for quantum systems $w(\{\mathbf{r}\},\{\mathbf{p}\},\beta)$ must satisfy,

$$e^{-\beta\mathcal{H}}e^{\frac{i}{\hbar}\sum_i \mathbf{p}_i\cdot\mathbf{r}_i} = e^{-\beta H}e^{\frac{i}{\hbar}\sum_i \mathbf{p}_i\cdot\mathbf{r}_i}w(\{\mathbf{r}\},\{\mathbf{p}\},\beta)$$
$$\equiv F(\{\mathbf{r}\},\{\mathbf{p}\},\beta). \tag{3.5}$$

The function $w(\{\mathbf{r}\},\{\mathbf{p}\},\beta)$ can be written using an independent particle approximation with an exchange-correlation correction as

$$w(\{\mathbf{r}\},\{\mathbf{p}\},\beta) = g_{xc}(\{\mathbf{r}\},\beta)\prod_{i=1}^{N}\tilde{w}(\mathbf{r}_i,\mathbf{p}_i,\beta) \tag{3.6}$$

where $g_{xc}(\{\mathbf{r}\},\beta)$ includes all quantum correlations and exchange effects necessary to enforce the indistinguishability of quantum particles, including the $\frac{1}{N!}$ factor. Although, $\tilde{w}(\mathbf{r}_i,\mathbf{p}_i,\beta)$ already depends on β this can also be included in $g_{xc}(\{\mathbf{r}\},\beta)$ so that the exchange-correlation function can be rewritten in a convenient form,

$$g_{xc}(\{\mathbf{r}\},\beta) \equiv e^{-\beta U_{xc}(\{\mathbf{r}\})}. \tag{3.7}$$

Using equation 3.6, the quantum partition function can be written as,

$$Q_N(\beta) = \frac{1}{h^{3N}}\int\cdots\int d\{\mathbf{r}\}d\{\mathbf{p}\}e^{-\beta\tilde{H}}\prod_{i=1}^{N}\tilde{w}(\mathbf{r}_i,\mathbf{p}_i,\beta) \tag{3.8}$$

where $\tilde{H} = H + U_{xc}(\{\mathbf{r}\})$. Now the potentials can be rewritten in terms of a density operator [25] given by,

$$\hat{n}(\mathbf{r}) = \sum_{i=1}^{N}\delta(\mathbf{r}-\mathbf{r}_i). \tag{3.9}$$

Including U_{xc} with the other potential terms, the Hamiltonian can be written as,

$$\tilde{H} = \sum_{i=1}^{N}\frac{\mathbf{p}_i^2}{2m} + U[\hat{n}] \tag{3.10}$$

where the potentials are functionals of the density operator. Inserting the expanded form of $\tilde{H}$ back into the quantum partition function,

$$Q_N(\beta) = \frac{1}{h^{3N}} \int \cdots \int d\{\mathbf{r}\} d\{\mathbf{p}\} e^{-\beta U[\hat{n}]} \prod_{i=1}^{N} e^{-\beta \frac{\mathbf{p}_i^2}{2m}} \tilde{w}(\mathbf{r}_i, \mathbf{p}_i, \beta). \tag{3.11}$$

To proceed, the definition of the functional Dirac delta is used,

$$e^{-\beta U[\hat{n}]} = \int \mathcal{D}\mathcal{N} \delta[\mathcal{N} - \hat{n}] e^{-\beta U[\mathcal{N}]} \tag{3.12}$$

where $\mathcal{D}\mathcal{N} = \lim_{N\to\infty} \prod_{i=1}^{N} d\mathcal{N}_i$ [26] is the functional integral over the electron density $\mathcal{N}$. Inserting the functional Dirac delta into the quantum partition function gives,

$$Q_N(\beta) = \frac{1}{h^{3N}} \int \mathcal{D}\mathcal{N} \delta[\mathcal{N} - \hat{n}] e^{-\beta U[\mathcal{N}]} \int \cdots \int d\{\mathbf{r}\} d\{\mathbf{p}\} \prod_{i=1}^{N} e^{-\beta \frac{\mathbf{p}_i^2}{2m}} \tilde{w}(\mathbf{r}_i, \mathbf{p}_i, \beta). \tag{3.13}$$

The Fourier transform definition of the functional Dirac delta is,

$$\delta[\mathcal{N} - \hat{n}] = \int \mathcal{D}\mathcal{W} e^{\beta \int d\mathbf{r}' \mathcal{W}(\mathbf{r}', \beta)(\mathcal{N}(\mathbf{r}', \beta) - \hat{n}(\mathbf{r}'))} \tag{3.14}$$

where $\mathcal{W}(\mathbf{r}', \beta)$ is an arbitrary field. Investigating the exponent in equation 3.14 and using the definition of the density operator,

$$\begin{aligned}
\beta \int d\mathbf{r}' \mathcal{W}(\mathbf{r}', \beta)(\mathcal{N}(\mathbf{r}', \beta) - \hat{n}(\mathbf{r}')) &= \beta \int d\mathbf{r}' \mathcal{W}(\mathbf{r}', \beta) \mathcal{N}(\mathbf{r}', \beta) - \beta \int d\mathbf{r}' \mathcal{W}(\mathbf{r}', \beta) \hat{n}(\mathbf{r}') \\
&= \beta \int d\mathbf{r}' \mathcal{W}(\mathbf{r}', \beta) \mathcal{N}(\mathbf{r}', \beta) \\
&\quad - \beta \int d\mathbf{r}' \mathcal{W}(\mathbf{r}', \beta) \sum_{i=1}^{N} \delta(\mathbf{r}' - \mathbf{r}_i) \\
&= \beta \int d\mathbf{r}' \mathcal{W}(\mathbf{r}', \beta) \mathcal{N}(\mathbf{r}', \beta) - \beta \mathcal{W}(\mathbf{r}_i, \beta).
\end{aligned}$$

Inserting the simplified Fourier transform Dirac delta into the quantum partition function,

$$Q_N(\beta) = \frac{1}{h^{3N}} \int \mathcal{D}\mathcal{N} \int \mathcal{D}\mathcal{W} e^{-\beta U[\mathcal{N}] + \beta \int d\mathbf{r}' \mathcal{W}(\mathbf{r}',\beta)\mathcal{N}(\mathbf{r}',\beta)} \times \int \cdots \int d\{\mathbf{r}\} d\{\mathbf{p}\} \prod_{i=1}^{N} e^{-\beta H_{\text{eff}}(\mathbf{r}_i,\mathbf{p}_i)} \tilde{w}(\mathbf{r}_i,\mathbf{p}_i,\beta) \tag{3.15}$$

where $H_{\text{eff}}(\mathbf{r}_i,\mathbf{p}_i,\beta) = \frac{\mathbf{p}_i}{2m} + \mathcal{W}(\mathbf{r}_i,\beta)$.

A single particle quantum partition function subject to the effective Hamiltonian can be defined as,

$$Q(\beta) = \frac{1}{h^3} \int \int d\mathbf{r} d\mathbf{p} e^{-\beta H_{\text{eff}}(\mathbf{r},\mathbf{p},\beta)} \tilde{w}(\mathbf{r},\mathbf{p},\beta). \tag{3.16}$$

The single partition function is then substituted into the full partition function,

$$Q_N(\beta) = \int \mathcal{D}\mathcal{N} \int \mathcal{D}\mathcal{W} Q(\beta)^N e^{-\beta U[\mathcal{N}] + \beta \int d\mathbf{r}' \mathcal{W}(\mathbf{r}',\beta)\mathcal{N}(\mathbf{r}',\beta)}. \tag{3.17}$$

To evaluate the integrals, a saddle point approximation is implemented that takes the general form [27],

$$\int dx e^{f(x)} = \int dx e^{f(x_0) + \frac{1}{2}(x-x_0)^2 f''(x_0) + \ldots} \tag{3.18}$$

where $f(x)$ is an arbitrary function that has been Taylor expanded around the point x_0 that is defined to be a minimum point on the real axis of the function and so $f'(x) = 0$. The Taylor series is truncated at either the first term or the second term so that the function can be integrated trivially or as a Gaussian, respectively.

Moving on to using the saddle point approximation for the full quantum partition function, it is assumed that $\mathcal{W}(\mathbf{r}',\beta)$ and $\mathcal{N}(\mathbf{r}',\beta)$ will obtain minimum field and electron density values at $\omega(\mathbf{r}',\beta)$ and, $n(\mathbf{r}',\beta)$ respectively. These mean field values will be the values the functional Taylor series is expanded upon and since they are minimums the first order derivatives will be zero and the series will be truncated at the first term. Relabelling $\mathbf{r}'$ as $\mathbf{r}$ the quantum partition function is

$$Q_N(\beta) = Q(\beta)^N e^{-\beta U[n] + \beta \int d\mathbf{r} \omega(\mathbf{r},\beta) n(\mathbf{r},\beta)}. \tag{3.19}$$

The expression can still be considered exact if the classical correlations which are ignored in the mean-field approximation are included in the exchange-correlation potential.

With the fully simplified form of the quantum partition function, the Helmholtz free energy of the system can now be obtained using the partition function relation from the canonical ensemble, $F = -k_B T \ln Q_N(\beta)$, giving,

$$\frac{F[n,\omega]}{k_B T} = -N \ln Q(\beta) + \beta U[n] - \beta \int d\mathbf{r} \omega(\mathbf{r},\beta) n(\mathbf{r},\beta). \tag{3.20}$$

The expression for the mean fields can be found by taking the functional derivative with respect to the mean field particle density in the free energy,

$$\begin{aligned}
\frac{\delta F[n,\omega]/k_B T}{\delta n(\mathbf{r}',\beta)} = 0 &= \beta \frac{\delta U[n]}{\delta n(\mathbf{r}',\beta)} - \beta \int d\mathbf{r} \omega(\mathbf{r},\beta) \frac{\delta n(\mathbf{r},\beta)}{\delta n(\mathbf{r}',\beta)} \\
&= \beta \frac{\delta U[n]}{\delta n(\mathbf{r}',\beta)} - \beta \int d\mathbf{r} \omega(\mathbf{r},\beta) \delta(\mathbf{r}-\mathbf{r}') \\
&= \beta \frac{\delta U[n]}{\delta n(\mathbf{r}',\beta)} - \beta \omega(\mathbf{r}',\beta).
\end{aligned}$$

Relabelling $\mathbf{r}'$ as $\mathbf{r}$, the mean fields are,

$$\omega(\mathbf{r},\beta) = \frac{\delta U[n]}{\delta n(\mathbf{r},\beta)}. \tag{3.21}$$

The mean field particle density is found by taking the functional derivative of the mean fields in the free energy,

$$\begin{aligned}
\frac{\delta F[n,\omega]/k_B T}{\delta \omega(\mathbf{r}',\beta)} = 0 &= -N \frac{\delta \ln\left(Q(\beta)\right)}{\delta \omega(\mathbf{r}',\beta)} - \beta \int d\mathbf{r} \frac{\delta \omega(\mathbf{r},\beta)}{\delta \omega(\mathbf{r}',\beta)} n(\mathbf{r},\beta) \\
&= -\frac{N}{Q(\beta)} \frac{\delta Q(\beta)}{\delta \omega(\mathbf{r}',\beta)} - \beta \int d\mathbf{r} \delta(\mathbf{r}-\mathbf{r}') n(\mathbf{r},\beta) \\
&= -\frac{N}{Q(\beta)} \frac{\delta Q(\beta)}{\delta \omega(\mathbf{r}',\beta)} - \beta n(\mathbf{r}',\beta)).
\end{aligned}$$

Relabelling $\mathbf{r}'$ as $\mathbf{r}$, the mean field particle density is,

$$n(\mathbf{r},\beta) = -\frac{N}{\beta Q(\beta)}\frac{\delta Q(\beta)}{\delta\omega(\mathbf{r},\beta)}. \tag{3.22}$$

These equations can be fully solved once the potentials $U[n]$ of the system are specified.

3.2.2 Modified Diffusion Equation

Revisiting the single particle partition function, it will obey the same relation between the classical and quantum partition function from equation 3.3 that the full partition function obeyed,

$$\begin{aligned} e^{-\beta\mathcal{H}_{\mathrm{KS}}}e^{\frac{i}{\hbar}\mathbf{p}\cdot\mathbf{r}} &= e^{-\beta H_{\mathrm{eff}}}e^{\frac{i}{\hbar}\mathbf{p}\cdot\mathbf{r}}\tilde{w}(\mathbf{r},\mathbf{p},\beta) \\ &\equiv Vq(\mathbf{r},\mathbf{p},\beta) \end{aligned} \tag{3.23}$$

where $\mathcal{H}_{\mathrm{KS}} = -\frac{\hbar^2}{2m}\nabla^2 + \mathcal{W}(\mathbf{r},\beta)$ and the subscript "KS" indicates that this is the same operator as in the Kohn-Sham equations of KS-DFT. A volume factor has been included in the definition for convenience. $q(\mathbf{r},\mathbf{p},\beta)$ is used instead of $F(\{\mathbf{r}\},\{\mathbf{p}\},\beta)$ to distinguish between the single particle and multi-particle comparison of the quantum partition function in classical form. Differentiating the above equation with respect to β, the following relation is obeyed,

$$\frac{\partial q(\mathbf{r},\mathbf{p},\beta)}{\partial\beta} = \frac{\hbar^2}{2m}\nabla^2 q(\mathbf{r},\mathbf{p},\beta) - \mathcal{W}(\mathbf{r},\beta)q(\mathbf{r},\mathbf{p},\beta). \tag{3.24}$$

Using the mean field value for the fields, the modified diffusion equation is,

$$\frac{\partial q(\mathbf{r},\mathbf{p},\beta)}{\partial\beta} = \frac{\hbar^2}{2m}\nabla^2 q(\mathbf{r},\mathbf{p},\beta) - \omega(\mathbf{r},\beta)q(\mathbf{r},\mathbf{p},\beta) \tag{3.25}$$

with initial condition,

$$q(\mathbf{r},\mathbf{p},0) = Ve^{\frac{i}{\hbar}\mathbf{r}\cdot\mathbf{p}}. \tag{3.26}$$

The single-particle partition function is then,

$$Q(\beta) = \frac{1}{V^2}\frac{1}{h^3}\int\int d\mathbf{r}d\mathbf{p}q(\mathbf{r},\mathbf{p},\beta)q^*(\mathbf{r},\mathbf{p},0). \tag{3.27}$$

The modified diffusion equation 3.25, can be solved more easily if the momentum coordinates, $\mathbf{p}$, are Fourier transformed to position coordinates, $\mathbf{r}_0$, in $q(\mathbf{r},\mathbf{p},\beta)$. The Fourier transform is

$$q(\mathbf{r},\mathbf{p},\beta) = h^3\int d\mathbf{r}_0 e^{\frac{i}{\hbar}\mathbf{r}_0\cdot\mathbf{p}}q(\mathbf{r},\mathbf{r}_0,\beta). \tag{3.28}$$

Substituting the Fourier transformed expression into the modified diffusion equation,

$$\frac{\partial q(\mathbf{r},\mathbf{r}_0,\beta)}{\partial\beta} = \frac{\hbar^2}{2m}\nabla^2 q(\mathbf{r},\mathbf{r}_0,\beta) - \omega(\mathbf{r},\beta)q(\mathbf{r},\mathbf{r}_0,\beta) \tag{3.29}$$

with initial condition,

$$q(\mathbf{r},\mathbf{r}_0,0) = V\int d\mathbf{p}e^{-\frac{i}{\hbar}\mathbf{r}_0\cdot\mathbf{p}}e^{\frac{i}{\hbar}\mathbf{r}\cdot\mathbf{p}} = V\int d\mathbf{p}e^{\frac{i}{\hbar}(\mathbf{r}-\mathbf{r}_0)\cdot\mathbf{p}} = V\delta(\mathbf{r}-\mathbf{r}_0). \tag{3.30}$$

The modified diffusion equation can now be solved and takes the same form as the Kac-Feynman solution from appendix D [21, 28],

$$q(\mathbf{r},\mathbf{r}_0,\beta) = V\mathfrak{N}\int_{\mathbf{r}_0}^{\mathbf{r}}\mathcal{D}\mathbf{r}e^{\int_0^\beta d\tau\{-\frac{m}{2\hbar^2}\left|\frac{d\mathbf{r}(\tau)}{d\tau}\right|^2-\omega(\mathbf{r}(\tau))\}} \tag{3.31}$$

where $\mathfrak{N}$ is a normalization constant, $\mathcal{D}\mathbf{r} = \lim_{N\to\infty}\prod_{i=1}^{N-1}d\mathbf{r}_i$ and the solution describes the thermal trajectory of a quantum particle which acts as an imaginary time component. Another interpretation is that the solution describes the unnormalized probability of a particle at a high classical temperature ($\beta = 0$) known to be at position $\mathbf{r}_0$, being found at position $\mathbf{r}$ when at low quantum temperature ($\beta > 0$). The solution takes the same form as an imaginary time quantum propagator.

Using the Fourier transformed expression, $q(\mathbf{r},\mathbf{r}_0,\beta)$, The single particle partition function can be rewritten as,

$$Q(\beta) = \frac{1}{V^2}\frac{1}{h^3}\int\int d\mathbf{r}d\mathbf{p}q(\mathbf{r},\mathbf{p},\beta)q^*(\mathbf{r},\mathbf{p},0) = \frac{1}{V}\int\int\int d\mathbf{r}d\mathbf{p}d\mathbf{r}_0 e^{\frac{i}{\hbar}\mathbf{r}_0\cdot\mathbf{p}}q(\mathbf{r},\mathbf{r}_0,\beta)e^{-\frac{i}{\hbar}\mathbf{r}\cdot\mathbf{p}}$$
$$= \frac{1}{V}\int\int d\mathbf{r}d\mathbf{r}_0\delta(\mathbf{r}_0-\mathbf{r})q(\mathbf{r},\mathbf{r}_0,\beta)$$
$$Q(\beta) = \frac{1}{V}\int d\mathbf{r}q(\mathbf{r},\mathbf{r},\beta). \tag{3.32}$$

With the solution to the modified diffusion equation and the explicit form of the quantum partition function, the mean-field particle density can be further specified as

$$n(\mathbf{r},\beta) = -\frac{N}{\beta Q(\beta)}\frac{\delta Q(\beta)}{\delta\omega(\mathbf{r},\beta)}$$
$$= -\frac{1}{V}\frac{N}{\beta Q(\beta)}\int d\mathbf{r}\frac{\delta q(\mathbf{r},\mathbf{r},\beta)}{\delta\omega(\mathbf{r},\beta)}$$
$$= -\frac{n_0}{\beta Q(\beta)}(-\beta q(\mathbf{r},\mathbf{r},\beta))$$
$$n(\mathbf{r},\beta) = \frac{n_0}{Q(\beta)}q(\mathbf{r},\mathbf{r},\beta) \tag{3.33}$$

where $n_0 = \frac{N}{V}$ is the uniform electron density.

3.2.3 Spectral Solution to the Modified Diffusion Equation

To solve for the ground-state electron density in the present case of molecular systems, the fields, electron density and modified diffusion equation are numerically solved self-consistently. In a brute force approach, the limiting computational factor is the requirement of solving the modified diffusion equation for each position coordinate $\mathbf{r}_0$. This is extremely computationally expensive, however, following Matsen [18], these same equations can be solved spectrally for the same numerical cost as solving a single modified diffusion equation, allowing complicated three-dimensional systems to be studied with reasonable computation power. The spectral method expands spatially dependent functions in a superposition of infinite orthonormal basis functions, $\{f_i(\mathbf{r})\}$, that encode the symmetry of the system and are chosen to be eigenvalues of the Laplacian operator, the modified diffusion equation then becomes a separable differential equation. The basis functions obey the eigenvalue equation for the Laplacian,

$$\nabla^2 f_i(\mathbf{r}) = \lambda_i f_i(\mathbf{r}) \tag{3.34}$$

where λ_i are the eigenvalues of the Laplacian operator with respect to the basis set $\{f_i(\mathbf{r})\}$. The basis functions also obey an orthonormality condition,

$$\frac{1}{V}\int d\mathbf{r} f_i(\mathbf{r}) f_j(\mathbf{r}) = \delta_{ij}. \tag{3.35}$$

An arbitrary function of position can be expanded using the basis functions as,

$$g(\mathbf{r}) = \sum_i g_i f_i(\mathbf{r}). \tag{3.36}$$

So, instead of solving directly for $g(\mathbf{r})$ at every position, a finite number of coefficients g_i can be solved to achieve the desired accuracy of the calculation. Additionally, for functions of two spatial coordinates a bilinear spectral expansion in position can be performed,

$$g(\mathbf{r}, \mathbf{r}_0) = \sum_{ij} g_{ij} f_i(\mathbf{r}) f_j(\mathbf{r}_0). \tag{3.37}$$

With this method, the single-particle quantum partition function, $Q(\beta)$, is spectrally expanded,

$$\begin{aligned} Q(\beta) &= \frac{1}{V}\int d\mathbf{r} q(\mathbf{r}, \mathbf{r}, \beta) \\ &= \sum_{ij} q_{ij}(\beta) \frac{1}{V}\int d\mathbf{r} f_i(\mathbf{r}) f_j(\mathbf{r}) \\ Q(\beta) &= \sum_i q_{ii}(\beta). \end{aligned} \tag{3.38}$$

The electron density $n(\mathbf{r})$ can also be spectrally expanded on both sides of the equation,

$$\begin{aligned} n(\mathbf{r}, \beta) &= \frac{n_0}{Q(\beta)} q(\mathbf{r}, \mathbf{r}, \beta) \\ \sum_i n_i(\beta) f_i(\mathbf{r}) &= \frac{n_0}{Q(\beta)} \sum_{jk} q_{jk}(\beta) f_j(\mathbf{r}) f_k(\mathbf{r}). \end{aligned}$$

Multiplying both sides of the equation by $\frac{1}{V}$ and $f_l(\mathbf{r})$ then integrating over $\mathbf{r}$ and relabelling indices, the electron density is,

$$n_k(\beta) = \frac{n_0}{Q(\beta)} \sum_{ij} q_{ij}(\beta)\Gamma_{ijk} \tag{3.39}$$

where,

$$\Gamma_{ijk} = \frac{1}{V} \int d\mathbf{r} f_i(\mathbf{r}) f_j(\mathbf{r}) f_k(\mathbf{r}) \tag{3.40}$$

is the gamma tensor. The only unspecified quantities are the spectral coefficients, $q_{ij}(\beta)$, these can be determined by spectrally expanding the modified diffusion equation and solving the resulting differential equation using the relation,

$$q(\mathbf{r}, \mathbf{r}_0, \beta) = \sum_{ij} q_{ij}(\beta) f_i(\mathbf{r}) f_j(\mathbf{r}_0). \tag{3.41}$$

Substituting into the modified diffusion equation,

$$\begin{aligned} \sum_{ij} \frac{\partial q_{ij}(\beta)}{\partial \beta} f_i(\mathbf{r}) f_j(\mathbf{r}_0) = \frac{\hbar^2}{2m} \sum_{i'j'} q_{i'j'}(\beta)\lambda_{i'} f_{i'}(\mathbf{r}) f_{j'}(\mathbf{r}_0) \\ - \sum_{i''j''k} q_{i''j''}(\beta)\omega_k(\beta) f_{i''}(\mathbf{r}) f_{j''}(\mathbf{r}_0) f_k(\mathbf{r}) \end{aligned} \tag{3.42}$$

where $\omega_k(\beta)$ are the spectral components of the fields. Multiplying both sides of the equation by $\frac{1}{V^2}$, $f_n(\mathbf{r})$, $f_m(\mathbf{r}_0)$, integrating both sides with respect to $\mathbf{r}$ and $\mathbf{r}_0$ and relabelling indices, the resulting equation is,

$$\frac{\partial q_{ij}(\beta)}{\partial \beta} = \frac{\hbar^2}{2m} \sum_k \lambda_i \delta_{ik} q_{kj}(\beta) - \sum_{kl} \omega_l(\beta)\Gamma_{ikl} q_{kj}(\beta) = \sum_k A_{ik} q_{kj}(\beta) \tag{3.43}$$

where

$$A_{ik} = \frac{\hbar^2}{2m}\lambda_i \delta_{ik} - \sum_l w_l(\beta)\Gamma_{ikl}. \tag{3.44}$$

The solution to this set of separable differential equations is,

$$q_{ij}(\beta) = \sum_k q_{kj}(0) e^{\beta A_{ik}} \tag{3.45}$$

where $q_{kj}(0)$ are the spectral components of the initial conditions which can be determined by spectrally expanding $q(\mathbf{r}, \mathbf{r}_0, 0)$,

$$q(\mathbf{r}, \mathbf{r}_0, 0) = \sum_{ij} q_{ij}(0) f_i(\mathbf{r}) f_j(\mathbf{r}_0) = V\delta(\mathbf{r} - \mathbf{r}_0). \tag{3.46}$$

Using equation 3.46, both sides of the equation are multiplied by $\frac{1}{V^2}$, $f_k(\mathbf{r})$, $f_l(\mathbf{r}_0)$ and integrated over $\mathbf{r}$ and $\mathbf{r}_0$. Relabelling indices the initial condition is,

$$q_{kj}(0) = \delta_{kj}. \tag{3.47}$$

The simplified spectral solution to the modified diffusion equation is,

$$q_{ij}(\beta) = e^{\beta A_{ij}}. \tag{3.48}$$

The exponential of the matrix can be calculated by diagonalization. The equivalent diagonalized representation is

$$q_{ij}(\beta) = \sum_k P_{ik} e^{\beta \alpha_k} P_{kj} \tag{3.49}$$

where α_k are the eigenvalues of the matrix A and the columns of P are the normalized eigenvectors of A. The problem of solving a modified diffusion equation for every point in coordinate space has been reduced to finding the eigenvalues and eigenvectors of the matrix A for a finite basis set size, significantly reducing the computational cost when calculating the modified diffusion equation solution. The quantum propagator is solved iteratively using an appropriate basis set size until self-consistency and the desired accuracy has been achieved. Compared to other DFT approaches, only a single modified diffusion equation needs to be solved each cycle, compared to a single eigenvalue equation per cycle in OF-DFT or a set of N eigenvalue equations per cycle for KS-DFT [8, 14, 20].

3.3 Cylindrically Symmetric Basis Set

The present theory has already been demonstrated to be valid for atomic systems, as shown by Thompson [20, 22]. However, further validation of the theory can be achieved by determining the ensemble average electron densities of diatomic molecular systems. Using the electron density values, the free energy can be calculated and used to determine other useful properties of diatomic molecules such as the bond length, bond dissociation energy and the fundamental vibrational frequency. Some approaches to OF-DFT that utilize the Thomas-Fermi or Von Weizsäcker functional as the non-interacting kinetic energy term, do not provide accurate results for most diatomic molecules and so establishing the occurrence of bonding in the present theory will validate its applicability beyond basic OF-DFT approaches [3, 8].

As ensemble average electron densities of diatomic molecules possess cylindrical symmetry, a suitable basis set will encode this symmetry, specifically, cylindrical Bessel functions for the radial, r, coordinate and a Fourier series for the axial, z, coordinate. The angular, θ, coordinate does not need to be explicitly represented in the basis set, as ensemble averaging of the electron densities will remove any angular dependence in the density. The motivation for this approximation is from the structure of electron orbitals in diatomic molecules. If the ensemble configurations of all the molecular orbitals present in a diatomic molecule are averaged, the resulting molecular orbitals will be cylindrically symmetric, with the angular dependence vanishing. For example, visualizing an ensemble of σ and π molecular orbitals that are averaged over all the possible configurations. The resulting ensemble-averaged electron density of these σ and π molecular orbitals would be the same for all angles, and so the electron density has no angular dependence.

For a diatomic molecule inside a cylindrical box, the orthonormalized basis set is given by,

$$f_{0j}(r,z) = \frac{\sqrt{2}}{J_1(\gamma_{0,j})} J_0\left(\gamma_{0,j}\frac{r}{R}\right) \cdot \frac{1}{\sqrt{2}} \tag{3.50}$$

$$f_{(2i)j}(r,z) = \frac{\sqrt{2}}{J_1(\gamma_{0,j})} J_0\left(\gamma_{0,j}\frac{r}{R}\right) \cdot \cos\frac{2\pi(2i)z}{Z} \tag{3.51}$$

$$f_{(2i-1)j}(r,z) = \frac{\sqrt{2}}{J_1(\gamma_{0,j})} J_0\left(\gamma_{0,j}\frac{r}{R}\right) \cdot \sin\frac{2\pi(2i-1)z}{Z} \tag{3.52}$$

where J_0, J_1 are the zeroth and first order cylindrical Bessel functions respectively, $\gamma_{0,j}$ is the j^{th} zero of the zeroth order cylindrical Bessel function, R is the radius of the cylindrical

box going from 0 to R and Z is the height of the cylindrical box going from $-\frac{Z}{2}$ to $\frac{Z}{2}$. Box dimensions are chosen large enough so that the electron densities go to zero at the boundary. The volume of the cylindrical box is $V = \pi R^2 Z$. The basis functions are eigenfunctions of the Laplacian operator with corresponding eigenvalues,

$$\lambda_{0j} = -\left(\frac{\gamma_{0,j}}{R}\right)^2 \tag{3.53}$$

$$\lambda_{ij} = -\left(\frac{\gamma_{0,j}}{R}\right)^2 - \left(\frac{2\pi i}{Z}\right)^2. \tag{3.54}$$

The indices i, j in the basis functions and eigenvalues both start at one. The summary of the basis set derivation is provided in appendix A. The values for the gamma tensor are summarized in appendix B. Although the basis functions and eigenvalues depend on two indices, i for the r coordinate and j for the z coordinate, the two indices will be suppressed to only one index to avoid cumbersome notation and keep the generality of the derivation. The calculations for a single index are nearly identical to when both indices are used. The full two index form will be used when either the basis functions or eigenvalues need to be explicitly written.

3.4 Potentials and Fields

3.4.1 External Potential

Now that the basis set has been specified, the field spectral coefficients, $\omega_i(\beta)$, for diatomic molecule systems can be determined. The spectral field coefficients can be used to specify A_{ik}, solve for the quantum propagator spectral coefficients, $q_{ij}(\beta)$, and calculate the electron density spectral coefficients, $n_i(\beta)$.

The external field spectral coefficients, ω_i^{ext}, that are due to the Coulomb interaction between the nuclei and the electrons will be investigated. The Coulomb potential for this interaction is,

$$U^{ext}[n] = -\sum_k \int\int d\mathbf{r}d\mathbf{r}' n(\mathbf{r},\beta)\mathcal{V}(|\mathbf{r}-\mathbf{r}'|)\ {}^k\rho^{nuc}(\mathbf{r}') \tag{3.55}$$

where $\mathcal{V}(|\mathbf{r}-\mathbf{r}'|) = \frac{1}{4\pi\epsilon_0}\frac{1}{|\mathbf{r}-\mathbf{r}'|}$ is the Coulomb potential, ${}^k\rho^{nuc}(\mathbf{r}')$ is the charge density of the k^{th} nucleus and $\sum_k$ is the sum over the number of nuclei, in the case of diatomic

molecules, this number is two. The nuclei are treated as stationary point particles and can be displaced symmetrically about the origin along the z-axis without loss of generality, to represent different atomic distances. The nuclear charge density will be represented by a Dirac delta as,

$$ {}^{k}\rho(\mathbf{r})^{nuc} = {}^{k}N\delta(r)\delta(z - {}^{k}z^{nuc})\delta(\theta) \tag{3.56} $$

where ${}^{k}N$ is the electric charge of the k^{th} nucleus and ${}^{k}z^{nuc}$ is the position along the z-axis of the k^{th} nucleus, for the present case of diatomic molecules ${}^{1}z^{nuc} = -{}^{2}z^{nuc}$. Using equation 3.21, the mean field of the external potential is

$$ \begin{aligned} \omega^{ext}(\mathbf{r}'') = \frac{\delta U^{ext}[n]}{n(\mathbf{r}'', \beta)} &= -\sum_{k} \int \int d\mathbf{r} d\mathbf{r}' \delta(\mathbf{r} - \mathbf{r}'') \mathcal{V}(|\mathbf{r} - \mathbf{r}'|)\ {}^{k}\rho^{nuc}(\mathbf{r}') \\ &= -\sum_{k} \int d\mathbf{r}' \mathcal{V}(|\mathbf{r}'' - \mathbf{r}'|)\ {}^{k}\rho^{nuc}(\mathbf{r}'). \end{aligned} $$

Relabelling $\mathbf{r}''$ as $\mathbf{r}$,

$$ \omega^{ext}(\mathbf{r}) = -\sum_{k} \int d\mathbf{r}' \mathcal{V}(|\mathbf{r} - \mathbf{r}'|)\ {}^{k}\rho^{nuc}(\mathbf{r}'). \tag{3.57} $$

The external potential can now be written in terms of its respective field as,

$$ U^{ext}[n] = \int d\mathbf{r} n(\mathbf{r}, \beta) \omega^{ext}(\mathbf{r}). \tag{3.58} $$

Spectrally expanding the electron density and the field,

$$ U^{ext}[n] = \sum_{ij} \int d\mathbf{r} n_i(\beta) \omega_j^{ext} f_i(\mathbf{r}) f_j(\mathbf{r}). $$

Multiplying the numerator and denominator by V, the orthonormality condition can be used to write the external potential as,

$$ U^{ext}[n] = V \sum_{i} n_i(\beta) \omega_i^{ext} \tag{3.59} $$

where $n_i(\beta)$ are the spectral components of the electron density and ω_i^{ext} are the spectral components of the external field. To determine the values of ω_i^{ext}, equation 3.57 is written as a Poisson equation, since its current form is the same as the solution to the Poisson equation. This equivalence is most easily seen when investigating the solution of the Poisson equation for an arbitrary function. The Poisson equation is,

$$\nabla^2 g(\mathbf{r}) = f(\mathbf{r}) \tag{3.60}$$

where g and f are arbitrary functions. The solution to equation 3.60 is,

$$g(\mathbf{r}) = -\int d\mathbf{r}' \frac{f(\mathbf{r}')}{4\pi|\mathbf{r}-\mathbf{r}'|}. \tag{3.61}$$

Back to $\omega_i^{ext}(\mathbf{r})$, its Poisson equation is,

$$\nabla^2 \omega^{ext}(\mathbf{r}) = \sum_k \frac{1}{\epsilon_0}\, {}^k\rho^{nuc}(\mathbf{r}). \tag{3.62}$$

The surface terms arising from the boundary conditions of the cylindrical box in the Poisson equation are taken to be zero. However, the actual form of the surface term has not been determined and so could likely be non-zero. It is possible that the Poisson surface term is only dependent on the size of the box, and so will become less significant as the size of the box increases. As well, the Poisson surface term will only affect the free energy of the system in the form of an additive constant, since the box size is the same throughout the calculations, and the physical quantities of interest for diatomic molecular systems will not be affected by this constant shift in the free energy. Specifically, the physical quantities involve differences between free energy values, the curvature of the free energy at different atomic separations and the atomic separation where the free energy is at a minimum, these measurements correspond to bond dissociation energy, fundamental vibrational frequency and bond length respectively.

In equation 3.62, multiplying the numerator and denominator by 4π and using natural units for the rest of the chapter where $\frac{1}{4\pi\epsilon_0} = 1$, $\hbar = 1$ and $m_e = 1$, m_e is the mass of the electron and spectrally expanding $\omega^{ext}(\mathbf{r})$ and ${}^k\rho^{nuc}(\mathbf{r})$, the Poisson equation is,

$$\sum_i \omega_i^{ext} \nabla^2 f_i(\mathbf{r}) = \sum_{jk} 4\pi \ {}^k\rho_j^{nuc} f_j(\mathbf{r})$$
$$\sum_i \omega_i^{ext} \lambda_i f_i(\mathbf{r}) = \sum_{jk} 4\pi \ {}^k\rho_j^{nuc} f_j(\mathbf{r}).$$

Multiplying both sides of the equation by $\frac{1}{V}$, $f_l(\mathbf{r})$ and integrating with respect to $\mathbf{r}$,

$$\sum_i \omega_i^{ext} \lambda_i \frac{1}{V} \int d\mathbf{r} f_i(\mathbf{r}) f_l(\mathbf{r}) = \sum_{jk} 4\pi \ {}^k\rho_j^{nuc} \frac{1}{V} \int d\mathbf{r} f_j(\mathbf{r}) f_l(\mathbf{r})$$
$$\omega_l^{ext} = \sum_k 4\pi \ {}^k\rho_l^{nuc}$$

relabel index l as i,

$$\omega_i^{ext} = \sum_k \frac{4\pi \ {}^k\rho_i^{nuc}}{\lambda_i}. \tag{3.63}$$

The spectral form of the nuclear charge density now needs to be determined,

$${}^k\rho^{nuc}(\mathbf{r}) = {}^kN\delta(r)\delta(z - {}^kz^{nuc})\delta(\theta) = \sum_i {}^k\rho_i^{nuc} f_i(\mathbf{r}).$$

Multiplying the equation by $\frac{1}{V}$, $f_j(\mathbf{r})$ and integrating with respect to $\mathbf{r}$,

$$\frac{1}{V} \int d\mathbf{r} \ {}^kN\delta(r)\delta(z - {}^kz^{nuc})\delta(\theta) f_j(\mathbf{r}) = \sum_i {}^k\rho_i^{nuc} \frac{1}{V} \int d\mathbf{r} f_i(\mathbf{r}) f_j(\mathbf{r})$$
$$\frac{{}^kN}{V} f_j(0, {}^kz^{nuc}) = {}^k\rho_j^{nuc}.$$

Relabel index j as i

$${}^k\rho_i^{nuc} = \frac{{}^kN}{V} f_i(0, {}^kz^{nuc}). \tag{3.64}$$

The external potential is

$$\omega_i^{ext} = \sum_k \frac{4\pi\ {}^kN}{V} \frac{f_i(0, {}^kz^{nuc})}{\lambda_i}. \tag{3.65}$$

Expanding the basis functions and eigenvalues in explicit form,

$$\omega_{0j}^{ext} = -\sum_k \frac{4\pi\ {}^kN}{V} \frac{\sqrt{2}}{J_1(\gamma_{0,j})} \left(\frac{1}{\sqrt{2}} \cdot \frac{1}{\left(\frac{\gamma_{0,j}}{R}\right)^2} \right) \tag{3.66}$$

$$\omega_{(2i)j}^{ext} = -\sum_k \frac{4\pi\ {}^kN}{V} \frac{\sqrt{2}}{J_1(\gamma_{0,j})} \left(\cos\left(\frac{2\pi(2i)\ {}^kz^{nuc}}{Z} \right) \cdot \frac{1}{\left(\frac{\gamma_{0,j}}{R}\right)^2 + \left(\frac{2\pi(2i)}{Z}\right)^2} \right) \tag{3.67}$$

$$\omega_{(2i-1)j}^{ext} = -\sum_k \frac{4\pi\ {}^kN}{V} \frac{\sqrt{2}}{J_1(\gamma_{0,j})} \left(\sin\left(\frac{2\pi(2i-1)\ {}^kz^{nuc}}{Z} \right) \cdot \frac{1}{\left(\frac{\gamma_{0,j}}{R}\right)^2 + \left(\frac{2\pi(2i-1)}{Z}\right)^2} \right). \tag{3.68}$$

3.4.2 Electron-Electron Potential

There is another Coulomb interaction, the electron-electron potential, $U^{ee}[n]$,

$$U^{ee}[n] = \frac{1}{2} \int\int d\mathbf{r} d\mathbf{r}' n(\mathbf{r}, \beta) \mathcal{V}(|\mathbf{r} - \mathbf{r}'|) n(\mathbf{r}', \beta). \tag{3.69}$$

The factor of $\frac{1}{2}$ is for double counting of the electrons in the electron densities. The spectrally expanded form of the electron-electron field follows a similar derivation as the external field. Using 3.21 the electron-electron mean-field is

$$\begin{aligned}
\omega^{ee}(\mathbf{r}'', \beta) = \frac{\delta U^{ee}[n]}{\delta n(\mathbf{r}'')} &= \frac{1}{2} \int\int d\mathbf{r} d\mathbf{r}' \delta(\mathbf{r} - \mathbf{r}'') \mathcal{V}(|\mathbf{r} - \mathbf{r}'|) n(\mathbf{r}, \beta') \\
&+ \frac{1}{2} \int\int d\mathbf{r} d\mathbf{r}' n(\mathbf{r}, \beta) \mathcal{V}(|\mathbf{r} - \mathbf{r}'|) \delta(\mathbf{r}' - \mathbf{r}'') \\
&= \frac{1}{2} \int d\mathbf{r}' \mathcal{V}(|\mathbf{r}'' - \mathbf{r}'|) n(\mathbf{r}', \beta) \\
&+ \frac{1}{2} \int d\mathbf{r} n(\mathbf{r}, \beta) \mathcal{V}(|\mathbf{r} - \mathbf{r}''|).
\end{aligned}$$

Since the Coulomb potential only depends on the absolute value of the distance between particles, the order of the position vectors can be swapped without changing the potential. In the second term, $\mathbf{r}$ can be relabelled as $\mathbf{r}'$ and after that for the entire expression $\mathbf{r}''$ can be relabelled as $\mathbf{r}$. The electron-electron field is

$$\omega^{ee}(\mathbf{r},\beta) = \int d\mathbf{r}'\mathcal{V}(|\mathbf{r}-\mathbf{r}'|)n(\mathbf{r}',\beta). \tag{3.70}$$

Substituting the electron-electron field into the electron-electron potential,

$$U^{ee}[n] = \frac{1}{2}\int d\mathbf{r} n(\mathbf{r},\beta)\omega^{ee}(\mathbf{r},\beta). \tag{3.71}$$

Spectrally expanding,

$$U^{ee}[n] = \frac{1}{2}\sum_{ij}\int d\mathbf{r} n_i(\beta)\omega_j^{ee}(\beta)f_i(\mathbf{r})f_j(\mathbf{r})$$

multiplying the numerator and denominator by V, and using the orthogonality condition, the electron-electron potential is

$$U^{ee}[n] = \frac{V}{2}\sum_{i} n_i(\beta)\omega_i^{ee}(\beta). \tag{3.72}$$

To determine the explicit form of ω_i^{ee} the integral expression of $\omega^{ee}(\mathbf{r})$ is written as a Poisson equation. As before, the surface terms in the Poisson equation will be ignored.

$$\nabla^2\omega^{ee}(\mathbf{r},\beta) = -4\pi n(\mathbf{r},\beta) \tag{3.73}$$

Spectrally expanding,

$$\sum_i \omega_i^{ee}(\beta)\nabla^2 f_i(\mathbf{r}) = -4\pi\sum_j n_j(\beta)f_j(\mathbf{r})$$
$$\sum_i \omega_i^{ee}(\beta)\lambda_i f_i(\mathbf{r}) = -4\pi\sum_j n_j(\beta)f_j(\mathbf{r}).$$

Multiplying both sides of the equation by $\frac{1}{V}$, $f_k(\mathbf{r})$ and integrating with respect to $\mathbf{r}$,

$$\sum_i \omega_i^{ee}(\beta)\lambda_i \frac{1}{V}\int d\mathbf{r} f_i(\mathbf{r})f_k(\mathbf{r}) = -4\pi \sum_j n_j(\beta)\frac{1}{V}\int d\mathbf{r} f_j(\mathbf{r})f_k(\mathbf{r})$$
$$\omega_k^{ee}(\beta)\lambda_k = -4\pi n_k(\beta).$$

Relabel index k as i,

$$\omega_i^{ee}(\beta) = \frac{-4\pi n_i(\beta)}{\lambda_i}. \tag{3.74}$$

To correct for self-interactions in the electron-electron potential, a Fermi-Amaldi factor of $(N-1)/N$ is included in the field and potential. The Fermi-Amaldi factor is the only exchange-correlation effect considered, it will correct for electron self-interactions exactly for $N = 1$ and asymptotically large N. Although, the Fermi-Amaldi factor is often considered crude for most values of N, it is simple to implement and the calculated diatomic molecule properties can be compared to well-known sources to determine the effect of the correction. The complete two index form of the electron-electron field is

$$\omega_{0j}^{ee}(\beta) = \left(\frac{N-1}{N}\right)\frac{4\pi n_{ij}(\beta)}{\left(\frac{\gamma_{0,j}}{R}\right)^2} \tag{3.75}$$
$$\omega_{ij}^{ee}(\beta) = \left(\frac{N-1}{N}\right)\frac{4\pi n_{ij}(\beta)}{\left(\frac{\gamma_{0,j}}{R}\right)^2 + \left(\frac{2\pi i}{Z}\right)^2}. \tag{3.76}$$

3.4.3 Pauli Potential

The last field that needs to be determined is the mean-field of the Pauli potential and will incorporate the quantum Pauli exclusion principle. Considering quantum particles in the present theory are equivalently described as ring polymers, the current implementation of the Pauli potential will be based on the classical analog of the exclusion principle, the excluded volume. Ring polymers are paired to account for the spin of the electron, each pair is considered a distinct chemical species and a Dirac delta function energy penalty is applied to different chemical species of ring polymers attempting to occupy the same space. The Pauli potential will then depend on the electron densities of the electron pairs,

and the sum of all the pair electron densities will be the total electron density. Using these ideas, the Pauli potential is,

$$U^P[\{n\}] = \frac{1}{2}\sum_{\substack{ij \\ i\neq j}} \int\int d\mathbf{r}d\mathbf{r}' \ {}_in(\mathbf{r},\beta)\mathcal{V}_{xv}(\mathbf{r}-\mathbf{r}') \ {}_jn(\mathbf{r}',\beta) \tag{3.77}$$

where $\{n\}$ is the set of all electron pair densities, the summations are over the electron pairs, ${}_in(\mathbf{r},\beta)$ indicates the i^{th} pair electron density and $\mathcal{V}_{xv}(\mathbf{r}-\mathbf{r}')$ is the excluded volume interaction energy,

$$\mathcal{V}_{xv}(\mathbf{r}-\mathbf{r}') = g_0^{-1}\delta(\mathbf{r}-\mathbf{r}'). \tag{3.78}$$

g_0^{-1} is a constant that needs to be determined and gives the strength of the interaction with units inverse density of states. The form of the Pauli potential in equation 3.78 is an approximation, as the exact form is

$$\mathcal{V}_{xv}(\mathbf{r}(s)-\mathbf{r}'(s)) = g_0^{-1}\delta(\mathbf{r}(s)-\mathbf{r}'(s)) \tag{3.79}$$

where $\mathbf{r}(s)$ is a parameterized curve describing the path of the polymer-like quantum particle through 4-D thermal space. Specifically, s is the imaginary time parameter that describes the thermal trajectory of the particle from 0 to β. The potential in equation 3.79 only acts on pairs of particles in the same place *and* at the same imaginary time. This is in comparison to equation 3.78 that is a mean-field approximation and only acts on pairs of particles when they are in the same place regardless of their imaginary time thermal trajectory and so overestimates the strength of the Pauli potential. The approximated Pauli potential is used instead, as implementing the exact Pauli potential is difficult. The expanded Pauli potential is,

$$\begin{aligned} U^P[\{n\}] &= \frac{1}{2}\sum_{\substack{ij \\ i\neq j}} \int\int d\mathbf{r}d\mathbf{r}' \ {}_in(\mathbf{r},\beta)g_0^{-1}\delta(\mathbf{r}-\mathbf{r}') \ {}_jn(\mathbf{r}',\beta) \\ &= \frac{1}{2}\sum_{\substack{ij \\ i\neq j}} g_0^{-1}\int d\mathbf{r}' \ {}_in(\mathbf{r}',\beta) \ {}_jn(\mathbf{r}',\beta) \\ &= \frac{1}{2}\sum_{ij} g_{ij}^{-1}\int d\mathbf{r}' \ {}_in(\mathbf{r}',\beta) \ {}_jn(\mathbf{r}',\beta) \end{aligned}$$

where $g_{ij}^{-1} = (1 - \delta_{ij})g_0^{-1}$. Relabelling $\mathbf{r}'$ as $\mathbf{r}$, the Pauli potential is,

$$U^P[\{n\}] = \frac{1}{2}\sum_{ij} g_{ij}^{-1} \int d\mathbf{r}\ {}_i n(\mathbf{r},\beta)\ {}_j n(\mathbf{r},\beta). \tag{3.80}$$

The Pauli potential interaction between quantum particles should be universal, and so the constant g_0^{-1} should not be free. The value for g_0^{-1} can be found by comparing predictions to experimental results, and in doing so, no assumptions about the internal structure of the polymer-like quantum particles need to be made as the internal structure is not known. Another, more straightforward approach is to use theoretical results from well-accepted exact models. Specifically, comparing the present theories' Pauli potential to a uniform gas of quantum particles that only interact through the exclusion principle [17]. The energy density of this system of electrons is the Thomas-Fermi energy density,

$$\frac{U^P}{V} = c_0 n_0^{5/3} \tag{3.81}$$

where c_0 is a constant with value,

$$c_0 = \frac{3}{10}(3\pi^2)^{2/3}. \tag{3.82}$$

Using these same assumptions for the Pauli potential, and rephrasing it as an energy density, c_0 can be used to determine the value of g_0^{-1}. Taking the uniform density limit of 3.80,

$$\begin{aligned} U^P[\{n\}] &= \frac{1}{2}\sum_{ij} g_{ij}^{-1} \int d\mathbf{r}\ {}_i n_0\ {}_j n_0 \\ U^P[\{n\}] &= \frac{V}{2}\sum_{ij} g_{ij}^{-1}\, {}_i n_0\ {}_j n_0 \end{aligned} \tag{3.83}$$

where ${}_i n_0$ is the uniform electron density for the pair of electrons with density ${}_i n(\mathbf{r},\beta)$. Multiplying both sides by $\frac{1}{V}$ and explicitly writing the uniform densities as ${}_i n_0 = \frac{{}_i N}{V}$, where ${}_i N$ is the number of particles in the pair, either 0, 1 or 2, gives

$$\frac{U^P[\{n\}]}{V} = \frac{1}{2V^2}\sum_{ij} g_{ij}^{-1}\, {}_i N\ {}_j N. \tag{3.84}$$

Using the same assumption as in the Thomas-Fermi energy density, assume a large number of electrons and so all pairs can be approximated to have $N_i = 2$ without loss of generality,

$$\begin{aligned}\frac{U^P[\{n\}]}{V} &= \frac{4}{2V^2}\sum_{ij} g_{ij}^{-1} \\ \frac{U^P[\{n\}]}{V} &= \frac{2g_0^{-1}}{V^2}\left(\frac{N^2}{4} - \frac{N}{2}\right)\end{aligned} \tag{3.85}$$

where N is the total number of electrons and each sum is over pairs containing two electrons and the number of terms in each sum is $\frac{N}{2}$ terms. For a large number of electrons, the $\frac{N}{2}$ term can be ignored as $N^2 >> N$. The uniform Pauli potential energy density is,

$$\frac{U^P[\{n\}]}{V} = \frac{g_0^{-1}}{2}n_0^2. \tag{3.86}$$

Comparing the Pauli potential energy density to the Thomas-Fermi energy density, they differ by a factor of $n_0^{1/3}$ and it may appear that the excluded volume type Pauli potential is inconsistent with the Pauli exclusion principle. Another approach that avoids the mean-filed approximation uses polymer scaling theory to show that the excluded volume Pauli potential correctly scales with the density [22]. The $n_0^{1/3}$ discrepancy could be accounted for by correlation corrections to the Pauli potential, but diatomic molecular systems do not necessarily have a large number of electrons and are not uniform in their electron density. As such, correlation corrections to the Pauli potential will not be explored.

Keeping with the uniform limit mean field approach of the Pauli potential, c_0 can be used to determine the value of g_0^{-1}, assuming both the Thomas-Fermi energy density and Pauli potential energy density have the same factor. Equating factors,

$$g_0^{-1} = 2c_0 = \frac{3}{5}(3\pi^2)^{2/3} \approx 5.742468. \tag{3.87}$$

With the value of the constant g_0^{-1} determined, the heterogeneous Pauli potential in 3.80 can be revisited to determine its mean field description. Using 3.21, the Pauli mean field is

$$
\begin{aligned}
{}_k\omega^P(\mathbf{r}',\beta) = \frac{\delta U^P[\{n\}]}{\delta\ {}_k n(\mathbf{r}',\beta)} &= \frac{1}{2}\sum_{\substack{ij\\ i\neq j}} g_0^{-1}\int d\mathbf{r}\delta_{ik}\delta(\mathbf{r}-\mathbf{r}')\ {}_j n(\mathbf{r},\beta) \\
&\quad + \frac{1}{2}\sum_{\substack{ij\\ i\neq j}} g_0^{-1}\int d\mathbf{r}\ {}_i n(\mathbf{r},\beta)\delta_{jk}\delta(\mathbf{r}-\mathbf{r}') \\
{}_k\omega^P(\mathbf{r}',\beta) &= \frac{1}{2}g_0^{-1}\sum_{j\neq k}\ {}_j n(\mathbf{r}',\beta) + \frac{1}{2}g_0^{-1}\sum_{i\neq k}\ {}_i n(\mathbf{r}',\beta).
\end{aligned}
$$

Since both sums are separate, the sum indices can be relabelled to an identical index, j without changing the result, relabel the k index as i and relabel $\mathbf{r}'$ to $\mathbf{r}$. The Pauli field is

$$
{}_i\omega^P(\mathbf{r},\beta) = g_0^{-1}\sum_{j\neq i}\ {}_j n(\mathbf{r},\beta). \tag{3.88}
$$

The Pauli field can be used to write the Pauli potential as,

$$
U^P[\{n\}] = \frac{1}{2}\sum_i \int d\mathbf{r}\ {}_i n(\mathbf{r},\beta)\ {}_i\omega^P(\mathbf{r},\beta). \tag{3.89}
$$

Multiplying the numerator and denominator by V and spectrally expanding, the Pauli potential is

$$
U^P[\{n\}] = \frac{V}{2}\sum_i\sum_{jk}\ {}_i n_j(\beta)\ {}_i\omega_k^P(\beta)\frac{1}{V}\int d\mathbf{r} f_j(\mathbf{r})f_k(\mathbf{r}).
$$

Using the orthonormality condition,

$$
U^P[\{n\}] = \frac{V}{2}\sum_i\sum_j\ {}_i n_j(\beta)\ {}_i\omega_j^P(\beta). \tag{3.90}
$$

To determine ${}_i\omega_j^P$, the expression for ${}_i\omega^P(\mathbf{r})$ can be spectrally expanded,

$$
\sum_k {}_i\omega_k^P(\beta)f_k(\mathbf{r}) = g_0^{-1}\sum_{j\neq i}\sum_l\ {}_j n_l(\beta)f_l(\mathbf{r}).
$$

Multiplying both sides by $\frac{1}{V}$, $f_m(\mathbf{r})$ and integrating with respect to $\mathbf{r}$,

$$\sum_k {}_i\omega_k^P(\beta)\frac{1}{V}\int d\mathbf{r} f_k(\mathbf{r})f_m(\mathbf{r}) = g_0^{-1}\sum_{j\neq i}\sum_l {}_jn_l(\beta)\frac{1}{V}\int d\mathbf{r} f_l(\mathbf{r})f_m(\mathbf{r})$$
$${}_i\omega_m^P(\beta) = g_0^{-1}\sum_{j\neq i} {}_jn_m(\beta).$$

Relabel index m as k, the Pauli field spectral form is

$${}_i\omega_k^P(\beta) = g_0^{-1}\sum_{j\neq i} {}_jn_k(\beta). \tag{3.91}$$

3.4.4 Nuclei Potential

All the fields under consideration have been fully specified. However, there is one last potential that does not have a corresponding field but needs to be determined for a diatomic molecular system, the Coulomb potential between the nuclei of the atoms, U^{nuc}. There is no corresponding field for the nuclei potential, as it does not depend on the electron density. U^{nuc} is given by,

$$U^{nuc} = \int d\mathbf{r}d\mathbf{r}' \; {}^1\rho^{nuc}(\mathbf{r})\mathcal{V}(|\mathbf{r}-\mathbf{r}'|) \; {}^2\rho^{nuc}(\mathbf{r}'). \tag{3.92}$$

Expanding the nuclear charge densities,

$$U^{nuc} = \int\int d\mathbf{r}d\mathbf{r}' \; {}^1N\delta(r)\delta(z-{}^1z^{nuc})\delta(\theta)\mathcal{V}(|\mathbf{r}-\mathbf{r}'|) \; {}^2N\delta(r')\delta(z'-{}^2z^{nuc})\delta(\theta')$$
$$U^{nuc} = {}^1N\mathcal{V}(|{}^1z^{nuc}-{}^2z^{nuc}|) \; {}^2N.$$

The nuclei potential is

$$U^{nuc} = \frac{{}^1N \; {}^2N}{|{}^1z^{nuc}-{}^2z^{nuc}|}. \tag{3.93}$$

It is not necessary to spectrally expand U^{nuc} as all the real space quantities in equation 3.93 are already known and can be easily computed.

It can be easily shown that the nuclei field is zero,

$$\omega^{nuc}(\mathbf{r},\beta) = \frac{\delta U^{nuc}}{\delta n(\mathbf{r},\beta)} = 0. \tag{3.94}$$

3.5 Helmholtz Free Energy

All the potentials and fields have been fully specified and the expanded form of the Helmholtz free energy can be established. To incorporate ideas of electron pairs into the free energy, the first term can be equivalently written, $(N/\beta)\ln Q(\beta) = \sum_i ({}_iN/\beta)\ln {}_iQ(\beta)$. The Helmholtz free energy is,

$$\begin{aligned}
F[n,w] &= -\sum_i \frac{{}_iN}{\beta}\ln {}_iQ(\beta) + U^{ext}[n] + U^{ee}[n] + U^P[\{n\}] + U^{nuc} \\
&\quad - \int d\mathbf{r}\omega^{ext}(\mathbf{r})n(\mathbf{r},\beta) - \int d\mathbf{r}\omega^{ee}(\mathbf{r},\beta)n(\mathbf{r},\beta) - \sum_i \int d\mathbf{r}\ {}_i\omega^P(\mathbf{r},\beta)\ {}_in(\mathbf{r},\beta) \\
&= -\sum_i \frac{{}_iN}{\beta}\ln {}_iQ(\beta) + \frac{{}^1N\ {}^2N}{|{}^1z^{nuc} - {}^2z^{nuc}|} \\
&\quad + \int d\mathbf{r}\omega^{ext}(\mathbf{r})n(\mathbf{r},\beta) + \frac{1}{2}\int d\mathbf{r}\omega^{ee}(\mathbf{r},\beta)n(\mathbf{r},\beta) + \frac{1}{2}\sum_i \int d\mathbf{r}\ {}_i\omega^P(\mathbf{r},\beta)\ {}_in(\mathbf{r},\beta) \\
&\quad - \int d\mathbf{r}\omega^{ext}(\mathbf{r})n(\mathbf{r},\beta) - \int d\mathbf{r}\omega^{ee}(\mathbf{r},\beta)n(\mathbf{r},\beta) - \sum_i \int d\mathbf{r}\ {}_i\omega^P(\mathbf{r},\beta)\ {}_in(\mathbf{r},\beta).
\end{aligned}$$

Simplifying, the free energy is

$$\begin{aligned}
F[n,w] &= -\sum_i \frac{{}_iN}{\beta}\ln {}_iQ(\beta) + \frac{{}^1N\ {}^2N}{|{}^1z^{nuc} - {}^2z^{nuc}|} \\
&\quad - \frac{1}{2}\int d\mathbf{r}\omega^{ee}(\mathbf{r},\beta)n(\mathbf{r},\beta) - \frac{1}{2}\sum_i \int d\mathbf{r}\ {}_i\omega^P(\mathbf{r},\beta)\ {}_in(\mathbf{r},\beta).
\end{aligned} \tag{3.95}$$

Spectrally expanding the fields,

$$F[n,w] = -\sum_i \frac{{}_iN}{\beta} \ln {}_iQ(\beta) + \frac{{}^1N\ {}^2N}{|{}^1z^{nuc} - {}^2z^{nuc}|}$$
$$- \frac{1}{2}\sum_{jk} \int d\mathbf{r}\omega_j^{ee}(\beta) n_k(\beta) f_j(\mathbf{r}) f_k(\mathbf{r}) - \frac{1}{2}\sum_i \sum_{jk} \int d\mathbf{r}\ {}_i\omega_j^P(\beta)\ {}_in_k(\beta)\ {}_if_j(\mathbf{r})\ {}_if_k(\mathbf{r}).$$

Multiplying the numerator and denominator of both field terms by V and integrating, the spectral field expansion of the free energy is

$$F[n,w] = -\sum_i \frac{{}_iN}{\beta} \ln {}_iQ(\beta) + \frac{{}^1N\ {}^2N}{|{}^1z^{nuc} - {}^2z^{nuc}|} - \frac{V}{2}\sum_j \left(\omega_j^{ee}(\beta) n_j(\beta) + \sum_i\ {}_i\omega_j^P(\beta)\ {}_in_j(\beta) \right). \tag{3.96}$$

The external field, w^{ext}, does not appear in the free energy expression as it does not explicitly depend on the electron density and so is cancelled out by the external potential.

Chapter 4

Diatomic Molecules

4.1 Introduction

The characteristics of diatomic molecules are calculated using the present theory, an alternative approach to OF-DFT based on ideas from SCFT. All homonuclear diatomic molecules composed of atomic pairs in the first two rows of the periodic table were investigated. Two heteronuclear diatomic molecules that are known to be stable under common conditions were also investigated. The electron density contours and bond lengths for all the diatomic molecules that exhibited bonding are presented and compared to known results. The bond dissociation energy and fundamental vibrational frequency for the hydrogen molecule are also compared. The free energy at different atomic separations for the hydrogen molecule is shown. The computational methods used to calculate the physical properties of the diatomic molecules are described.

Demonstrating the ability of the present theory to predict molecular bonding and calculate the physical properties of diatomic molecules is a fundamental step in validating the usefulness of the theory. It proves that the electron density structure emulates the physical system more closely than other OF-DFT theories that implement the Thomas-Fermi functional or Von Weizsäcker functional as their non-interacting kinetic energy functional since both functionals are inaccurate for multi-orbital systems, such as most diatomic molecules [8]. It will also demonstrate that a wider variety of quantum systems can be investigated in the future with the expectation that the theory will give reasonable results. Some of these systems may be larger molecules or solid-state lattices, where OF-DFT is commonly implemented [29, 30, 31].

The calculation results for diatomic molecules presented in this chapter using the present

theory with a cylindrically symmetric basis set were performed independently.

4.2 Computational Methods

The method for determining the electron density that gives the ground-state free energy of the system was performed computationally in Python.

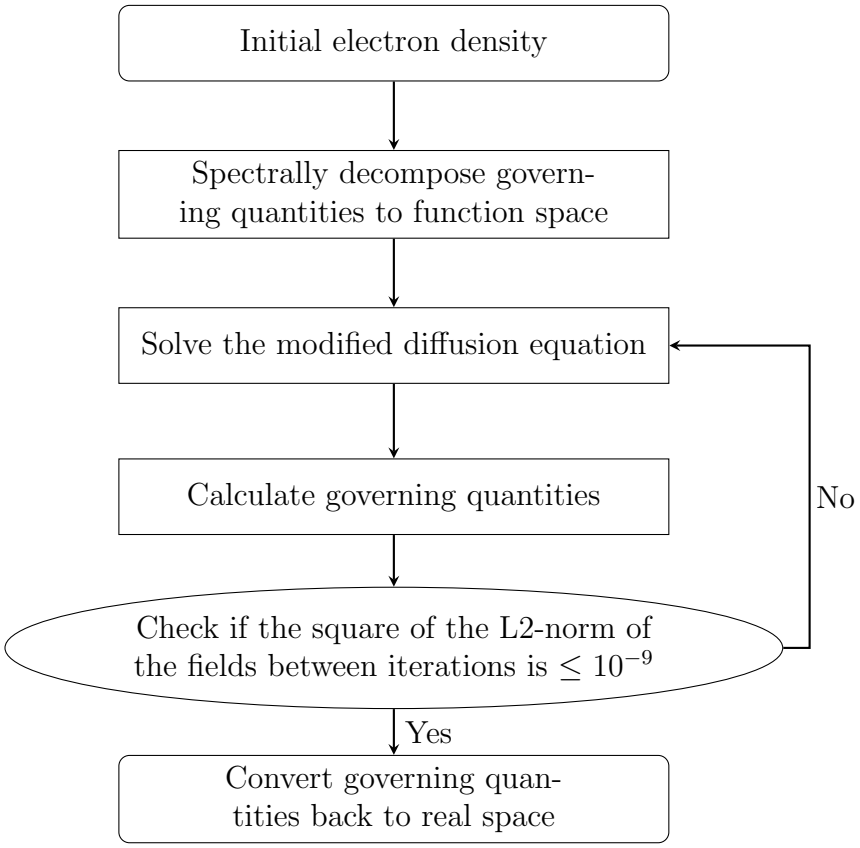

Figure 4.1: Flowchart of the computational algorithm used to determine the electron density of diatomic molecules.

The self-consistent calculation process obeys the flowchart in figure 4.1. Start with a guess for the initial electron density, in the case of diatomic molecules, the individual atoms were calculated separately, and then the results combined as an initial guess for the molecule composed of those two atoms. To calculate the ground-state electron density of

the individual atoms, the analytical hydrogen atom solution is used as an initial guess and the ground-state electron density of the hydrogen atom is found. The atom the next atomic number up is then calculated using the previous atom's ground-state electron density as the initial guess. This process of building up the atom is done until the desired atomic element has been reached. After the initial guess, the governing quantities, the electron density, quantum propagator and fields are spectrally decomposed to the function space of the basis set. The modified diffusion equation is then solved, and the new governing quantities are calculated. The square of the L2-norm for the total field values between the current iteration and previous iteration is then calculated. If the square of the L2-norm is less than 10^{-9} the convergence criterion has been met and the electron density, quantum propagator and fields are converted back to real space. The ground-state free energy is then calculated. If the square of the L2-norm is greater than 10^{-9}, the governing quantities are plugged back into the modified diffusion equation and the cycle repeats until the convergence criterion has been met. To improve the computational efficiency, Picard and Anderson mixing algorithms were implemented so that the convergence criterion is met more quickly. During the computational procedure, the value for the thermal parameter, β, was chosen to be large enough such that the system had reached the ground-state temperature. Note that a large β value corresponds to a low temperature.

4.3 Electron Density

Using the alternative approach to OF-DFT with cylindrically symmetric basis functions, the total electron density contours for common stable diatomic molecules in the first two rows of the periodic table are presented. The total electron density contour plots provide a fundamental test of the theory, as the electron density is used to determine the ground-state free energy as well as any of the other physical properties relevant to the molecules.

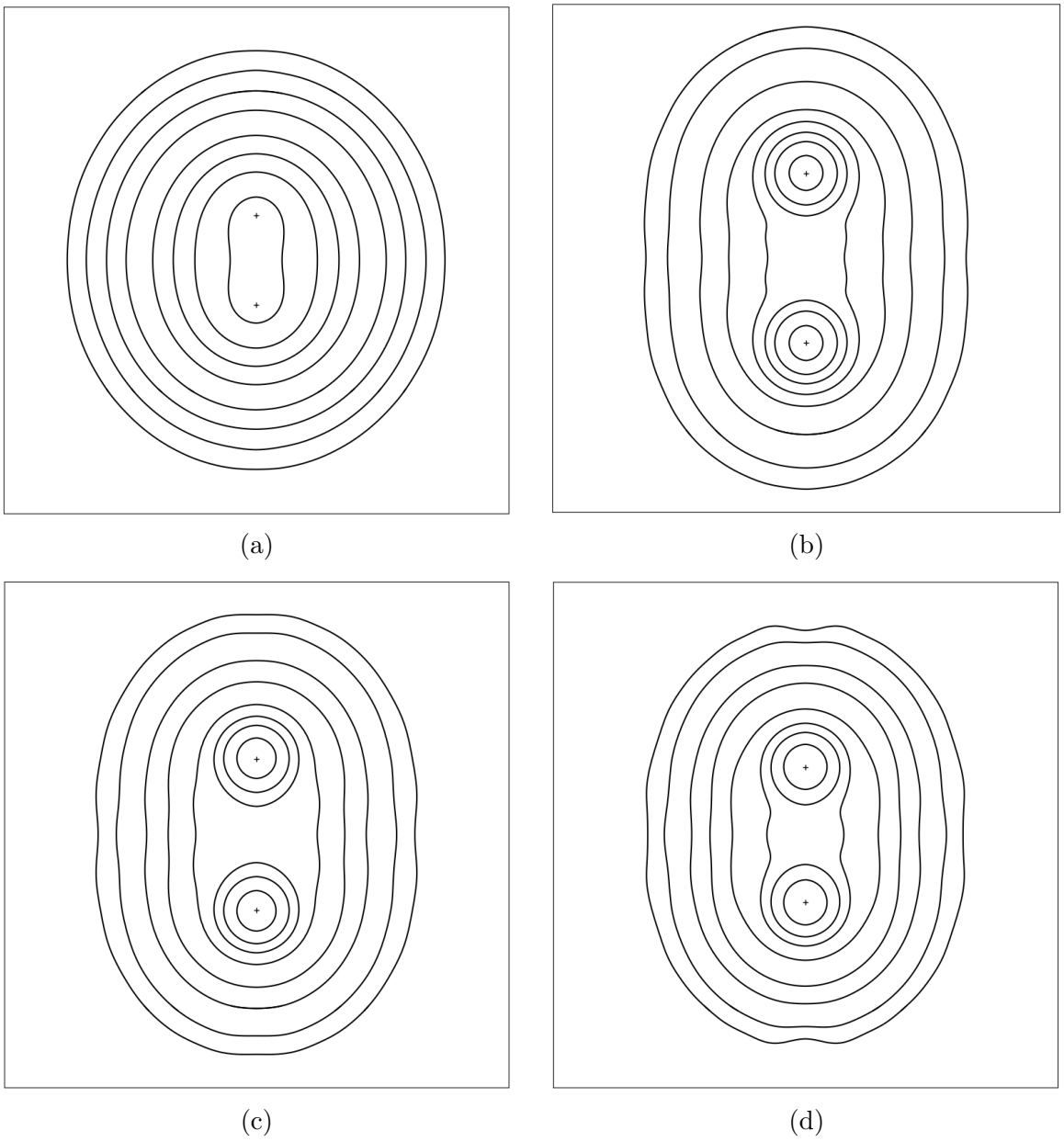

Figure 4.2: Total electron density contour plot of homonuclear diatomic molecules, (a) H_2, (b) N_2, (c) O_2, (d) F_2. For (a), both axes are identically spaced from -4 to 4 Bohr radii, a_0. The outermost contour is 0.001 e/a_0^3 and the innermost contour is 0.2 e/a_0^3. For the remaining contour plots (b), (c), and (d) both axes are identically spaced from -3 to 3 a_0. The outermost contour is 0.04 e/a_0^3 and the innermost contour is 8 e/a_0^3.

All the contour plots have been post-processed to eliminate high-frequency noise and to increase the readability of the plots. The post-processing was done by averaging each data point with a small number of other data points in its vicinity. The source of the noise is the oscillatory nature of the Bessel functions, sines and cosines in the basis set. This leads to high-frequency oscillations near the edge of the box where a larger number of basis functions are required to capture the comparatively small electron density in that region. Averaging each data point with nearby points within a single period of the oscillations allows for the underlying structure of the electron density to be captured. This averaging process allows for the true predictions of the electron density structure from the theory to be viewed without the basis set choice obscuring the results.

The separation distance of atomic centers is such that the total free energy of the molecule is minimized. The location of the atomic centers are artificially marked with a cross. The contour plots of the diatomic molecules are cross-sections of the r-z plane in cylindrical coordinates, with the z-axis along the vertical and r-axis along the horizontal. The negative r-axis contour values are the positive r-axis values reflected along the z-axis mirror plane so that complete contours are formed. The contour plots for each molecule share a similar contour distribution scheme that follows the format of Matta and Gillespie [32], starting at the outermost contour with 0.001 e/a_0^3 then 2×10^n e/a_0^3, 4×10^n e/a_0^3, 8×10^n e/a_0^3 where n starts at -3 and increases in steps of unity. Depending on the molecule, the outermost contour is the minimum electron density that still makes up a relevant portion of the total electron density and is not dominated by noise, and the innermost contour is the maximum electron density value rounded down to meet the nearest electron density value in the contour distribution scheme.

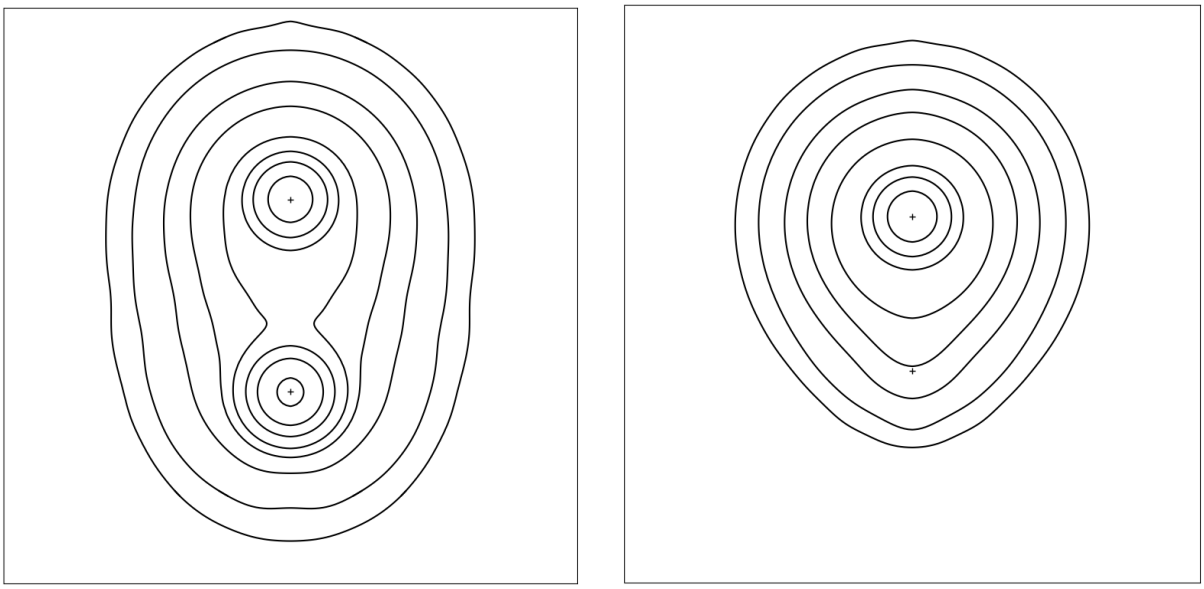

(a) (b)

Figure 4.3: Total electron density contour plot of heteronuclear diatomic molecules, (a) CO, (b) HF. For (a) and (b), both axes are identically spaced from -3 to 3 a_0. The outermost contour is 0.04 e/a_0^3 and the innermost contour is 8 e/a_0^3. In (a), the carbon nucleus is on the bottom and the oxygen nucleus is on the top. In (b), the hydrogen nucleus is on the bottom and the fluorine nucleus is on the top.

The electron density of the hydrogen molecule is the simplest case and represents a first test of the theory, demonstrating that molecular bonding occurs and that the electron densities are shared between the individual atoms. The electron density contour plot can be found in figure 4.2 (a). The hydrogen molecule only hosts two electrons in total and so, there is no Pauli exclusion principle and the excluded volume description of the Pauli potential will not impact the electron density distribution. However, the Fermi-Amaldi self-interaction correction factor will be at its least accurate value.

The remaining stable homonuclear diatomic molecules are N_2, O_2 and F_2, their more complex electron density structure provides the ability to examine the effects of the approximations in the theory due to the increased number of electrons and the presence of the Pauli potential. It can be seen in figure 4.2 (b), (c) and (d), that the contours for these three molecules obey the correct trend with the innermost contour at 8 e/a_0^3 moving outward as the number of electrons increase, indicating that the peak electron density is larger, and the density gradient is steeper near the nucleus. For all the homonuclear

diatomic molecules, the contours are symmetric about the r axis mirror plane, indicating that the electron densities around each atomic center are symmetric.

The electron density contours for HF and CO in figure 4.3, both have asymmetric electron density distributions about the r axis mirror plane, as would be expected since the individual atoms are different. Interestingly, for HF, the external potential from the hydrogen nucleus is so small that there are no contours centered around its nucleus, this does not occur in any other contour plot. However, the influence of the potential from the hydrogen nucleus is still clearly visible in the total electron density distribution. For the contour plot of CO, it can be directly compared to a similar contour plot of the same molecule from Matta and Gillespie. In agreement with Matta and Gillespie, the electron density gradient is steeper near the oxygen nucleus than it is near the carbon nucleus. However, the electron densities from Matta and Gillespie reach a higher peak near the nuclei compared to the present theory. This is not unexpected, as the limited basis set size prevents regions of highly varying electron densities from being captured, and the electron density varies significantly in these peak regions. Overall, the peak electron densities are not expected to affect physical predictions and are not of great concern. The electron density contours for all the diatomic molecules studied are qualitatively accurate compared to known results from other DFT methods.

4.4 Bond Lengths

The bonding characteristics were studied for homonuclear pairs of atoms in the first two rows of the periodic table. The only homonuclear pairs of atoms that displayed a clear free energy minimum when observing different atomic separations and therefore exhibited molecular boding, were H_2, N_2, O_2, and F_2. There was an exception where C_2 displayed a very shallow minimum, much lower than the other diatomic molecules and with a bond dissociation energy significantly lower than the bond dissociation energy of single carbon bonds in alkanes [33]. On the other hand, it is known that diatomic carbon can exist as vapour under exotic conditions [34], and the predicted bond length for C_2 of 2.2 Bohr radii is only 6.4 % of the experimental value of 2.35 [34, 35]. Considering the approximations made within the model and the shallowness of the minimum, it was judged that the minimum should not be considered as molecular bonding. All other homonuclear atomic pairs in the first two rows of the periodic table that were not mentioned above did not display free energy minimums.

Two heteronuclear diatomic molecules, CO and HF, bonding characteristics were also investigated. Both molecules had clear free energy minimums, and therefore molecular

bonding occurred.

Molecule	SCFT Bond Length	KS-DFT Bond Length [36, 37]	NIST Bond Length [38, 39]	SCFT KS-DFT % Difference	SCFT NIST % Difference
H_2	1.42 ± 0.01	1.404[a]	1.401	1.14	1.35
N_2	2.0 ± 0.1	2.088[a]	2.074	4.21	3.57
O_2	1.8 ± 0.1	2.285[b]	2.282	21.23	21.12
F_2	1.6 ± 0.1	2.651[a]	2.668	39.65	40.03
CO	2.0 ± 0.1	2.151[a]	2.132	7.02	6.19
HF	1.6 ± 0.1	1.748[a]	1.733	8.47	7.67

Table 4.1: Differences in OF-DFT based on SCFT, KS-DFT and experimental bond lengths for diatomic molecules. [a]Using B3LYP exchange-correlation functional and the 6-31G(d,p) basis set. [b]Using B3LYP exchange-correlation functional and the aug-CC-PVDZ basis set.

Using the location of the free energy minimums, the bond lengths were determined for all six diatomic molecules studied. The results are summarized in Table 4.1. The SCFT bond length results were fairly accurate when compared with NIST experimental values. The majority of molecules had under an 8% difference, the exceptions being O_2 and F_2. The large deviation of these molecules' bond lengths from the experimental values could be attributed to the high electronegativity of the O and F atoms [40]. The Fermi-Amaldi and Pauli potential approximations present in the theory may not model the electronegative character of atoms properly, leading to inaccurate physical properties. For all diatomic molecules, except for H_2, the calculated bond length underestimates the experimental bond length. Observing trends in the bond lengths, calculated from the present theory, the homonuclear diatomic molecule bond length decreases as the number of electrons increases, whereas the bond length increases as the number of electrons increases for the experimental bond length values. There are too few results to indicate that this trend is significant, and the two heteronuclear molecules do not follow this incorrect bond length trend, as HF has a shorter bond length and fewer electrons than CO. However, a possible explanation for this trend behaviour could be attributed to the lower-than-expected electron density near the core, as mentioned in the comparison of the CO contour plot with the same plot from Matta and Gillespie. The lower electron density near the core could be improperly shielding the valence electron densities and so the external potential from the nucleus will be stronger than expected in the valence region, resulting in an over-binding of the valence electron densities and a decreased bond length. Comparing the SCFT bond lengths with the KS-DFT calculated bond lengths, a similar discrepancy is observed as in the comparison with

NIST bond length values. The KS-DFT and NIST bond lengths both have similar values, and so this is expected. Interestingly, for the majority of diatomic molecules, the KS-DFT method overestimates bond lengths except for F_2, whereas the SCFT method generally underestimates the bond lengths except for H_2. This leads to the discrepancy in bond length values between SCFT and KS-DFT being generally greater than the discrepancy between SCFT and NIST bond length values.

The SCFT bond lengths can also be compared with the results of Finzel [35, 41] which uses a first-order atomic fragment OF-DFT method for several dimers, both exotic and common. Due to the approximations in the present theory, only the common diatomic molecules with robust bonding were investigated. Comparing the results for N_2, O_2, and CO with those of Finzel, they find percentage differences from experimental results as 10.9, 18.9, and 3.2, respectively. So, the estimate for N_2 in the present theory is significantly better, but the estimates for O_2 and CO are somewhat worse. Finzel reports mean absolute percentage errors (MAPE) which is the average of the percentage differences. For these three molecules, their results give a MAPE of 11 % compared to 10.3 % in this work. In other words, the two methods for these three molecules are comparable. For more exotic molecules, Finzel predicts bonding for Be_2 but not C_2 whereas the reverse is found for the results presented here. As mentioned, the minimum energy found for C_2 is not considered to be bonding, despite a respectable prediction of the bond length.

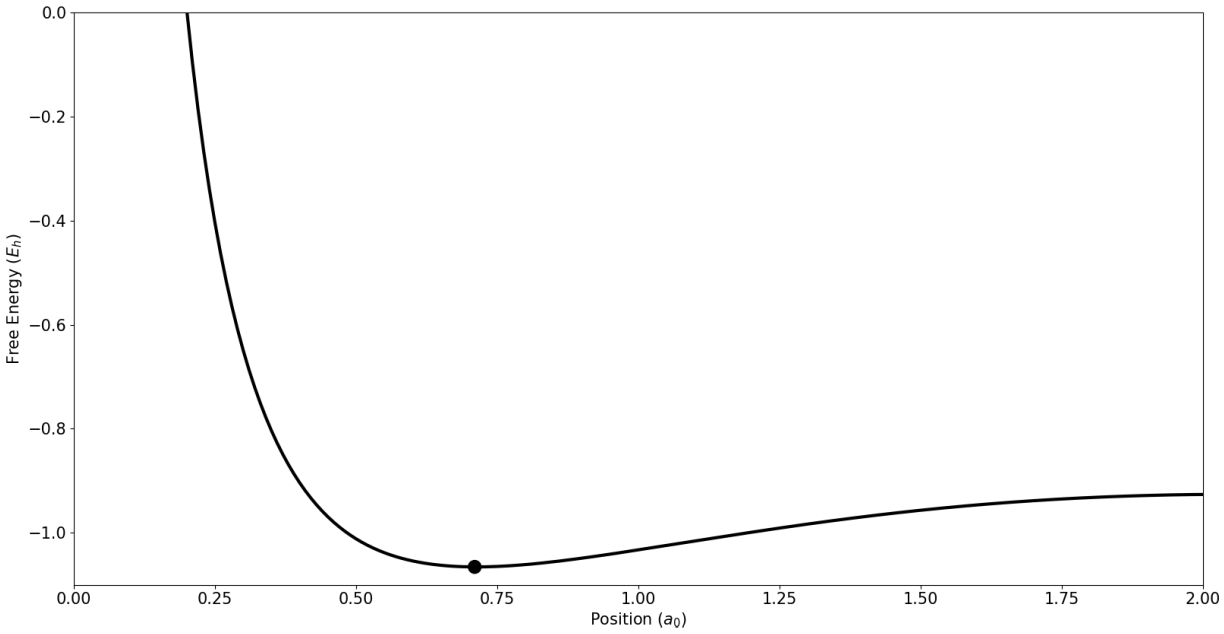

Figure 4.4: Free energy for two hydrogen atoms at different atomic separations. The position coordinate is in reference to the origin, the actual distance between the two atoms will be twice the position value. The dot marks the free energy minimum.

The plot of the free energy at different atomic separations for a pair of hydrogen atoms can be found in figure 4.4. Similar plots were constructed for all homonuclear atomic pairs from hydrogen to neon, as well as the two heteronuclear pairs, HF and CO. The presence of a minimum free energy value in these plots was used to determine if bonding occurred, and the position of the free energy minimum was used to calculate bond length.

4.5 Bond Dissociation Energy and Fundamental Vibrational Frequency for Hydrogen

For all the diatomic molecules, excluding hydrogen, the bond dissociation energies could not be accurately determined. To calculate the bond dissociation energies of the diatomic molecules, the difference must be taken between the free energy values at different atomic separations, specifically, the difference between the free energy minimum and the asymptotic free energy. Although these molecules exhibited a clear free energy minimum, at large separations, the size of the box was too small, and the free energy did not asymptote.

As well, at these large separations where the individual atoms should not be interacting with one another, the Fermi-Amaldi correction does not completely cancel the Coulomb electron-electron interaction. This issue could be remedied by increasing the size of the box, but this would require an even larger basis set, and the basis set size is one of the primary limitations of the current construction of the theory. It was possible to make the box size sufficiently large for hydrogen and so its bond dissociation energy was calculated as 0.14 $Hartrees$ compared to the experimental value [33] of 0.1661 $Hartrees$, a 15.71% discrepancy between results. As mentioned earlier, the Fermi-Amaldi factor would be at its least accurate value for hydrogen, and so it is surprising how closely the calculated bond dissociation energy resembles the experimental value. This is a good indication that given an improved basis set with a larger box size, reasonable bond dissociation energies could be found for the other diatomic molecules. Alternatively, the bond dissociation energy could be calculated by taking the difference of the molecular free energy minimum and twice the free energy from the independent atom calculation. However, the Poisson surface term arising from the finite box size would not cancel correctly, and so this method was not explored.

The fundamental vibrational frequencies of the diatomic molecules could be calculated as well. This is performed by examining the free energy at different atomic separations and mapping the curvature of the region around the minimum free energy to a spring constant for the simple harmonic oscillator. This was only done for hydrogen, as a preliminary test, and the agreement with NIST experimental results was poor. The calculated value from the present theory, 8367 cm^{-1}, is nearly double the NIST value [38], 4161 cm^{-1}, a difference of 101%. There is no reason to expect the results would improve for the other diatomic molecules, and so they were not calculated.

4.6 Limitations

The basis functions used to calculate the properties of the diatomic molecules are convenient as they are a complete orthonormal set, so building up the basis set is trivial. They are also eigenfunctions of the Laplacian, and so the governing modified diffusion equation is easily spectrally decomposed. However, due to the oscillator nature of the basis functions, they are not computationally efficient, and a large number of basis sets are required to achieve results with negligible noise. The need for a large basis set size is due to the fact that for each additional coordinate being modelled, the actual number of basis functions representing each coordinate is the total number of coordinates root the total number of basis functions. For example, in a system of 3 coordinates and modelled by 1000 basis functions, the number of basis functions per coordinate is $\sqrt[3]{1000} = 10$. As mentioned in

the theory chapter, this is why a cylindrical averaging approximation was implemented in the calculation process. It captures the general electron density structure of the diatomic molecule without the need to model the angular coordinate. This approximation is physically reasonable as the present theory is an ensemble interpretation, and it significantly improves the computational efficiency of the calculation. The computational efficiency is further improved by grouping all angular-dependent physical orbitals with the same radial and axial dependence into the same artificial shell in the theory. This orbital grouping approximation is motivated by the energy difference between angular dependent orbitals being significantly smaller than the energy difference between radially and axially dependent orbitals. The culmination of these orbital approximations is that the core electrons of each atom are represented in their own shells, whereas the valence electrons in each atom are grouped into a single shell. Unfortunately, in doing this, the angular dependence of the molecular orbitals is not captured. Another drawback of this approach is that all the valence electrons in the single-shell do not feel a Pauli exclusion principle from other electrons in the same shell, which should occur in a full, physically equivalent theory.

The current results for diatomic molecules are fine for the proof-of-concept nature of this work where qualitative and semi-quantitative results are of interest, but in the future, to obtain increased quantitative accuracy Gaussian basis sets can be used. The use of Gaussians is more computationally efficient and would remove the need to use cylindrical averaging on the orbitals and the grouping of multiple electron pairs into a single shell [42]. They have not been implemented, as Gaussian basis sets are a large field of research and the proof that this alternative approach to OF-DFT demonstrates molecular bonding is the primary concern. Other improvements to the theory would include the use of pseudopotentials, where the effect of the core electrons on the valence electrons are described as a potential instead of fully modelling the core electron densities, improving computational efficiency [14]. As well, using more advanced exchange-correlation functionals beyond the current implementation of the Pauli potential and Fermi-Amaldi correction would improve the overall accuracy of the theory [43, 44].

Chapter 5

Conclusions

In this work, the alternative approach to OF-DFT based on ideas from SCFT has been successfully applied to systems of diatomic molecules. In doing so, the validity of this theory in predicting correct electron density structure and molecular bonding has been achieved. Demonstrating that the theory provides a more accurate picture of the properties of diatomic molecules compared to other basic OF-DFT methods that implement the Thomas-Fermi or von Weizsäcker functional as their non-interacting kinetic energy functional.

The necessary physics and mathematics for understanding the present OF-DFT theory and the motivation behind the theory was reviewed in chapter 2. The foundational Hohenberg-Kohn theorems of DFT were proven and applied to the construction of KS-DFT and OF-DFT. The different approximation schemes between these two approaches were outlined, and common approximation methods for each theory were presented. The SCFT of Gaussian distributed polymers in an external field was reviewed.

The complete OF-DFT theory based on ideas from SCFT was fully constructed in chapter 3. The governing quantities of the theory, the electron density, fields and quantum propagator as well as the governing modified diffusion equation were derived from a "first principles" approach. The theory demonstrates a useful comparison that 4-D thermal space Gaussian ring polymers and 3-D quantum particles are isomorphic. This provides an alternative ensemble interpretation viewpoint of constructing DFT from SCFT. Special consideration is given to the cylindrical basis set that is necessary to determine the electron density and ground-state free energy of diatomic molecules. This demonstrates that in the present theory, it is possible to model any system with cylindrical symmetry and extends the applicability of the theory beyond just atoms [20].

The physical properties of a variety of homonuclear and heteronuclear diatomic molecules were calculated using the present theory and the results presented in chapter 4. Six diatomic molecules were investigated in total, H_2, N_2, O_2, F_2, CO and HF. For the electron density contour plots of diatomic molecules, they were shown to be in qualitative agreement with known DFT results. Specifically, when comparing the electron density of CO with a similar plot from Matta and Gillespie [32], it was found that the structure of the contours were very similar, with a slight deviation in peak electron density that should not affect the physical properties that are calculated using the electron density. The bond lengths for all the diatomic molecules were compared with known experimental values from NIST [38, 39] and KS-DFT calculations [36, 37], with the majority being in agreement to within less than 8% and 9% respectively, with notable deviations being O_2 and F_2. The bond dissociation energy and fundamental vibrational frequency for hydrogen was calculated, with the bond dissociation energy deviating 16% from the experimental value and the vibrational frequency varying significantly from the experimental value. Limitations to the theory were discussed, providing reasoning for the discrepancy in some of the calculated physical properties, as well as, why only the bond dissociation energy and fundamental vibrational frequency for hydrogen was calculated.

Overall, the present theory was successfully applied to modelling homonuclear and heteronuclear diatomic molecules. Molecular bonding was demonstrated between pairs of atoms, producing semi-quantitative and qualitative results for the diatomic molecules' physical properties. The electron density contours were found to be in qualitative agreement with known DFT results. Bond lengths were quantitatively accurate for the majority of diatomic molecules studied, with notable exceptions O_2 and F_2. For H_2, the bond dissociation energy was semi-quantitatively accurate and the fundamental vibrational frequency varied significantly from the experimental value. The results could potentially be improved if a Gaussian basis set centered around the atomic centers was implemented.

The current OF-DFT approach has its advantages in that the symmetry of the system can be encoded in the basis set and that the exact form of the non-interacting kinetic energy functional is only limited by the exchange-correlation functional. In contrast, to other OF-DFT theories where the non-interacting kinetic energy functional and exchange-correlation functional are both approximated. The disadvantage being the large number of basis sets required to model the system and the use of the crude Fermi-Amaldi factor to correct for electron-electron interactions. The present work provides a steppingstone for the model to continue to be applied to more complex quantum systems.

References

[1] H. Taube. Mechanisms of oxidation with oxygen. *The Journal of general physiology*, 49(1), 1965.

[2] M. A. Sutton et al. Challenges in quantifying biosphere-atmosphere exchange of nitrogen species. *Environmental Pollution*, 150(1):125–139, 2007.

[3] R. Parr and Y. Weitao. *Density-Functional Theory of Atoms and Molecules*. Oxford University Press, 1989.

[4] A. D. Becke. Perspective: Fifty years of density-functional theory in chemical physics. *Journal of Chemical Physics*, 140(18), 2014.

[5] W. Kohn and L. J. Sham. Self-Consisten Equations Including Exchange and Correlation Effects. *Physical Review Letters*, 140(4A):1133–1139, 1965.

[6] P. Hohenberg and W. Kohn. Inhomogeneous Electron Gas. *Physical Review Letters*, 136(3B):864–872, 1964.

[7] K. Burke. Perspective on density functional theory. *Journal of Chemical Physics*, 136(15), 2012.

[8] V. L. Lignères and E. A. Carter. An Introduction to Orbital-Free Density Functional Theory. In *Handbook of Materials Modeling*, volume 7, pages 137–148. Springer Netherlands, Dordrecht, 2005.

[9] E. Schrödinger. Quantisierung als Eigenwertproblem. *Annalen der Physik*, 384(6):489–527, 1926.

[10] Viraht Sahni. The Hohenberg-Kohn Theorems and Kohn-Sham Density Functional Theory. In *Quantal Density Functional Theory*, pages 99–123. Springer-Verlag Berlin Heidelberg, 2004.

[11] K. A. Baseden and J. W. Tye. Introduction to density functional theory: Calculations by hand on the helium atom. *Journal of Chemical Education*, 91(12):2116–2123, 2014.

[12] G. E. Scuseria and V. N. Staroverov. Progress in the development of exchange-correlation functionals. In *Theory and Applications of Computational Chemistry*, pages 669–724. Elsevier B.V., 2005.

[13] D. Bagayoko. Understanding density functional theory (DFT) and completing it in practice. *AIP Advances*, 4(12), 2014.

[14] Y. A. Wang and E. A. Carter. Orbital-Free Kinetic-Energy Density Functional Theory. In *Theoretical Methods in Condensed Phase Chemistry*, volume 184, pages 117–184. Springer Netherlands, 2000.

[15] W. C. Witt, B. G. Del Rio, J. M. Dieterich, and E. A. Carter. Orbital-free density functional theory for materials research. *Journal of Materials Research*, 33(7):777–795, 2018.

[16] K. Finzel. A simple approximation for the Pauli potential yielding self-consistent electron densities exhibiting proper atomic shell structure. *International Journal of Quantum Chemistry*, 115(23):1629–1634, 2015.

[17] N. W. Ashcroft and N. D. Mermin. *Solid State Physics*. Holt, Rinehart and Winston, 1976.

[18] M. W. Matsen. Self-Consistent Field Theory and Its Applications. In *Soft Matter, Volume 1: Polymer Melts and Mixtures*, volume 1, pages 3–83. Wiley-VCH, 2006.

[19] A. Arora, J. Qin, D. C. Morse, K. T. Delaney, G. H. Fredrickson, F. S. Bates, and K. D. Dorfman. Broadly Accessible Self-Consistent Field Theory for Block Polymer Materials Discovery. *Macromolecules*, 49(13):4675–4690, 2016.

[20] R. B. Thompson. An alternative derivation of orbital-free density functional theory. *Journal of Chemical Physics*, 150(20), 2019.

[21] R. P. Feynman and A. R. Hibbs. *Quantum Mechanics and Path Integrals*. Dover Publications, Inc., 2010.

[22] R. B. Thompson. Atomic shell structure from an orbital-free-related density-functional-theory Pauli potential. *Physical Review A*, 102(1):1–10, 2020.

[23] O. A. Von Lilienfeld and M. E. Tuckerman. Molecular grand-canonical ensemble density functional theory and exploration of chemical space. *Journal of Chemical Physics*, 125(15), 2006.

[24] R. Sundararaman, W. A. Goddard, and T. A. Arias. Grand canonical electronic density-functional theory: Algorithms and applications to electrochemistry. *Journal of Chemical Physics*, 146(11), 2017.

[25] A. U. Von Barth. Basic Density-Functional Theory — an Overview. *Physica Scripta*, 9, 2004.

[26] A. Altland and B. Simons. *Condensed Matter Field Theory*. Cambridge University Press, 210.

[27] David Derbes. Feynman's derivation of the Schrodinger Equation. *American Journal of Physics*, 64(881), 1996.

[28] E. Helfand. Theory of inhomogeneous polymers: Fundamentals of the Gaussian random-walk model. *The Journal of Chemical Physics*, 62(3):999–1005, 1975.

[29] G. S. Ho, C. Huang, and E. A. Carter. Describing metal surfaces and nanostructures with orbital-free density functional theory. *Current Opinion in Solid State and Materials Science*, 11(5-6):57–61, 2007.

[30] J. Xia and E. A. Carter. Density-decomposed orbital-free density functional theory for covalently bonded molecules and materials. *Physical Review B - Condensed Matter and Materials Physics*, 86(23):1–15, 2012.

[31] L. A. Constantin, E. Fabiano, and F. Della Sala. Semilocal Pauli-Gaussian Kinetic Functionals for Orbital-Free Density Functional Theory Calculations of Solids. *Journal of Physical Chemistry Letters*, 9(15):4385–4390, 2018.

[32] C. F. Matta and R. J. Gillespie. Understanding and interpreting molecular electron density distributions. *Journal of Chemical Education*, 79(9):1141, 2002.

[33] Y. R. Luo. *Comprehensive handbook of chemical bond energies*. CRC Press, 2007.

[34] R. Hoffmann. C2 in All Its Guises, 1995.

[35] K. Finzel. Equilibrium bond lengths from orbital-free density functional theory. *Molecules*, 25(8), 2020.

[36] Valérie Wathelet, Benoît Champagne, David H. Mosley, Jean Marie André, and Sandro Massidda. Vibrational frequencies of diatomic molecules from Car and Parrinello molecular dynamics. *Chemical Physics Letters*, 275(5-6):506–512, 1997.

[37] Jian Wang, Benny G. Johnson, and Russell J. Boyd. Electron densities of several small molecules as calculated from density functional theory. *Journal of Physical Chemistry*, 100(15):6317–6324, 1996.

[38] K. P. Huber and G. Herzberg. *Molecular Spectra and Molecular Structure*. Van Nostrand Reinhold Inc., 1979.

[39] F. J. Lovas, E. Tiemann, J. S. Coursey, S. A. Kotochigova, J. Chang, K. Olsen, and R. A. Dragoset. NIST Diatomic Spectral Database, 2005.

[40] R.G. Parr, R. A. Donnelly, M. Levy, and W. E. Palke. Electronegativity: The density functional viewpoint. *The Journal of Chemical Physics*, 68(8):3801–3807, 1977.

[41] K. Finzel. The first order atomic fragment approach - An orbital-free implementation of density functional theory. *Journal of Chemical Physics*, 151(2):1–7, 2019.

[42] J. G. Hill. Gaussian basis sets for molecular applications. *International Journal of Quantum Chemistry*, 113(1):21–34, 2013.

[43] A. J. Cohen, P. Mori-Sánchez, and W. Yang. Development of exchange-correlation functionals with minimal many-electron self-interaction error. *Journal of Chemical Physics*, 126(19):10–15, 2007.

[44] V.G. Tsirelson, A. I. Stash, V. V. Karasiev, and S. Liu. Pauli potential and Pauli charge from experimental electron density. *Computational and Theoretical Chemistry*, 1006:92–99, 2013.

[45] P. Moon and D. E. Spencer. *Field Theory Handbook Including Coordinate Systems, Differential Equations and Their Solutions*. Springer-Verlag Berlin Heidelberg, 2 edition, 1971.

[46] D. A. McQuarrie. *Statistical Mechanics*. Harper & Row, 1976.

[47] J. G. Kirkwood. Quantum statistics of almost classical assemblies. *Physical Review*, 44(1):31–37, 1933.

[48] John G. Kirkwood. Quantum statistics of almost classical assemblies. *Physical Review*, 45(2):116–117, 1 1934.

[49] J. J. Sakurai and J. Napolitano. *Modern Quantum Mechanics*. Cambridge University Press, 2020.

[50] R. Shankar. *Principles of Quantum Mechanics*. Plenum Publishers, 2 edition, 1994.

APPENDICES

Appendix A

Derivation of Cylindrically Symmetric Basis Set

To determine the basis set with the desired cylindrical symmetry, the orthonormal eigenfunctions of the Laplacian need to be determined. This is done by solving the Helmholtz equation in cylindrical coordinates. The solution is [45],

$$f_{nm}(r,z) = J_0(mr)\left(A_0 + A_n\cos(nz) + B_n\sin(nz)\right) \tag{A.1}$$

where J_0 is the zeroth order cylindrical Bessel function, n, m are constants and A_0, A_n, B_n are the normalization constants, all of which need to be determined. The simplest method for determining the constants n, m is to perform the calculations for each coordinate separately. Starting with the radial coordinate, the orthogonality condition requires

$$\int_0^R r dr J_0(mr)J_0(m'r) = R\frac{mJ_0(m'R)J_1(mR) - m'J_0(mR)J_1(m'R)}{m^2 - m'^2} = 0 \tag{A.2}$$

where J_1 is the first order cylindrical Bessel function and $m \neq m'$. The most obvious choice is to let $J_0(mR) = 0$ and $J_0(m'R) = 0$. So, $m = \frac{\gamma_{0,j}}{R}$ and $m' = \frac{\gamma_{0,j'}}{R}$ where $\gamma_{0,j}$ is the j^{th} zero of the zeroth-order cylindrical Bessel function. To determine the constant of the axial coordinate, different combinations of orthogonality conditions for each term will be investigated. The orthogonality condition involving two constant terms does not need to be calculated as it does not explicitly depend on the n constant and only one constant term exists in the basis set. Starting with the constant and cosine term, the orthogonality condition requires

$$\int_{-Z/2}^{Z/2} dz \cos(nz) = \frac{2}{n} \sin\left(n\frac{Z}{2}\right) = 0. \tag{A.3}$$

Requiring $\sin\left(n\frac{Z}{2}\right) = 0$. So, $n = i\frac{2\pi}{Z}$ where i is an integer. The solution to the constant, n, can be used to determine if the solution is valid for all other orthogonality condition combinations. The next combination is the constant and sine term,

$$\int_{-Z/2}^{Z/2} dz \sin\left(i\frac{2\pi z}{Z}\right) = 0. \tag{A.4}$$

So, the orthogonality condition holds. The next combination is a sine and sine term,

$$\int_{-Z/2}^{Z/2} dz \sin\left(i\frac{2\pi z}{Z}\right) \sin\left(i'\frac{2\pi z}{Z}\right) = Z\frac{i\cos(i\pi)\overbrace{\sin(i'\pi)}^{0} - i'\cos(i'\pi)\overbrace{\sin(i\pi)}^{0}}{i'^2\pi - i^2\pi} = 0. \tag{A.5}$$

Again, the orthogonality condition holds. The cosine and cosine term combination is next,

$$\int_{-Z/2}^{Z/2} dz \cos\left(i\frac{2\pi z}{Z}\right) \cos\left(i'\frac{2\pi z}{Z}\right) = Z\frac{i'\cos(i\pi)\overbrace{\sin(i'\pi)}^{0} - i\cos(i'\pi)\overbrace{\sin(i\pi)}^{0}}{i'^2\pi - i^2\pi} = 0. \tag{A.6}$$

The orthogonality condition holds. Next is cosine and sine term,

$$\int_{-Z/2}^{Z/2} dz \cos\left(i\frac{2\pi z}{Z}\right) \sin\left(i'\frac{2\pi z}{Z}\right) = 0. \tag{A.7}$$

The orthogonality condition holds. The axial coordinate orthogonality constant has been verified for all z component basis functions combinations. The basis functions can be written with different z component index labels as

$$f_{0j}(r,z) = J_0\left(\gamma_{0,j}\frac{r}{R}\right)\cdot A_0 \tag{A.8}$$

$$f_{(2i)j}(r,z) = J_0\left(\gamma_{0,j}\frac{r}{R}\right)\cdot A_{(2i)}\cos\left(\frac{2\pi(2i)z}{Z}\right) \tag{A.9}$$

$$f_{(2i-1)j}(r,z) = J_0\left(\gamma_{0,j}\frac{r}{R}\right)\cdot B_{(2i-1)}\sin\left(\frac{2\pi(2i-1)z}{Z}\right). \tag{A.10}$$

The cosine and sine index are even and odd respectively, as to which z component basis function term is used, that depends on whether the z component index is even or odd. The basis set needs to be normalized for each z component basis set, starting with the constant term

$$\begin{aligned}
1 &= \frac{1}{V}\int_0^R\int_0^{2\pi}\int_{-Z/2}^{Z/2} drd\theta dzr|f_{0j}(r,z)|^2 \\
&= \frac{1}{V}\int_0^R\int_0^{2\pi}\int_{-Z/2}^{Z/2} drd\theta dzr J_0^2(\gamma_{0,j}\frac{r}{R})A_0^2 \\
&= \frac{2\pi Z}{\pi R^2 Z}A_0^2\frac{R^2}{2}(\overbrace{J_0^2(\gamma_{0,j})}^{0}+J_1^2(\gamma_{0,j})) \\
1 &= A_0^2 J_1^2(\gamma_{0,j}).
\end{aligned}$$

The normalization constant for the z component constant term is,

$$A_0 = \frac{1}{J_1(\gamma_{0,j})}. \tag{A.11}$$

Next is the normalization constant for the z component cosine term,

$$
\begin{aligned}
1 &= \frac{1}{V}\int_0^R \int_0^{2\pi} \int_{-Z/2}^{Z/2} dr d\theta dz r |f_{(2i)j}(r,z)|^2 \\
&= \frac{1}{V}\int_0^R \int_0^{2\pi} \int_{-Z/2}^{Z/2} dr d\theta dz r J_0^2(\gamma_{0,j}\frac{r}{R}) A_{(2i)}^2 \cos^2(\frac{2\pi(2i)z}{Z}) \\
&= A_{(2i)}^2 \frac{J_1^2(\gamma_{0,j})}{Z}\frac{Z}{2} \\
1 &= A_{(2i)}^2 \frac{J_1^2(\gamma_{0,j})}{2}.
\end{aligned}
$$

The normalization constant for the z component cosine term is,

$$
A_{(2i)} = \frac{\sqrt{2}}{J_1(\gamma_{0,j})}. \tag{A.12}
$$

Lastly, the normalization constant for the z component sine term,

$$
\begin{aligned}
1 &= \frac{1}{V}\int_0^R \int_0^{2\pi} \int_{-Z/2}^{Z/2} dr d\theta dz r |f_{(2i-1)j}(r,z)|^2 \\
&= \frac{1}{V}\int_0^R \int_0^{2\pi} \int_{-Z/2}^{Z/2} dr d\theta dz r J_0^2(\gamma_{0,j}\frac{r}{R}) B_{(2i-1)}^2 \sin^2(\frac{2\pi(2i-1)z}{Z}) \\
&= B_{(2i-1)}^2 \frac{J_1^2(\gamma_{0,j})}{Z}\frac{Z}{2} \\
1 &= B_{(2i-1)}^2 \frac{J_1^2(\gamma_{0,j})}{2}.
\end{aligned}
$$

The normalization constant for the z component sine term is,

$$
B_{(2i-1)} = \frac{\sqrt{2}}{J_1(\gamma_{0,j})}. \tag{A.13}
$$

All the constants have been determined and the orthonormal basis function is fully specified. The full basis function is,

$$f_{0j}(r,z) = \frac{\sqrt{2}}{J_1(\gamma_{0,j})} J_0\left(\gamma_{0,j}\frac{r}{R}\right) \cdot \frac{1}{\sqrt{2}} \tag{A.14}$$

$$f_{(2i)j}(r,z) = \frac{\sqrt{2}}{J_1(\gamma_{0,j})} J_0\left(\gamma_{0,j}\frac{r}{R}\right) \cdot \cos\frac{2\pi(2i)z}{Z} \tag{A.15}$$

$$f_{(2i-1)j}(r,z) = \frac{\sqrt{2}}{J_1(\gamma_{0,j})} J_0\left(\gamma_{0,j}\frac{r}{R}\right) \cdot \sin\frac{2\pi(2i-1)z}{Z}. \tag{A.16}$$

The eigenvalues of the Laplacian operator for the basis set now need to be calculated. As before, the procedure is split up into the different z component basis set terms. Starting with the constant term,

$$\begin{aligned}
\nabla^2 f_{0j}(r,z) &= \left(\frac{1}{r}\frac{\partial}{\partial r}\left(r\frac{\partial}{\partial r}\right) + \frac{1}{r^2}\frac{\partial^2}{\partial\theta^2} + \frac{\partial^2}{\partial z^2}\right) \frac{1}{J_1(\gamma_{0,j})} J_0\left(\gamma_{0,j}\frac{r}{R}\right) \\
&= \frac{1}{J_1(\gamma_{0,j})}\frac{1}{r}\frac{\partial}{\partial r}\left(r\frac{\partial}{\partial r}\right) J_0\left(\gamma_{0,j}\frac{r}{R}\right) \\
&= -\left(\frac{\gamma_{0,j}}{R}\right)^2 \frac{1}{J_1(\gamma_{0,j})} J_0\left(\gamma_{0,j}\frac{r}{R}\right) \\
&= -\left(\frac{\gamma_{0,j}}{R}\right)^2 f_{0j}(r,z).
\end{aligned}$$

The constant term eigenvalue of the Laplacian operator is

$$\lambda_{0j} = -\frac{\gamma_{0,j}^2}{R^2}. \tag{A.17}$$

Next, is the eigenvalue for the z component cosine term,

$$\begin{aligned}
\nabla^2 f_{(2i)j}(r,z) &= \frac{\sqrt{2}}{J_1(\gamma_{0,j})} \cos\left(\frac{2\pi(2i)z}{Z}\right) \frac{1}{r}\frac{\partial}{\partial r}\left(r\frac{\partial}{\partial r}\right) J_0\left(\gamma_{0,j}\frac{r}{R}\right) \\
&\quad + \frac{\sqrt{2}}{J_1(\gamma_{0,j})} J_0\left(\gamma_{0,j}\frac{r}{R}\right) \frac{\partial^2}{\partial z^2} \cos\left(\frac{2\pi(2i)z}{Z}\right) \\
&= \left(-\left(\frac{\gamma_{0,j}}{R}\right)^2 - \left(\frac{2\pi(2i)}{Z}\right)^2\right) f_{(2i)j}(r,z).
\end{aligned}$$

The cosine term eigenvalue is,

$$\lambda_{(2i)j} = -\left(\frac{\gamma_{0,j}}{R}\right)^2 - \left(\frac{2\pi(2i)}{Z}\right)^2. \tag{A.18}$$

Lastly, the eigenvalue for the z component sine term is calculated,

$$\begin{aligned}
\nabla^2 f_{(2i-1)j}(r,z) &= \frac{\sqrt{2}}{J_1(\gamma_{0,j})} \sin\left(\frac{2\pi(2i-1)z}{Z}\right) \frac{1}{r}\frac{\partial}{\partial r}\left(r\frac{\partial}{\partial r}\right) J_0\left(\gamma_{0,j}\frac{r}{R}\right) \\
&+ \frac{\sqrt{2}}{J_1(\gamma_{0,j})} J_0\left(\gamma_{0,j}\frac{r}{R}\right) \frac{\partial^2}{\partial z^2} \sin\left(\frac{2\pi(2i-1)z}{Z}\right) \\
&= \left(-\left(\frac{\gamma_{0,j}}{R}\right)^2 - \left(\frac{2\pi(2i-1)}{Z}\right)^2\right) f_{(2i-1)j}(r,z).
\end{aligned}$$

The sine term eigenvalue is,

$$\lambda_{(2i-1)j} = -\left(\frac{\gamma_{0,j}}{R}\right)^2 - \left(\frac{2\pi(2i-1)}{Z}\right)^2. \tag{A.19}$$

Appendix B

Gamma Tensor

To determine the full explicit form of the gamma tensor with all the different z component index combinations is quite cumbersome and so only the unique gamma tensor indices will be explicitly calculated, and all the other indices can be determined by permuting the indices of the unique expressions. The fully expanded index form of the gamma tensor is,

$$\Gamma_{ij,i'j',i''j''} = \frac{1}{V}\int d\mathbf{r} f_{ij}(\mathbf{r}) f_{i'j'}(\mathbf{r}) f_{i''j''}(\mathbf{r}). \tag{B.1}$$

It should be noted that the integral of the product of three zeroth-order Bessel functions do not have an analytical solution and so needs to be numerically integrated to determine the value of the gamma tensor indices. To avoid obscuring the results of the different indices in the gamma tensor, this Bessel function integral as well as any factors that are consistent for all gamma tensor indices will be written in a compact form as,

$$I^r_{j,j',j''} = \frac{2}{R^2}\cdot\frac{\sqrt{2}}{J_1(\gamma_{0,j})}\cdot\frac{\sqrt{2}}{J_1(\gamma_{0,j'})}\cdot\frac{\sqrt{2}}{J_1(\gamma_{0,j''})}\int_0^R dr\ rJ_0(\gamma_{0,j}\frac{r}{R})\cdot J_0(\gamma_{0,j'}\frac{r}{R})\cdot J_0(\gamma_{0,j''}\frac{r}{R}) \tag{B.2}$$

where $I^r_{j,j',j''}$ indicates that it is the integral expression for the radial r component of the gamma tensor. The different combinations of the axial coordinate, z, terms for the gamma tensor will now be explored, starting with all constant terms for the z component,

$$\Gamma_{0j,0j',0j''} = I^r_{j,j',j''}\frac{1}{Z}\int_{-Z/2}^{Z/2} dz\frac{1}{2^{3/2}} = \frac{I^r_{j,j',j''}}{2^{3/2}}. \tag{B.3}$$

Next is two constant terms and one cosine term for the z component,

$$\Gamma_{(2i)j,0j',0j''} = I^r_{j,j',j''} \frac{1}{Z} \int_{-Z/2}^{Z/2} dz \frac{1}{2} \cdot \cos \frac{2\pi(2i)z}{Z} = \frac{I^r_{j,j',j''}}{2} \cdot \operatorname{sinc} \pi(2i) \tag{B.4}$$

where $\operatorname{sinc} x = \frac{\sin x}{x}$. Now two constant terms and one sine term,

$$\Gamma_{(2i-1)j,0j',0j''} = I^r_{j,j',j''} \frac{1}{Z} \int_{-Z/2}^{Z/2} dz \frac{1}{2} \cdot \sin \frac{2\pi(2i-1)z}{Z} = 0. \tag{B.5}$$

Now, one constant term and two cosine terms,

$$\begin{aligned} \Gamma_{(2i)j,(2i')j',0j''} &= I^r_{j,j',j''} \frac{1}{Z} \int_{-Z/2}^{Z/2} dz \frac{1}{\sqrt{2}} \cdot \cos \frac{2\pi(2i)z}{Z} \cdot \cos \frac{2\pi(2i')z}{Z} \\ &= \frac{I^r_{j,j',j''}}{2^{3/2}} \left(\operatorname{sinc} \pi((2i) - (2i')) + \operatorname{sinc} \pi((2i) + (2i')) \right). \end{aligned} \tag{B.6}$$

Now, one constant term and two sine terms,

$$\begin{aligned} \Gamma_{(2i-1)j,(2i'-1)j',0j''} &= I^r_{j,j',j''} \frac{1}{Z} \int_{-Z/2}^{Z/2} dz \frac{1}{\sqrt{2}} \cdot \sin \frac{2\pi(2i-1)z}{Z} \cdot \sin \frac{2\pi(2i'-1)z}{Z} \\ &= \frac{I^r_{j,j',j''}}{2^{3/2}} \left(\operatorname{sinc} \pi((2i-1) - (2i'-1)) - \operatorname{sinc} \pi((2i-1) + (2i'-1)) \right). \end{aligned} \tag{B.7}$$

Now, one constant term, one cosine term and one sine term,

$$\Gamma_{(2i)j,(2i'-1)j',0j''} = I^r_{j,j',j''} \frac{1}{Z} \int_{-Z/2}^{Z/2} dz \frac{1}{\sqrt{2}} \cdot \cos \frac{2\pi(2i)z}{Z} \cdot \sin \frac{2\pi(2i'-1)z}{Z} = 0. \tag{B.8}$$

Now, one cosine term and two sine terms,

$$\begin{aligned}\Gamma_{(2i)j,(2i'-1)j',(2i''-1)j''} &= I^r_{j,j',j''}\frac{1}{Z}\int_{-Z/2}^{Z/2} dz \cos\frac{2\pi(2i)z}{Z}\cdot\sin\frac{2\pi(2i'-1)z}{Z}\cdot\sin\frac{2\pi(2i''-1)z}{Z}\\ &= \frac{I^r_{j,j',j''}}{4}\left(-\operatorname{sinc}\pi((2i)-(2i'-1)-(2i''-1))\right.\\ &+\operatorname{sinc}\pi((2i)+(2i'-1)-(2i''-1))\\ &+\operatorname{sinc}\pi((2i)-(2i'-1)+(2i''-1))\\ &\left.-\operatorname{sinc}\pi((2i)+(2i'-1)+(2i''-1))\right). \end{aligned} \tag{B.9}$$

Now, two cosine terms and one sine term,

$$\Gamma_{(2i)j,(2i')j',(2i''-1)j''} = I^r_{j,j',j''}\frac{1}{Z}\int_{-Z/2}^{Z/2} dz \cos\frac{2\pi(2i)z}{Z}\cdot\cos\frac{2\pi(2i')z}{Z}\cdot\sin\frac{2\pi(2i''-1)z}{Z} = 0. \tag{B.10}$$

Now, three cosine terms,

$$\begin{aligned}\Gamma_{(2i)j,(2i')j',(2i'')j''} &= I^r_{j,j',j''}\frac{1}{Z}\int_{-Z/2}^{Z/2} dz \cos\frac{2\pi(2i)z}{Z}\cdot\cos\frac{2\pi(2i')z}{Z}\cdot\cos\frac{2\pi(2i'')z}{Z}\\ &= \frac{I^r_{j,j',j''}}{4}\left(\operatorname{sinc}\pi((2i)-(2i')-(2i''))+\operatorname{sinc}\pi((2i)+(2i')-(2i''))\right.\\ &\left.+\operatorname{sinc}\pi((2i)-(2i')+(2i''))+\operatorname{sinc}\pi((2i)+(2i')+(2i''))\right). \end{aligned} \tag{B.11}$$

Now, three sine terms,

$$\begin{aligned}\Gamma_{(2i-1)j,(2i'-1)j',(2i''-1)j''} &= I^r_{j,j',j''}\frac{1}{Z}\\ &\cdot\int_{-Z/2}^{Z/2} dz \sin\frac{2\pi(2i-1)z}{Z}\cdot\sin\frac{2\pi(2i'-1)z}{Z}\cdot\sin\frac{2\pi(2i''-1)z}{Z}\\ &= 0. \end{aligned} \tag{B.12}$$

All other gamma tensor indices will have the same form but with the i, i', i'', j, j' and j'', indices reordered.

Appendix C

Quantum and Classical Partition Function

A direct relation from the quantum partition function to the classical partition function can be demonstrated through an expansion of the quantum partition function in powers of $\hbar$ with the leading term being the classical partition function [46, 47, 48]. The complete derivation involves a permutation operator to describe the symmetric or anti-symmetric properties in coordinate particle exchange, resulting in a $\frac{1}{N!}$ factor in the final expression. The inclusion of such effects would detract from the overall intent of the derivation, that is, to demonstrate the expansion of the quantum partition function. As such, particle exchange effects will be ignored.

Starting with an ensemble of N quantum particles, the quantum partition function in the position basis is

$$Q = \sum_{i=1}^{N} \int d\{\mathbf{r}\} \psi_i^*(\{\mathbf{r}\}) e^{-\beta \mathcal{H}} \psi_i(\{\mathbf{r}\}) \tag{C.1}$$

where $\mathcal{H}$ is the quantum Hamiltonian,

$$\mathcal{H} = \sum_i -\frac{\hbar^2}{2m} \nabla_i^2 + U[\{\mathbf{r}\}] \tag{C.2}$$

and $\psi_i(\{\mathbf{r}\})$ are a complete orthonormal set of eigenfunctions of the Hamiltonian. Introducing eigenfunctions of the momentum operator in the position representation ($i\hbar\nabla_i \psi(\mathbf{r}) = \mathbf{p}_i \psi(\mathbf{r})$),

$$\phi(\{\mathbf{r}\},\{\mathbf{p}\}) = \exp\left(\frac{i}{\hbar}\sum_{i=1}^{N}\mathbf{p}_i\cdot\mathbf{r}_i\right). \tag{C.3}$$

$\psi_i(\{\mathbf{r}\})$ can be expanded in terms of momentum eigenfunction basis,

$$\psi_i(\{\mathbf{r}\}) = \int d\{\mathbf{p}\}a_i(\{\mathbf{p}\})\exp\left(\frac{i}{\hbar}\sum_{j=1}^{N}\mathbf{p}_j\cdot\mathbf{r}_j\right). \tag{C.4}$$

This expression takes the form of a Fourier transform and, thus, the $a_i(\{\mathbf{p}\})$ coefficients are the Fourier transform of $\psi_i(\{\mathbf{r}\})$. Taking the inverse Fourier transform,

$$a_i(\{\mathbf{p}\}) = \frac{1}{(2\pi\hbar)^{3N}}\int d\{\mathbf{r}\}\psi_i(\{\mathbf{r}\})\exp\left(-\frac{i}{\hbar}\sum_{j=1}^{N}\mathbf{p}_j\cdot\mathbf{r}_j\right). \tag{C.5}$$

Equation C.4 can be substituted into the quantum partition function,

$$Q = \sum_{i=1}^{N}\int d\{\mathbf{r}\}\int d\{\mathbf{p}\}\psi_i^*(\{\mathbf{r}\})a_i(\{\mathbf{p}\})e^{-\beta\mathcal{H}}\exp\left(\frac{i}{\hbar}\sum_{j=1}^{N}\mathbf{p}_j\cdot\mathbf{r}_j\right). \tag{C.6}$$

The explicit form of $a_i(\{\mathbf{p}\})$ can be substituted into the partition function using equation C.5,

$$Q = \frac{1}{(2\pi\hbar)^{3N}}\int d\{\mathbf{r}\}\int d\{\mathbf{r}'\}\int d\{\mathbf{p}\}\left(\sum_{i=1}^{N}\psi_i^*(\{\mathbf{r}\})\psi_i(\{\mathbf{r}'\})\right) \cdot\exp\left(-\frac{i}{\hbar}\sum_{j=1}^{N}\mathbf{p}_j\cdot\mathbf{r}'_j\right)e^{-\beta\mathcal{H}}\exp\left(\frac{i}{\hbar}\sum_{j=1}^{N}\mathbf{p}_j\cdot\mathbf{r}_j\right). \tag{C.7}$$

TO proceed, the orthogonality condition of the wave function is required,

$$\int d\{\mathbf{r}'\}\left(\sum_{i=1}^{N}\psi_i^*(\{\mathbf{r}\})\psi_i(\{\mathbf{r}'\})\right)f(\{\mathbf{r}'\}) = \int d\{\mathbf{r}'\}\delta(\{\mathbf{r}'-\mathbf{r}\})f(\{\mathbf{r}'\}) = f(\{\mathbf{r}\})$$

where $f(\{\mathbf{r}'\})$ is any integrable function. Using the orthogonality condition, the partition function can be simplified to,

$$Q = \frac{1}{h^{3N}} \int d\{\mathbf{r}\} \int d\{\mathbf{p}\} \exp\left(-\frac{i}{\hbar}\sum_{i=1}^{N} \mathbf{p}_i \cdot \mathbf{r}_i\right) e^{-\beta\mathcal{H}} \exp\left(\frac{i}{\hbar}\sum_{i=1}^{N} \mathbf{p}_i \cdot \mathbf{r}_i\right). \tag{C.8}$$

In the partition function, if the quantum Hamiltonian ($\mathcal{H}$) were to be replaced by its classical counterpart (H) the exponents would commute and the partition function would be for a continuous system of N classical particles. A function $w(\{\mathbf{r}\},\{\mathbf{p}\},\beta)$ can be defined that contains all the non-classical effects in the quantum partition function, using this function the following relation can be formulated,

$$e^{-\beta\mathcal{H}} \exp\left(\frac{i}{\hbar}\sum_{i=1}^{N} \mathbf{p}_i \cdot \mathbf{r}_i\right) = e^{-\beta H} \exp\left(\frac{i}{\hbar}\sum_{i=1}^{N} \mathbf{p}_i \cdot \mathbf{r}_i\right) w(\{\mathbf{r}\},\{\mathbf{p}\},\beta) = F(\{\mathbf{r}\},\{\mathbf{p}\},\beta). \tag{C.9}$$

Rewriting the quantum partition function using this relation,

$$Q = \frac{1}{h^{3N}} \int d\{\mathbf{r}\} \int d\{\mathbf{p}\} e^{-\beta H} w(\{\mathbf{r}\},\{\mathbf{p}\},\beta). \tag{C.10}$$

To investigate the classical limit of the quantum partition function, the following limits should hold, $w(\{\mathbf{r}\},\{\mathbf{p}\},\beta) \to 1$ as $\lim_{\hbar\to 0}$. To prove this $F(\{\mathbf{r}\},\{\mathbf{p}\},\beta)$ is differentiated with respect to β,

$$\begin{aligned}\frac{\partial F(\{\mathbf{r}\},\{\mathbf{p}\},\beta)}{\partial\beta} &= \frac{\partial}{\partial\beta} e^{-\beta\mathcal{H}} \exp\left(\frac{i}{\hbar}\sum_{i=1}^{N} \mathbf{p}_i \cdot \mathbf{r}_i\right) \\ &= \frac{\partial}{\partial\beta}(\mathbb{1} - \beta\mathcal{H} + \frac{\beta^2}{2}\mathcal{H}^2 + \ldots) \exp\left(\frac{i}{\hbar}\sum_{i=1}^{N} \mathbf{p}_i \cdot \mathbf{r}_i\right),\end{aligned}$$

with the boundary condition, $F(\{\mathbf{r}\},\{\mathbf{p}\},0) = \exp\left(\frac{i}{\hbar}\sum_{i=1}^{N} \mathbf{p}_i \cdot \mathbf{r}_i\right)$. Taking derivatives,

$$\frac{\partial F(\{\mathbf{r}\},\{\mathbf{p}\},\beta)}{\partial\beta} = -\mathcal{H} F(\{\mathbf{r}\},\{\mathbf{p}\},\beta). \tag{C.11}$$

The differential equation can be solved using a variation on the WKB method [49] which uses successive approximations of $w(\{\mathbf{r}\},\{\mathbf{p}\},\beta)$ in powers of $\hbar$, assuming that $\hbar$ is small compared to other quantities in the equation. The expansion is,

$$w(\{\mathbf{r}\},\{\mathbf{p}\},\beta) = \sum_{i=0}^{\infty} h^i w_i(\{\mathbf{r}\},\{\mathbf{p}\},\beta). \tag{C.12}$$

Substituting the classical expression for $F(\{\mathbf{r}\},\{\mathbf{p}\},\beta)$ from equation C.9 into equation C.11 and writing out the first few terms of the $w(\{\mathbf{r}\},\{\mathbf{p}\},\beta)$ expansion,

$$\begin{aligned}
&\left(\frac{\partial w_0}{\partial\beta} + \hbar\frac{\partial w_1}{\partial\beta} + \mathcal{O}(\hbar^2)\right) e^{-\beta H} \exp\left(\frac{i}{\hbar}\sum_{i=1}^{N}\mathbf{p}_i\cdot\mathbf{r}_i\right) \\
&- He^{-\beta H}\exp\left(\frac{i}{\hbar}\sum_{i=1}^{N}\mathbf{p}_i\cdot\mathbf{r}_i\right)\left(w_0+\hbar w_1+\mathcal{O}(\hbar^2)\right) \\
&= -\left(-\frac{\hbar^2}{2m}\nabla^2 + U(\{\mathbf{r}\})\right) e^{-\beta H}\exp\left(\frac{i}{\hbar}\sum_{i=1}^{N}\mathbf{p}_i\cdot\mathbf{r}_i\right)\left(w_0+\hbar w_1+\mathcal{O}(\hbar^2)\right).
\end{aligned}$$

Expanding the classical Hamiltonian, $H = \frac{p^2}{2m} + U(\{\mathbf{r}\})$, operating with the Laplacian, cancelling the $e^{-\beta H}\exp\left(\frac{i}{\hbar}\sum_{i=1}^{N}\mathbf{p}_i\cdot\mathbf{r}_i\right)$ factors on both sides of the equation and grouping the second order or higher $\hbar$ terms,

$$\begin{aligned}
&\left(\frac{\partial w_0}{\partial\beta} + \hbar\frac{\partial w_1}{\partial\beta} + \mathcal{O}(\hbar^2)\right) - H\left(w_0+\hbar w_1+\mathcal{O}(\hbar^2)\right) \\
&= -U(\{\mathbf{r}\})\left(w_0+\hbar w_1+\mathcal{O}(\hbar^2)\right) - \frac{p_i^2}{2m}\left(w_0+\hbar w_1+\mathcal{O}(\hbar^2)\right) \\
&+ \frac{i\hbar}{m}\left(\sum_{i=1}^{N}\mathbf{p}_i\cdot\nabla_i w_0 - \beta w_0\sum_{i=1}^{N}\mathbf{p}_i\cdot\nabla_i U(\{\mathbf{r}\})\right) + \mathcal{O}(\hbar^2).
\end{aligned}$$

Cancelling the classical Hamiltonian terms on both sides of the equation,

$$\left(\frac{\partial w_0}{\partial\beta} + \hbar\frac{\partial w_1}{\partial\beta} + \mathcal{O}(\hbar^2)\right) = \frac{i\hbar}{m}\left(\sum_{i=1}^{N}\mathbf{p}_i\cdot\nabla_i w_0 - \beta w_0\sum_{i=1}^{N}\mathbf{p}_i\cdot\nabla_i U(\{\mathbf{r}\})\right) + \mathcal{O}(\hbar^2). \tag{C.13}$$

Splitting the equation in powers of $\hbar$, the zeroth order equation gives,

$$\frac{\partial w_0}{\partial \beta} = 0.$$

So,

$$w_0 = C$$

where C is an arbitrary constant. The boundary condition for $F(\{\mathbf{r}\}, \{\mathbf{p}\}, 0)$ can be rephrased as $w(\{\mathbf{r}\}, \{\mathbf{p}\}, 0) = 1$. So, expansion of $w(\{\mathbf{r}\}, \{\mathbf{p}\}, 0)$ in terms of $\hbar$ can be written as,

$$1 = w_0(\{\mathbf{r}\}, \{\mathbf{p}\}, 0) + \hbar w_1(\{\mathbf{r}\}, \{\mathbf{p}\}, 0) + \mathcal{O}(\hbar^2). \tag{C.14}$$

Comparing terms with the same order of $\hbar$,

$$w_0(\{\mathbf{r}\}, \{\mathbf{p}\}, 0) = 1 \tag{C.15}$$
$$w_j(\{\mathbf{r}\}, \{\mathbf{p}\}, 0) = 0, \ j \geq 1. \tag{C.16}$$

Since the value of $w(\{\mathbf{r}\}, \{\mathbf{p}\}, \beta)$ is a constant and therefore independent of the value for β,

$$w(\{\mathbf{r}\}, \{\mathbf{p}\}, \beta) = 1. \tag{C.17}$$

Looking back at the original expression for $F(\{\mathbf{r}\}, \{\mathbf{p}\}, \beta)$ it is now obvious that as $\hbar \to 0$ or $\beta \to 0$ the quantum partition function is equivalent to the classical partition function.

Appendix D

Kac-Feynman Differential Equation Solution

Starting with the time-dependent Schrödinger equation for a time-independent Hamiltonian, the Kac-Feynman path integral solution is proven [21, 50]. It is then shown that the path integral solution is equivalent to the partition function and satisfies the modified diffusion equation at an imaginary time of $\hbar\beta$.

The time-dependent Schrödinger equation is,

$$i\hbar\frac{\partial}{\partial t}\left|\psi(t)\right\rangle = \mathcal{H}\left|\psi(t)\right\rangle. \tag{D.1}$$

Solving the separable differential equation at a time t and initial time $t_0 = 0$,

$$\left|\psi(t)\right\rangle = \exp\left(-\frac{i}{\hbar}\mathcal{H}t\right)\left|\psi(t_0 = 0)\right\rangle \tag{D.2}$$

multiplying $\langle\mathbf{r}_N|$ to both sides of the equation and writing the initial state in the position basis, $|\psi(t_0 = 0)\rangle = \int_{-\infty}^{\infty} d\mathbf{r}_0 \langle\mathbf{r}_0|\psi(t_0 = 0)\rangle |\mathbf{r}_0\rangle$,

$$\langle\mathbf{r}_N|\psi(t)\rangle = \int_{-\infty}^{\infty} d\mathbf{r}_0 \langle\mathbf{r}_N| \exp\left(-\frac{i}{\hbar}\mathcal{H}t\right)|\mathbf{r}_0\rangle \langle\mathbf{r}_0|\psi(t_0 = 0)\rangle. \tag{D.3}$$

The matrix elements of the time evolution operator will be referred to as the propagator $U(\mathbf{r}_N, t; \mathbf{r}_0, 0)$ and is explicitly written as

$$U(\mathbf{r}_N, t; \mathbf{r}_0, 0) = \langle \mathbf{r}_N | \exp\left(-\frac{i}{\hbar}\mathcal{H}t\right) |\mathbf{r}_0\rangle \,. \tag{D.4}$$

Discretizing the time evolution over N intervals, the time evolution operator is,

$$\left[\exp\left(-\frac{i}{\hbar}\mathcal{H}\frac{t}{N}\right)\right]^N .$$

Defining the time intervals as $\epsilon = \frac{t}{N}$ and taking the limit as $N \to \infty$ the time evolution operator is,

$$\exp\left(-\frac{i\epsilon}{\hbar}\mathcal{H}\right) = \exp\left(-\frac{i\epsilon}{\hbar}\left(\frac{\hat{\mathbf{P}}^2}{2m} + V(\hat{\mathbf{R}})\right)\right) \simeq \exp\left(-\frac{i\epsilon}{\hbar}\frac{\hat{\mathbf{P}}^2}{2m}\right)\exp\left(-\frac{i\epsilon}{\hbar}V(\hat{\mathbf{R}})\right). \tag{D.5}$$

Assuming that the values for the operators are not too large and ϵ is small. The commutator terms in the Baker-Campbell-Hausdorff formula $e^A e^B = e^{A+B+\frac{1}{2}[A,B]+\cdots}$ are of increasing order in ϵ and therefore go to zero. Expanding the propagator for N time intervals,

$$\begin{aligned} &U(\mathbf{r}_N, t; \mathbf{r}_0, 0) \\ &= \langle \mathbf{r}_N | \underbrace{\exp\left(-\frac{i\epsilon}{\hbar}\frac{\hat{\mathbf{P}}^2}{2m}\right)\exp\left(-\frac{i\epsilon}{\hbar}V(\hat{\mathbf{R}})\right)\cdot\exp\left(-\frac{i\epsilon}{\hbar}\frac{\hat{\mathbf{P}}^2}{2m}\right)\exp\left(-\frac{i\epsilon}{\hbar}V(\hat{\mathbf{R}})\right)\cdot\ldots}_{N \text{ time evolution operators}} |\mathbf{r}_0\rangle \,. \end{aligned} \tag{D.6}$$

Introducing a resolution of the identity in the position basis, $\mathbb{1} = \int_{-\infty}^{\infty} d\mathbf{r}\, |\mathbf{r}\rangle\,, \langle \mathbf{r}|$, between each time evolution operator,

$$U(\mathbf{r}_N, t; \mathbf{r}_0, 0) = \int \prod_{i=1}^{N-1} d\mathbf{r}_i \, \langle \mathbf{r}_N | \exp\left(-\frac{i\epsilon}{\hbar}\frac{\hat{\mathbf{P}}^2}{2m}\right) \exp\left(-\frac{i\epsilon}{\hbar}V(\hat{\mathbf{R}})\right) |\mathbf{r}_{N-1}\rangle$$
$$\langle \mathbf{r}_{N-1} | \exp\left(-\frac{i\epsilon}{\hbar}\frac{\hat{\mathbf{P}}^2}{2m}\right) \exp\left(-\frac{i\epsilon}{\hbar}V(\hat{\mathbf{R}})\right) |\mathbf{r}_{N-2}\rangle$$
$$\cdots$$
$$\langle \mathbf{r}_2 | \exp\left(-\frac{i\epsilon}{\hbar}\frac{\hat{\mathbf{P}}^2}{2m}\right) \exp\left(-\frac{i\epsilon}{\hbar}V(\hat{\mathbf{R}})\right) |\mathbf{r}_1\rangle$$
$$\langle \mathbf{r}_1 | \exp\left(-\frac{i\epsilon}{\hbar}\frac{\hat{\mathbf{P}}^2}{2m}\right) \exp\left(-\frac{i\epsilon}{\hbar}V(\hat{\mathbf{R}})\right) |\mathbf{r}_0\rangle \, .$$

Examining a single time evolution operator matrix element,

$$\langle \mathbf{r}_N | \exp\left(-\frac{i\epsilon}{\hbar}\frac{\hat{\mathbf{P}}^2}{2m}\right) \exp\left(-\frac{i\epsilon}{\hbar}V(\hat{\mathbf{R}})\right) |\mathbf{r}_{N-1}\rangle$$
$$= \langle \mathbf{r}_N | \exp\left(-\frac{i\epsilon}{\hbar}\frac{\hat{\mathbf{P}}^2}{2m}\right) |\mathbf{r}_{N-1}\rangle \exp\left(-\frac{i\epsilon}{\hbar}V(\mathbf{r}_{N-1})\right) .$$

To evaluate $\langle \mathbf{r}_N | \exp\left(-\frac{i\epsilon}{\hbar}\frac{\hat{\mathbf{P}}^2}{2m}\right) |\mathbf{r}_{N-1}\rangle$ a resolution of the identity in the momentum basis, $\mathbb{1} = \frac{1}{2\pi\hbar}\int_{-\infty}^{\infty} d\mathbf{p} \, |\mathbf{p}\rangle \langle \mathbf{p}|$, is inserted,

$$\frac{1}{2\pi\hbar}\int_{-\infty}^{\infty} d\mathbf{p} \, \langle \mathbf{r}_N | \exp\left(-\frac{i\epsilon}{\hbar}\frac{\hat{\mathbf{P}}^2}{2m}\right) |\mathbf{p}\rangle \langle \mathbf{p}|\mathbf{r}_{N-1}\rangle$$
$$= \frac{1}{2\pi\hbar}\int_{-\infty}^{\infty} d\mathbf{p} \, \langle \mathbf{r}_N|\mathbf{p}\rangle \exp\left(-\frac{i\epsilon}{\hbar}\frac{\mathbf{p}^2}{2m}\right) \langle \mathbf{p}|\mathbf{r}_{N-1}\rangle \, .$$

Substituting the inner product of position and momentum $\langle \mathbf{r}|\mathbf{p}\rangle = \exp\left(\frac{i}{\hbar}\mathbf{p}\cdot\mathbf{r}\right)$,

$$\begin{aligned}
&\frac{1}{2\pi\hbar}\int_{-\infty}^{\infty} d\mathbf{p}\exp\left(\frac{i}{\hbar}\mathbf{p}\cdot(\mathbf{r}_N-\mathbf{r}_{N-1})\right)\exp\left(-\frac{i\epsilon}{\hbar}\frac{\mathbf{p}^2}{2m}\right)\\
&\quad=\frac{1}{2\pi\hbar}\int_{-\infty}^{\infty} d\mathbf{p}\exp\left(-\frac{i\epsilon}{\hbar}\frac{\mathbf{p}^2}{2m}+\frac{i}{\hbar}\mathbf{p}\cdot(\mathbf{r}_N-\mathbf{r}_{N-1})\right)\\
&\quad=\sqrt{\frac{m}{2\pi i\hbar\epsilon}}\exp\left(\frac{im(\mathbf{r}_N-\mathbf{r}_{N-1})^2}{2\hbar\epsilon}\right).
\end{aligned}$$

Taking this logic and applying it to the N time evolution matrix elements, a compact form of the propagator can be determined,

$$U(\mathbf{r}_N,t;\mathbf{r}_0,0)=\left(\frac{m}{2\pi i\hbar\epsilon}\right)^{\frac{N}{2}}\int\prod_{i=1}^{N-1}d\mathbf{r}_i\exp\left(\sum_{i=1}^{N}\frac{im(\mathbf{r}_i-\mathbf{r}_{i-1})^2}{2\hbar\epsilon}-\frac{i\epsilon}{\hbar}V(\mathbf{r}_{i-1})\right). \tag{D.7}$$

Taking the limit as $N\to\infty$, so $\epsilon\to 0$ the time evolution will be continuous, as before. The propagator is written as,

$$U(\mathbf{r}_N,t;\mathbf{r}_0,0)=\int D\mathbf{r}\exp\left(\frac{i}{\hbar}\int_0^t dt\left[\frac{m}{2}\left|\frac{d\mathbf{r}}{dt}\right|^2-V(\mathbf{r}(t))\right]\right) \tag{D.8}$$

where,

$$D\mathbf{r}=\lim_{N\to\infty}\left(\frac{m}{2\pi i\hbar\epsilon}\right)^{\frac{N}{2}}\int\prod_{i=1}^{N-1}d\mathbf{r}_i. \tag{D.9}$$

If a Wick rotation $t=-i\tau$ is performed so that the propagator now describes an imaginary time trajectory. The derivation of this imaginary time propagator can be easily performed following the same procedure as outlined previously. The imaginary time propagator is,

$$U(\mathbf{r}_N,\tau;\mathbf{r}_0,0)=\langle\mathbf{r}_N|\exp\left(-\frac{1}{\hbar}\mathcal{H}\tau\right)|\mathbf{r}_0\rangle=\int D\mathbf{r}\exp\left(-\frac{1}{\hbar}\int_0^\tau d\tau\left[\frac{m}{2}\left|\frac{d\mathbf{r}}{d\tau}\right|^2+V(\mathbf{r}(\tau))\right]\right). \tag{D.10}$$

Moving on to consider the quantum partition function,

$$Q = \mathrm{Tr} \exp\left(-\beta \mathcal{H}\right). \tag{D.11}$$

The trace is invariant under unitary change of basis and so can be expanded in the position basis,

$$Q = \int_{-\infty}^{\infty} d\mathbf{r} \left\langle \mathbf{r} \right| \exp\left(-\beta \mathcal{H}\right) \left| \mathbf{r} \right\rangle. \tag{D.12}$$

Focusing on the argument in the integrand and multiplying both the numerator and denominator by $\hbar$

$$Q = \int_{-\infty}^{\infty} d\mathbf{r} \left\langle \mathbf{r} \right| \exp\left(-\frac{1}{\hbar}\beta\hbar \cdot \mathcal{H}\right) \left| \mathbf{r} \right\rangle. \tag{D.13}$$

The partition function now takes the same form as the imaginary time propagator, with an integral endpoint $\tau = \beta\hbar$. The solution is already known from equation D.10,

$$Q = U(\mathbf{r}, \beta\hbar; \mathbf{r}, 0) = \int D\mathbf{r} \exp\left(-\frac{1}{\hbar}\int_0^{\beta\hbar} d\tau \left[\frac{m}{2}\left|\frac{d\mathbf{r}}{d\tau}\right|^2 + V(\mathbf{r}(\tau))\right]\right). \tag{D.14}$$